CHAPTER III

RESULTS AND DISCUSSION

3.1 The Primary Screening Results on Plant Growth Regulator of Various Plants

The screening results of dichloromethane and methanolic crude extracts of twelve plants are presented in Tables 3.1and 3.2.

Table 3.1 Effect of dichloromethane crude extract of various plants on seedling growth of *B. pekinensis* Rupr.

Plant	Level of inhibition at various concentration*		
	10 ppm	100 ppm	1000 ppm
Fagraea fragrans Roxb.	+	--	--
Enkleia siamensis Nervling.	+	+	+
Allophylus cobbe Bl.	+	+	++
Breynia glauca Craib.	+	++	+++
Gendarussa vulgaris Nees.	+	++	++
Strychnos nux-blanda A.W. Hill.	+	+	+
Tylophora indica (Burm.f.) Merr.	+	+++	+++
Tagetes erecta Linn.	+	+	++
Cosmos sulphureus Cav.	+	+	+
Tinospora cordifolia Willd.	+	+	++
Wedelia trilobata (Linn.) Hitchc	+	+	+
Melampodium paludosum HBK.	+	+	+++

* The level of plant growth inhibition was determined by using the approximation of root and shoot length compare with the control ; thus, the level was classified as inhibition more than 70 % (+++), 40-70 % (++), less than 40% (+), and was contrasted (-).

Table 3.2 Effect of methanolic crude extract of various plants on seedling growth of *B. pekinensis* Rupr.

Plant	Level of inhibition at various concentration		
	10 ppm	100 ppm	1000 ppm
Fagraea fragrans Roxb.	+	+	--
Enkleia siamensis Nervling.	+	++	++
Allophylus cobbe Bl.	+	++	++
Breynia glauca Craib.	+	++	++
Gendarussa vulgaris Nees.	+	+	+++
Strychnos nux-blanda A.W. Hill.	+	+	+
Tylophora indica (Burm.f.) Merr.	+	+++	+++
Tagetes erecta Linn.	+	+	++
Cosmos sulphureus Cav.	+	+	++
Tinospora cordifolia Willd.	+	+	++
Wedelia trilobata (Linn.) Hitchc	+	+	+
Melampodium paludosum HBK.	+	+	++

Based on the result of *B. pekinensis* Rupr. seedling growth inhibitory effect, both dichloromethane and methanolic crude extracts of the roots of *T. indica* Merr. revealed the best inhibition results. The growth inhibition was completed at 1000 ppm and 100 ppm (Tables 3.1 and 3.2).

Then, the other parts of this plant such as leaves and stems were selected for further investigation on plant growth regulator activity against *B. pekinensis* Rupr.

Three parts of *T. indica* Merr. (roots, stems and leaves) were extracted by methanol. The result of plant growth regulator activity against *B. pekinensis* Rupr. of methanolic crude extracts of roots, stems and leaves of *T. indica* Merr. are shown in Table 3.3.

Table 3.3 Effect of methanolic crude extract of roots, stems and leaves of *T. indica* Merr. on seedling growth of *B. pekinensis* Rupr.

Part of *T. indica* Merr.	Level of inhibition at various concentration		
	10 ppm	100 ppm	1000 ppm
root	+	++	+++
stem	+	+	+
leaf	+	+	+

From the bioassay results on Table 3.3, this research will be focused only on the constituents of the roots of *T. indica* Merr. and its plant growth regulation against *B. pekinensis* Rupr.

3.2 Plant Growth Regulation Activity Results of the Crude Extracts of the Roots of *T. indica* Merr.

Each crude extract of the roots of *T. indica* Merr. which was derived from the extraction procedure described in Chapter II (2.5.2) was preliminary bioassayed for plant growth regulation activity. The results are displayed in Table 3.4, Figures 3.1 and 3.2.

Table 3.4 Effect of each crude extract of the roots of *T. indica* Merr. on seedling growth of *B. pekinensis* Rupr.

Crude extract	Part of *B. pekinensis*	% Inhibition at various concentration		
		10 ppm	100 ppm	1000 ppm
Hexane	Root	-7.5	-21.8	-27.1
	Shoot	-29.2	1.9	28.2
Dichloromethane	Root	1.4	81.4	94.1
	Shoot	2.7	66.8	100
Ethyl acetate	Root	-22.0	66.4	94.8
	Shoot	9.8	59.8	100
Methanol	Root	-17.4	-8.8	92.6
	Shoot	-10.5	9.6	95.7

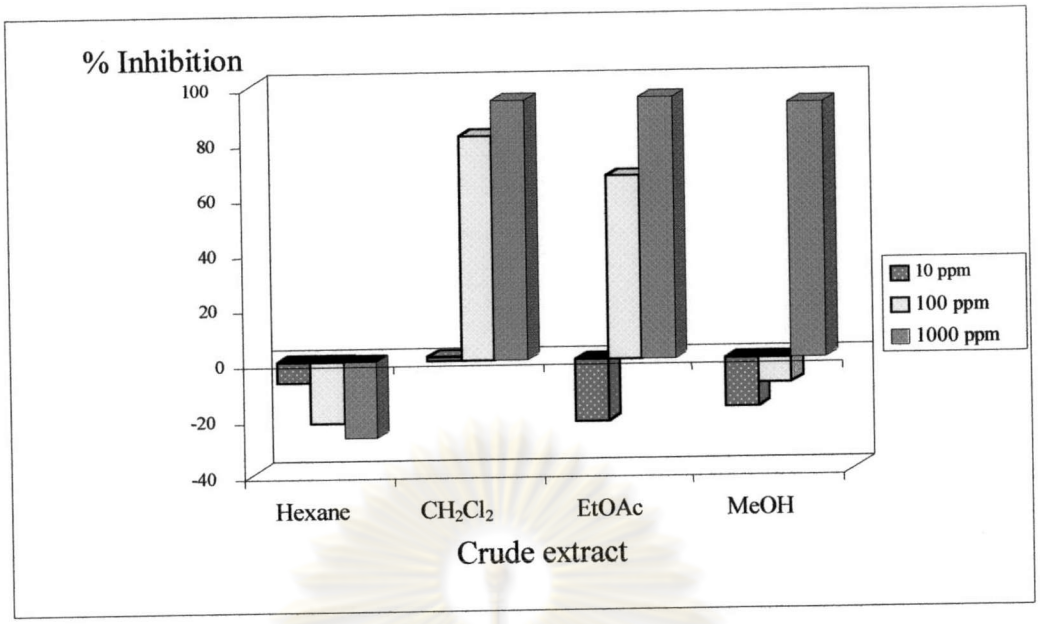

Figure 3.1 Effect of each crude extract of the root of *T. indica* Merr. on root length of *B. pekinensis* Rupr. at various concentration (ppm)

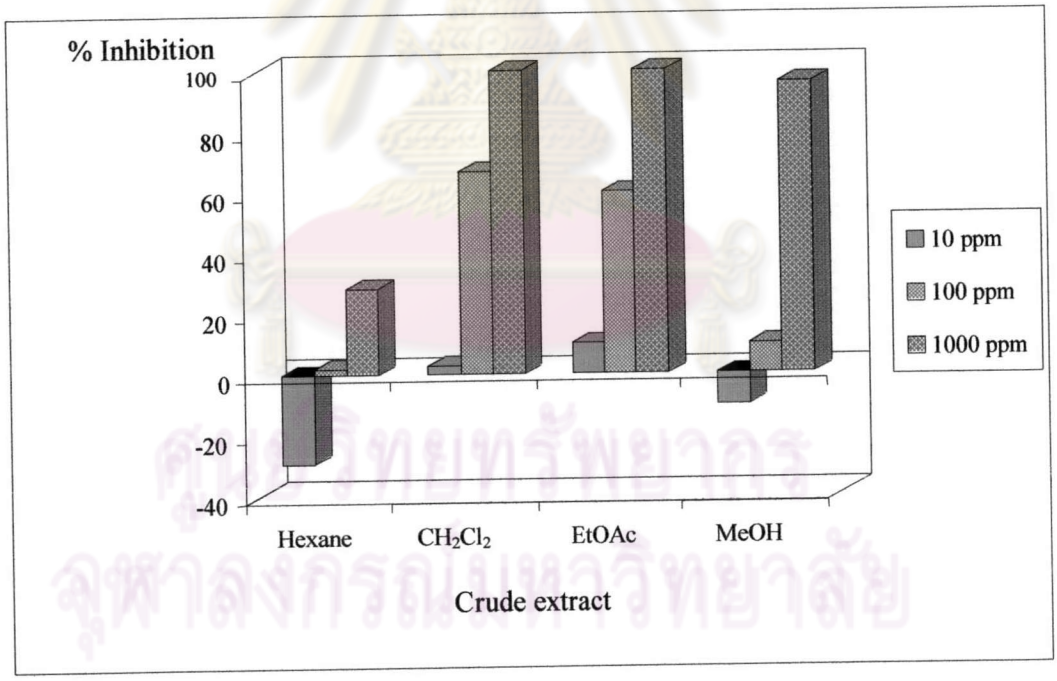

Figure 3.2 Effect of each crude extract of the root of *T. indica* Merr. on shoot length of *B. pekinensis* Rupr. at various concentration (ppm)

For the inhibitory effect on the root and shoot length of *B. pekinensis* Rupr., dichloromethane and ethyl acetate crude extracts showed the strongest inhibitory effect, followed by methanolic and hexane crude extract, respectively. Therefore, the dichloromethane and ethyl acetate crude extracts were selected for further separation.

3.3 Plant Growth Regulation Activity of Fractionation of Dichloromethane and Ethyl acetate Crude Extracts of the Roots of *T. indica* Merr.

According to plant growth regulation activity of crude extracts (see Table 3.4), dichloromethane and ethyl acetate crude extracts indicated that these fractions contain allelopathic chemicals against *B. pekinensis* Rupr. The separation by quick column chromatography of both crude extracts into small portions was carried out and the plant growth regulation activity test of each derived fraction was also observed.

3.3.1 Plant Growth Inhibition Activity of Dichloromethane Subfractions of the Roots of *T. indica* Merr.

The result of plant growth inhibition against *B. pekinensis* Rupr. of each subfraction which derived from the separation of dichloromethane crude extract by quick column chromatography (Table 2.1) are shown in Table 3.5, Figures 3.3 and 3.4.

Table 3.5 Effect of dichloromethane subfractions of the roots of *T. indica* Merr. on seedling growth of *B. pekinensis* Rupr.

Crude subfraction	Part of *B. pekinensis*	% Inhibition at various concentration		
		10 ppm	100 ppm	1000 ppm
A	Root	-7.4	2.6	13.1
	Shoot	-5.8	0.7	10.3
B	Root	1.4	8.6	14.6
	Shoot	0.6	5.6	12.1
C	Root	-12.3	17.4	24.6
	Shoot	-8.9	10.5	19.4
D	Root	-8.0	-0.1	19.2
	Shoot	-10.6	-1.2	10.8
E	Root	8.5	91.5	100
	Shoot	6.2	90.2	100
F	Root	3.4	90.2	100
	Shoot	5.7	88.3	100

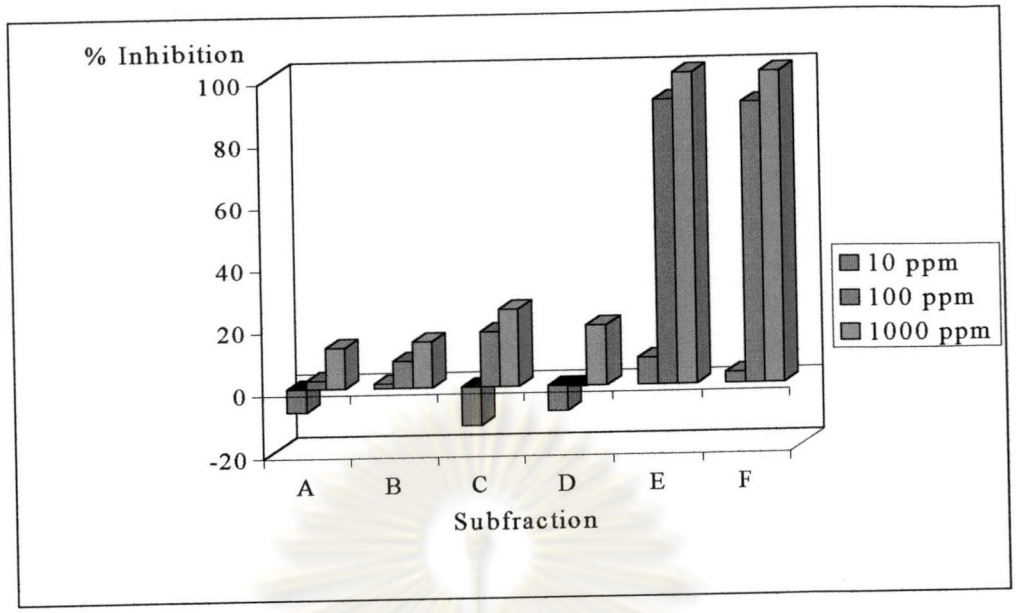

Figure 3.3 Effect of dichloromethane subfractions of the roots of *T. indica* Merr. on root length of *B. pekinensis* Rupr.

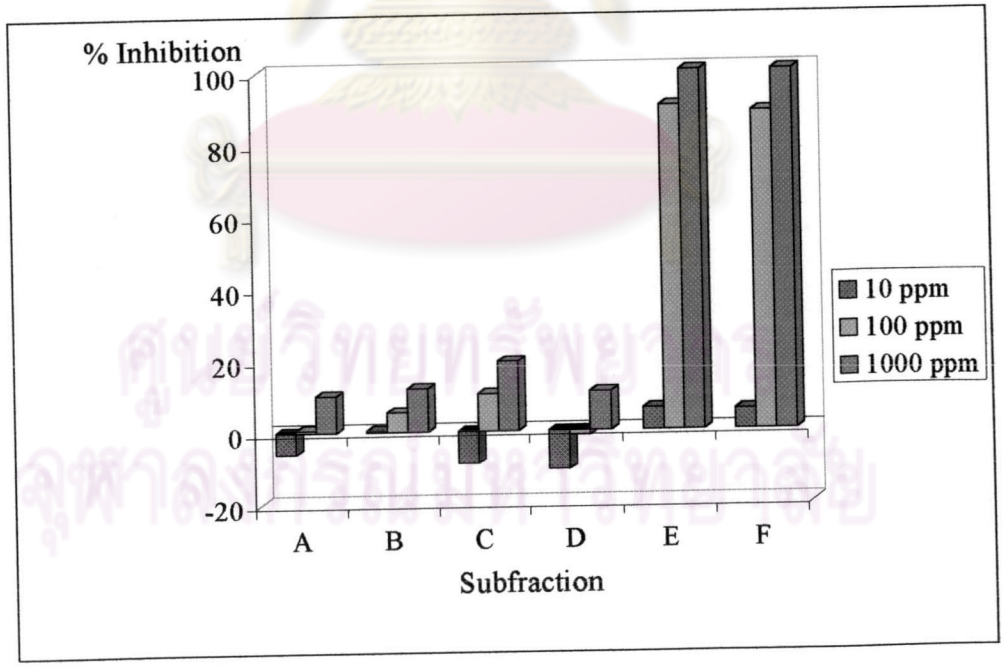

Figure 3.4 Effect of dichloromethane subfractions of the roots of *T. indica* Merr. on shoot length of *B. pekinensis* Rupr.

3.3.2 Plant Growth Inhibition Activity of Ethyl acetate Subfractions of the roots of *T. indica* Merr.

The result of seedling growth inhibition against *B. pekinensis* Rupr. of each subfraction which derived from the separation of ethyl acetate crude extract by quick column chromatography (Table 2.2) are displayed in Table 3.6, Figures 3.5 and 3.6.

Table 3.6 Effect of ethyl acetate subfractions of the roots of *T. indica* Merr. on seedling growth of *B. pekinensis* Rupr.

Crude subfraction	Part of *B. pekinensis*	% Inhibition at various concentration		
		10 ppm	100 ppm	1000 ppm
1	Root	13.3	17.9	21.1
	Shoot	8.9	11.1	19.5
2	Root	23.8	29.5	57.7
	Shoot	1.0	19.4	34.2
3	Root	25.1	78.4	100
	Shoot	34.6	53.0	100
4	Root	27.4	95.6	100
	Shoot	27.5	92.6	100
5	Root	14.0	23.5	100
	Shoot	15.4	54.4	100
6	Root	33.2	42.9	100
	Shoot	2.2	61.5	100

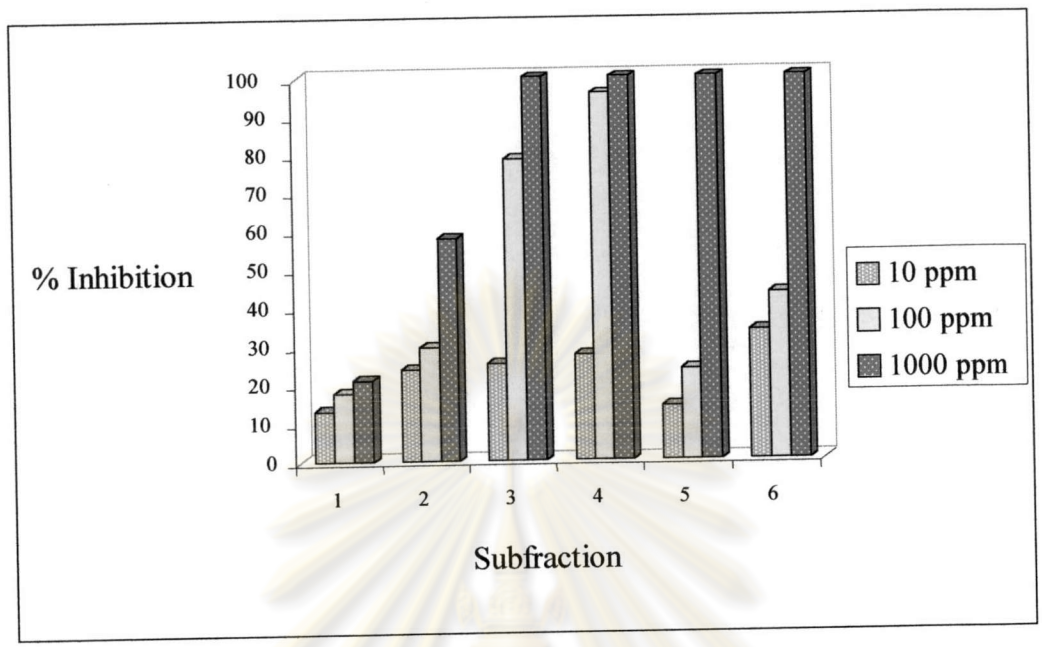

Figure 3.5 Effect of ethyl acetate subfractions of the roots of *T. indica* Merr. on root length of *B. pekinensis* Rupr.

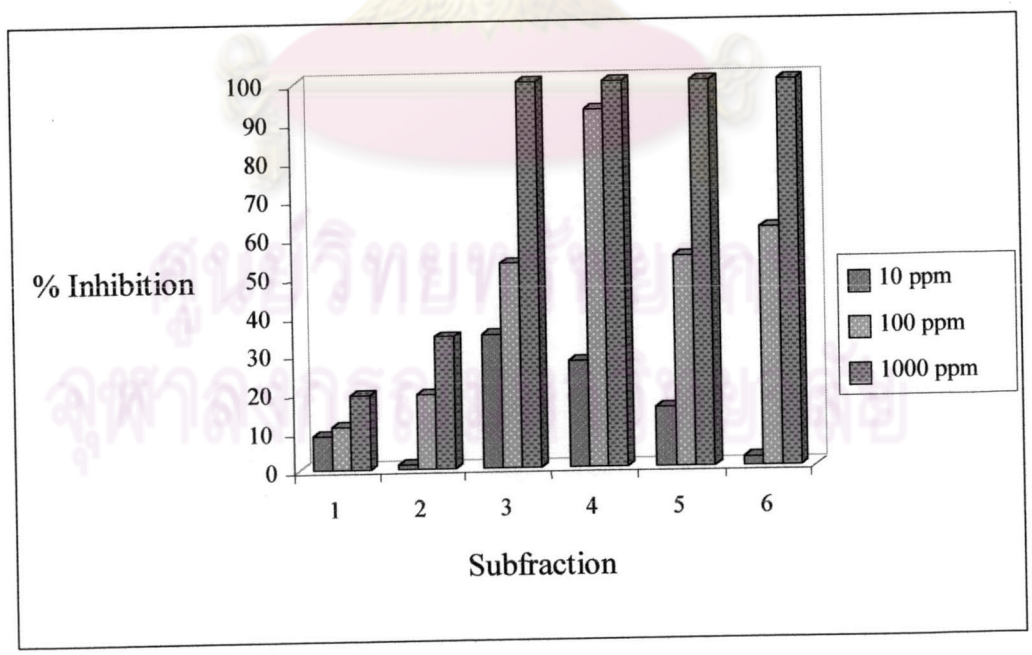

Figure 3.6 Effect of ethyl acetate subfractions of the roots of *T. indica* Merr. on shoot length of *B. pekinensis* Rupr.

From the results of plant growth regulators activity against *B. pekinensis* Rupr., subfractions E and F achieved from dichloromethane crude extract exposed very good activity. The growth inhibition of both root and shoot at 100 ppm were still highly active of approximately 90%. For ethyl acetate crude extract, subfractions 3, 4, 5 and 6 showed good activity with 100% inhibition on both root and shoot length on *B. pekinensis* Rupr. at 1000 ppm. At 100 ppm, subfraction 4 displayed the highest percent inhibition with more than 90%, followed by subfractions 3, 6 and 5 at 78.4%, 42.9% and 23.5% inhibition of root elongation, respectively.

Based on the result in Tables 3.5 and 3.6, it was implied that subfraction E, F, 3, 4, 5, 6 should contained some bioactive substances. Thus, they were subjected to the isolation, purification, and elucidation structural of bioactive compounds which were affected the seedling growth of *B. pekinensis* Rupr.

3.4 Properties and Structure Elucidation of Isolated Compounds

3.4.1 Structural Elucidation of Mixture 1

Mixture 1, a white wax of melting point 43-45 °C (125 mg), was isolated from the subfraction E of dichloromethane crude extract. It was fractionated by column chromatography over silica gel eluting with 1:4 EtOAc/CH_2Cl_2, and was purified by several crystallization from 1:1 EtOAc/CH_2Cl_2.

The IR spectrum (Figure 3.7) exhibited the characteristic absorption peaks at V_{max} 3454 cm^{-1} (OH stretching of hydroxy group), 2919 and 2846 cm^{-1} (C-H stretching), 1712 cm^{-1}(C=O stretching), 1464 cm^{-1} (CH_2 bending) and 1299 cm^{-1} (C-O stretching). The IR spectrum clearly supported that this compound should be long chain carboxylic acid.

The EI mass spectrum (Figure 3.8) of this mixture displayed the molecular peak, M^+ at m/z 284. It corresponded to the molecular formula $C_{18}H_{36}O_2$ (Calcd. For $C_{18}H_{36}O_2$: MW 284.48) of octadecanoic acid from analogy with library data.

Mixture 1 was methylated with trimethylsilyl diazomethane ($TMSCHN_2$). A solution of compound 1 in CH_2Cl_2 was treated with excess $TMSCHN_2$ led to yield methyl ester of Mixture 1(1A). The methyl ester derivative was examined by GC-MS analysis. This derivative was subjected to GC-MS analysis for determine the mixture component. The chromatogram of this derivative exhibited 3 components as I, II and III was shown in Figure 3.9

The compound I had retention time at 8.27 min. Mass spectrum of this compound gave the molecular peak, M^+, at m/z 270 (Calcd. For $C_{17}H_{34}O_2$: MW 270.45). It was hexadecanoic acid, methyl ester from comparison with library data. It was obvious to conclude that compound I was hexadecanoic acid or palmitic acid. The mass spectrum of this compound and library data of hexadecanoic acid methyl ester are shown in Figure 3.10. The mass fragmentation pattern of compound I is shown in Scheme 3.1.

The mass spectrum of compound II, that had retention time at 9.08 min, gave the molecular peak at m/z 296 (Calcd. For $C_{19}H_{36}O_2$: MW 296.49). From the comparison with library data, it was cis-9-octadecenoic acid, methyl ester. Then compound II was cis-9-octadecenoic acid or oleic acid. The mass spectrum of this compound and library data of cis-9-octadecenoic acid methyl ester are shown in

Figure 3.11. The mass fragmentation pattern of compound II is shown in Scheme 3.2.

The last compound, compound III, had retention time at 9.17 min. Mass spectrum gave the molecular peak at m/z 298 (Calcd. For $C_{19}H_{38}O_2$: MW 298.50). It was octadecanoic acid, methyl ester from comparison with library data. It was clear to complete that compound III was octadecanoic acid or stearic acid. The mass spectrum of this compound and library data of octadecenoic acid methyl ester are shown in Figure 3.12. The mass fragmentation pattern of compound III is shown in Scheme 3.3.

Hence, it was concluded that mixture 1 was a mixture of hexadecanoic acid, cis-9-octadecenoic acid and octadecanoic acid. The composition of three compounds in Mixture 1 was revealed in Table 3.7.

Table 3.7 The composition of each compound in Mixture 1

Name	R_t (min)	% Composition
hexadecanoic acid	8.27	85
cis-9-octadecenoic acid	9.08	8
octadecanoic acid	9.17	7

The structure of these three compounds are shown below:

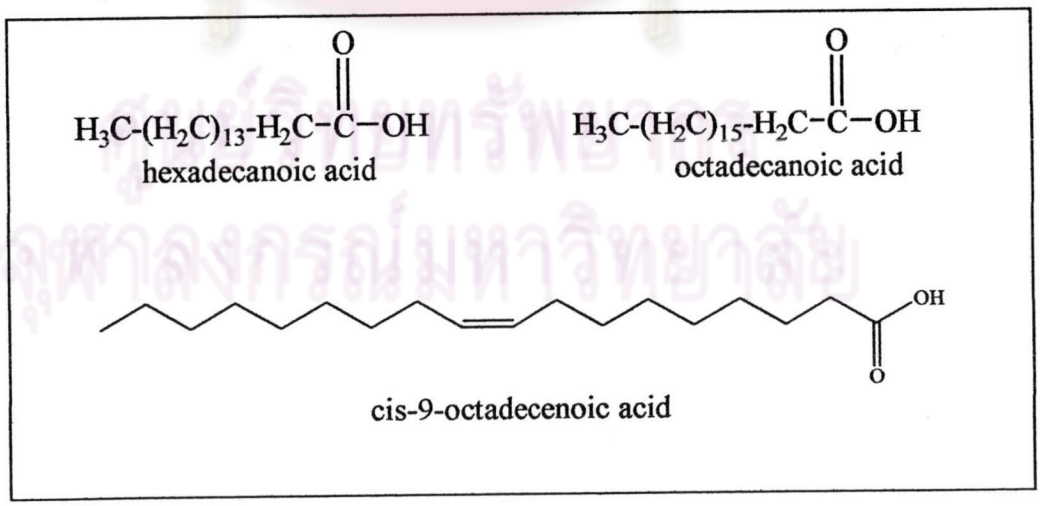

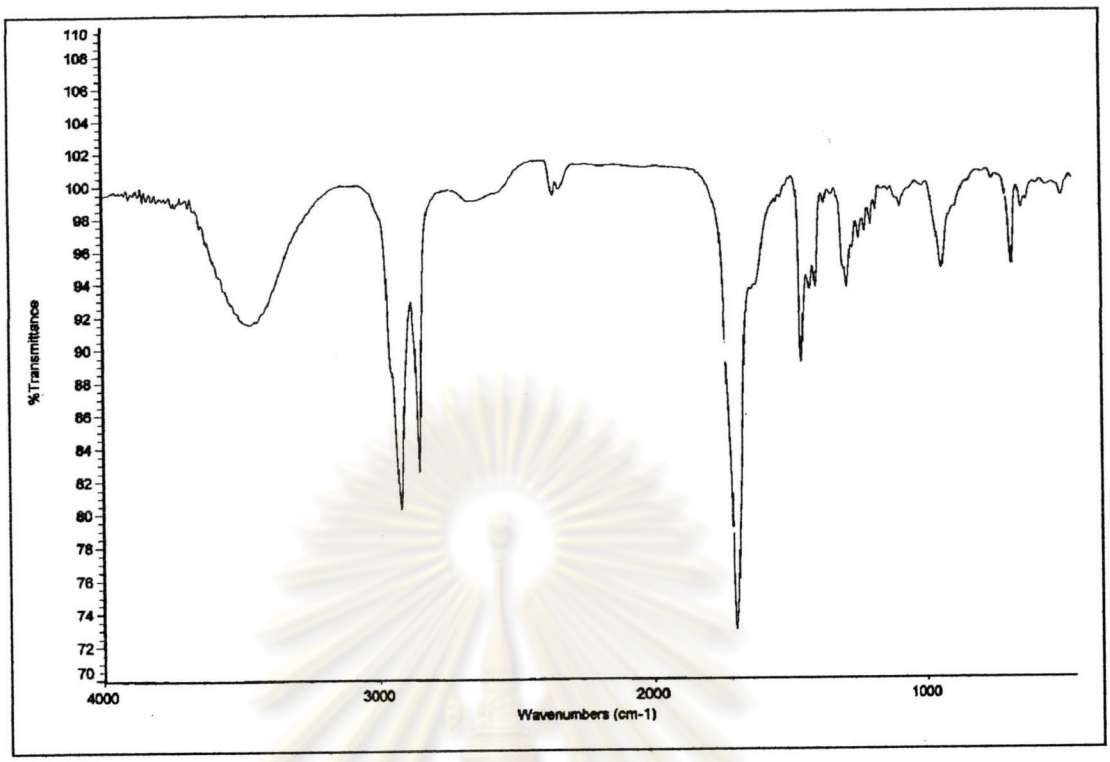

Figure 3.7 The IR spectrum of mixture 1

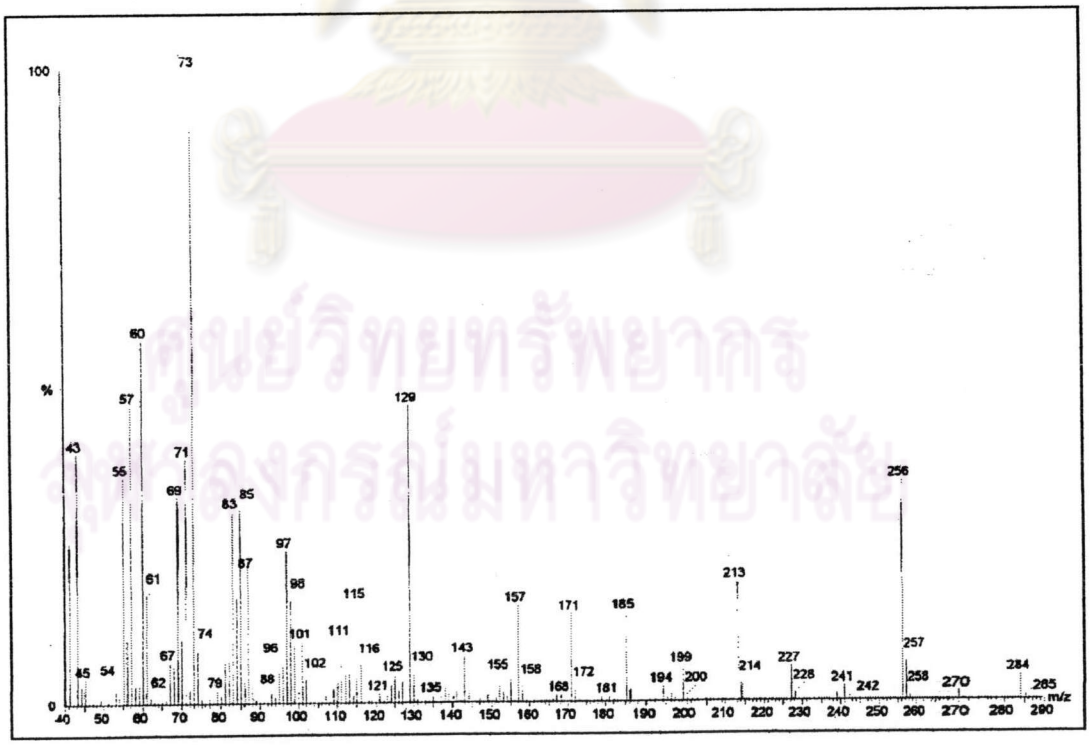

Figure 3.8 The EI mass spectrum of mixture 1

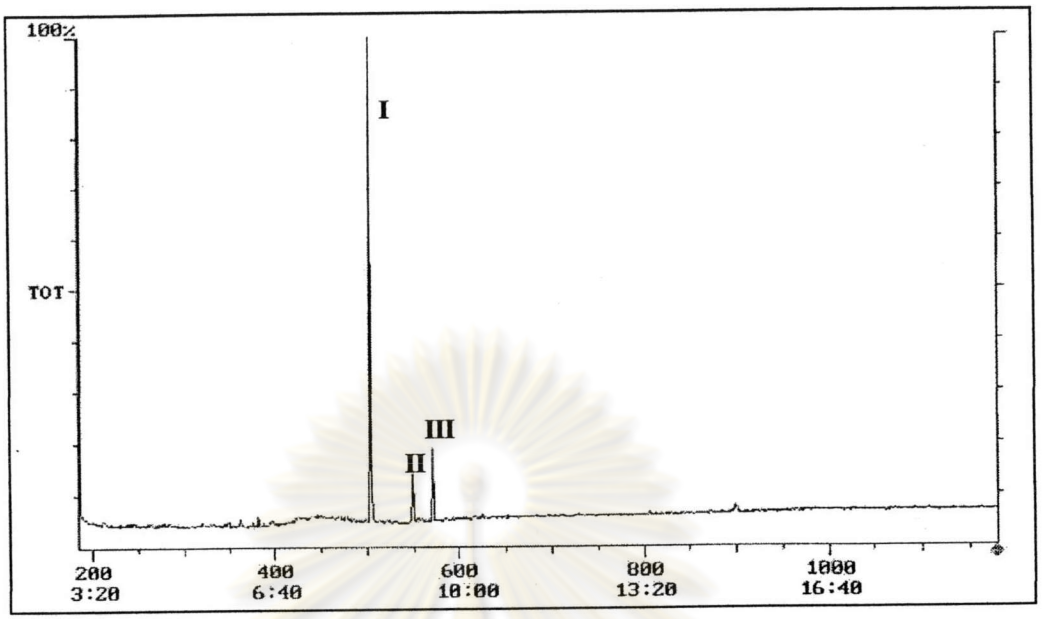

Figure 3.9 The GC chromatogram of mixture 1

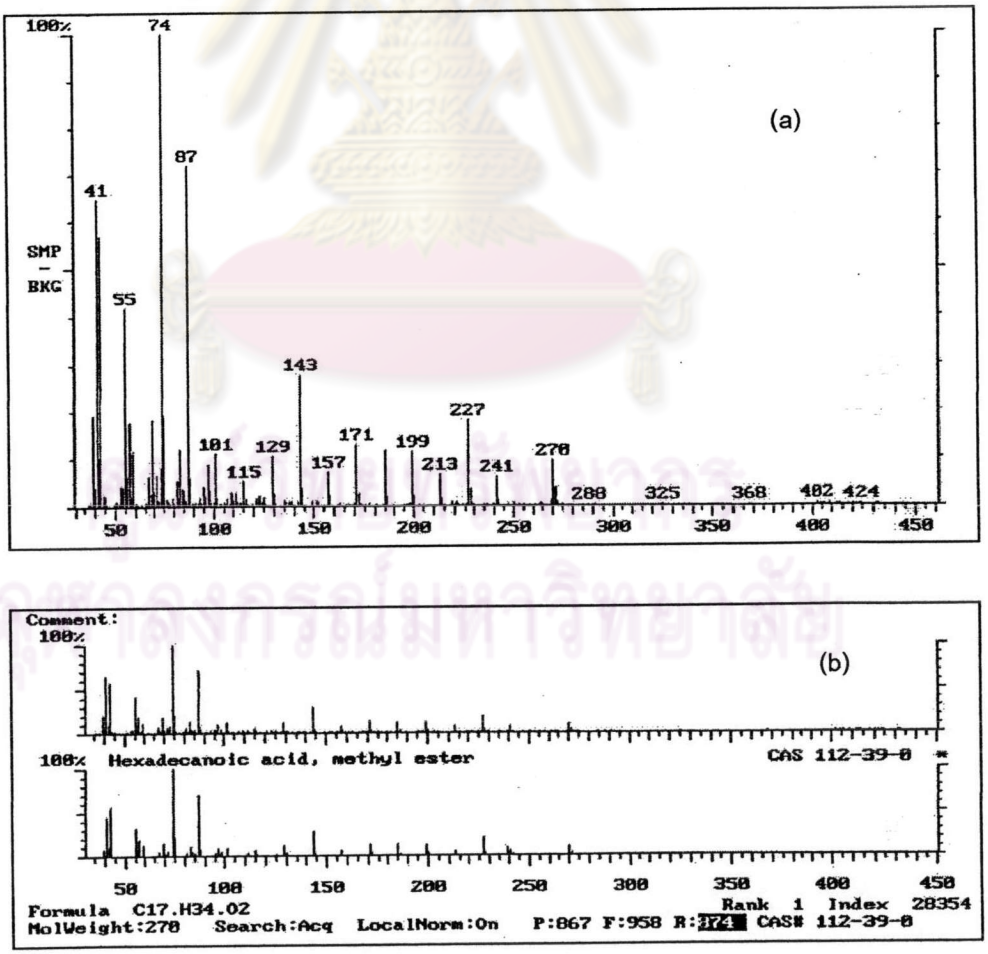

Figure 3.10 The mass spectrum of compound I (a) and library data of hexadecanoic acid, methyl ester (b)

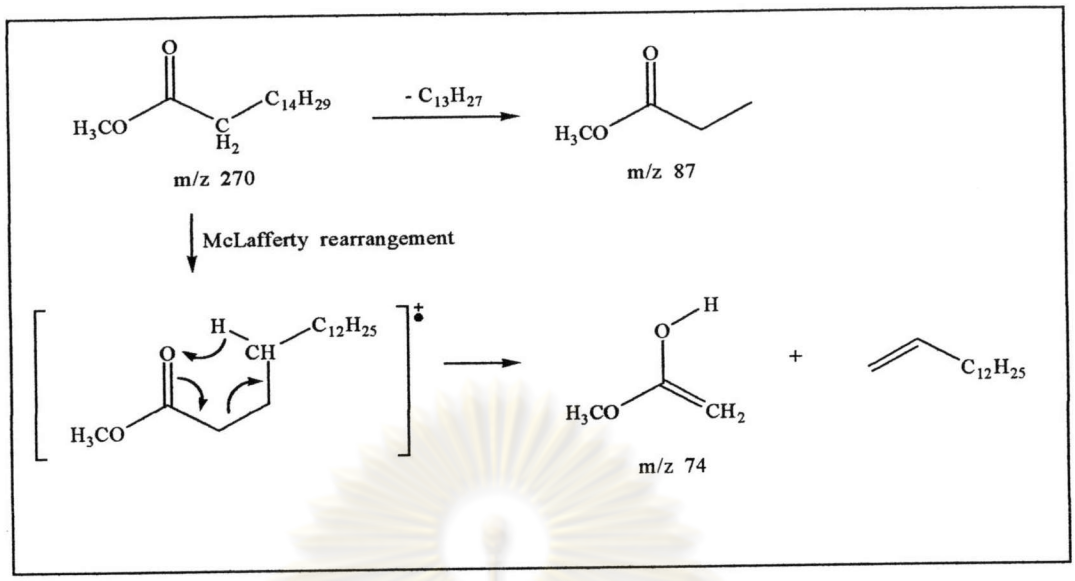

Scheme 3.1 The mass fragmentation pattern of hexadecanoic acid, methyl ester

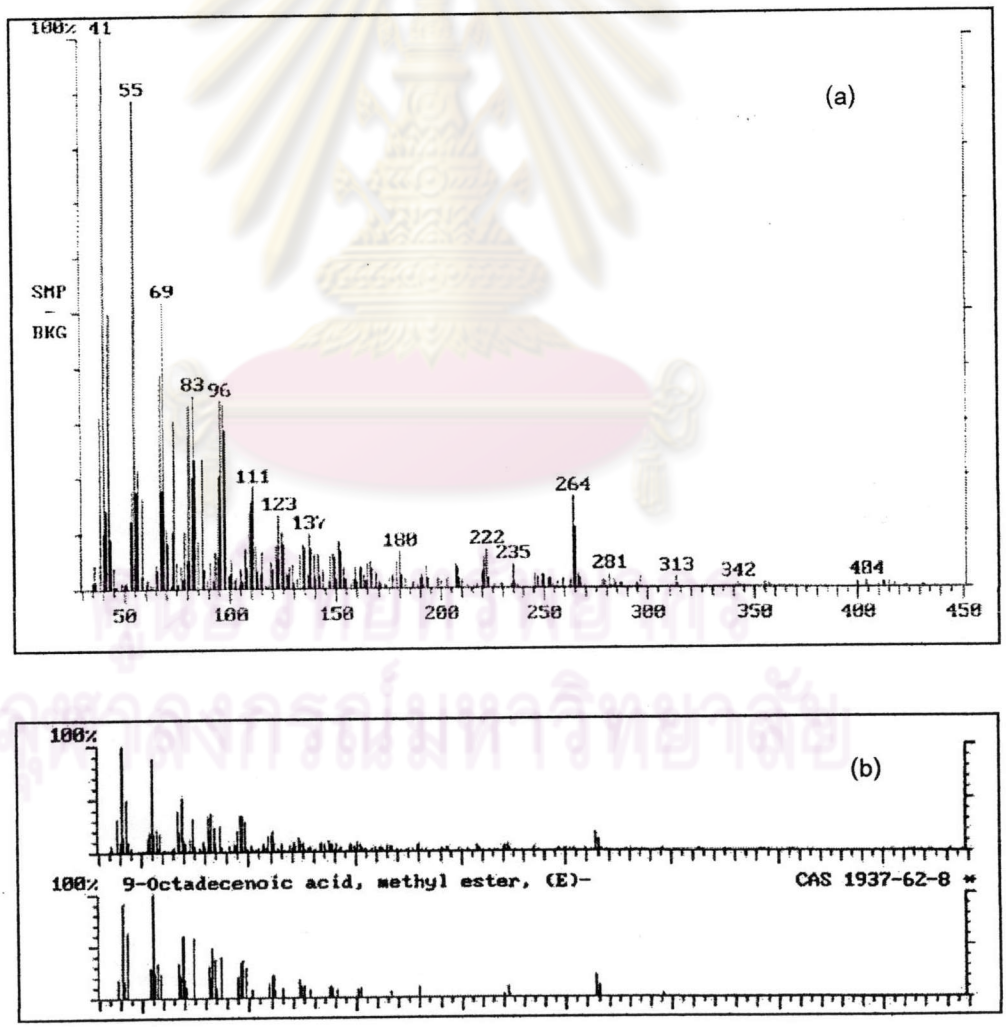

Figure 3.11 The mass spectrum of compound II (a) and library data of cis-9-octadecanoic acid, methyl ester (b)

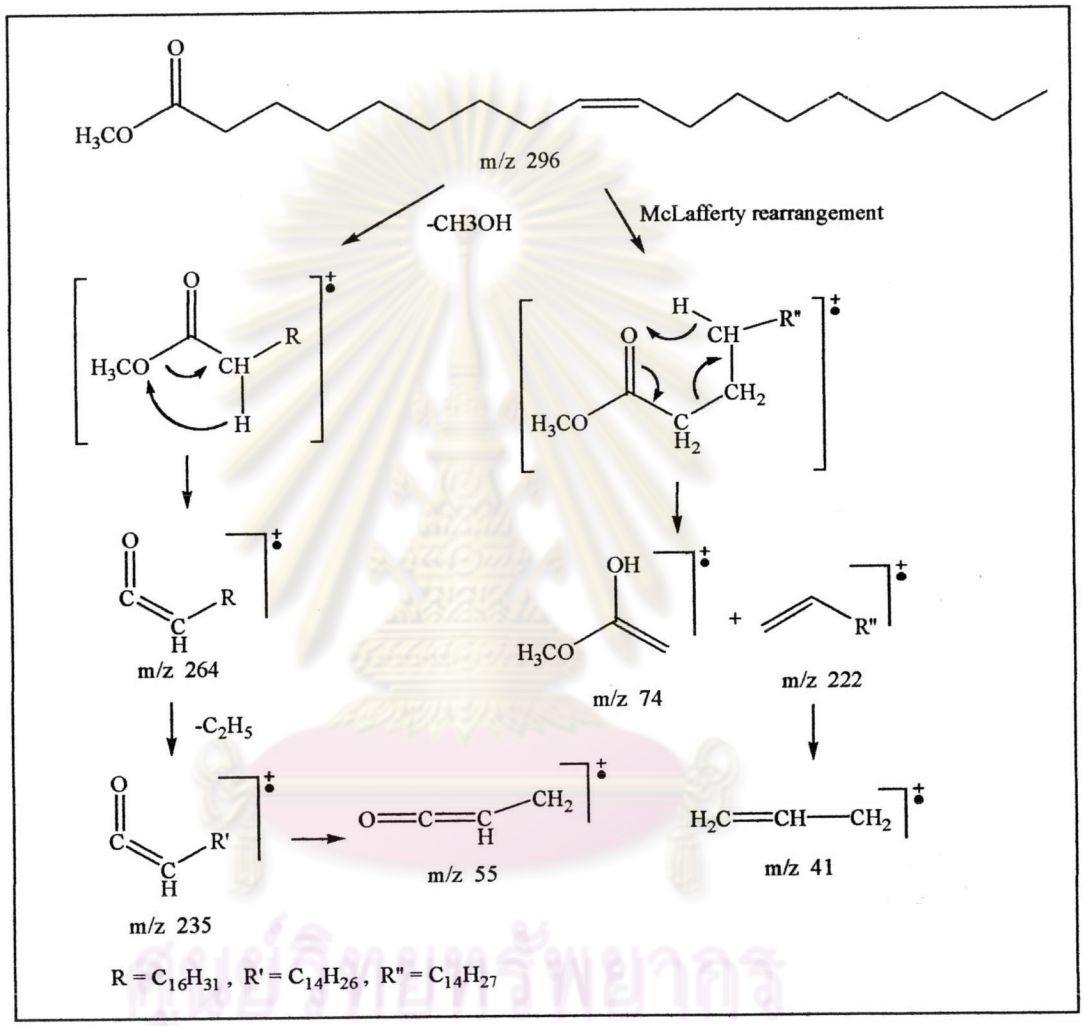

Scheme 3.2 The mass fragmentation pattern of cis-9-octadecenoic acid methyl ester

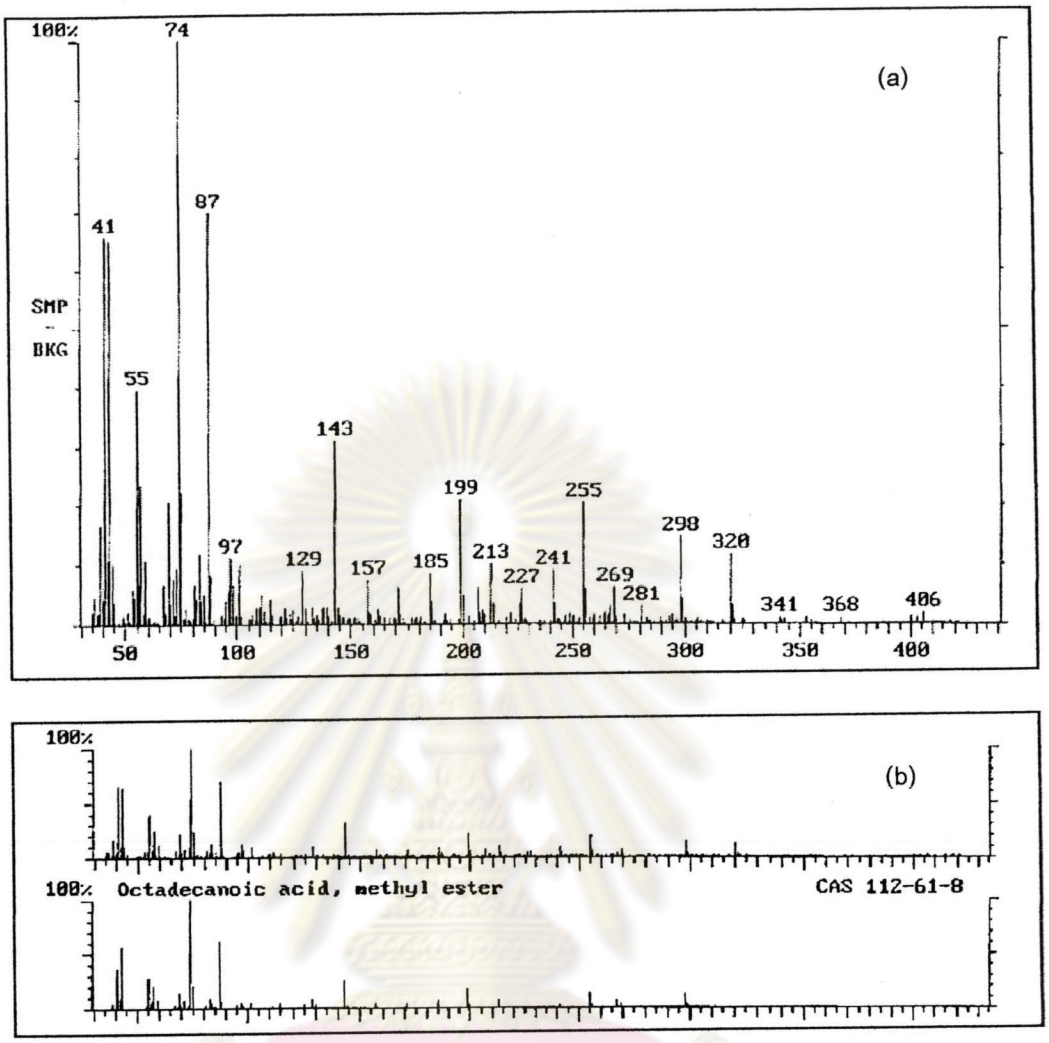

Figure 3.12 The mass spectrum of compound III (a) and library data of octadecanoic acid, methyl ester (b)

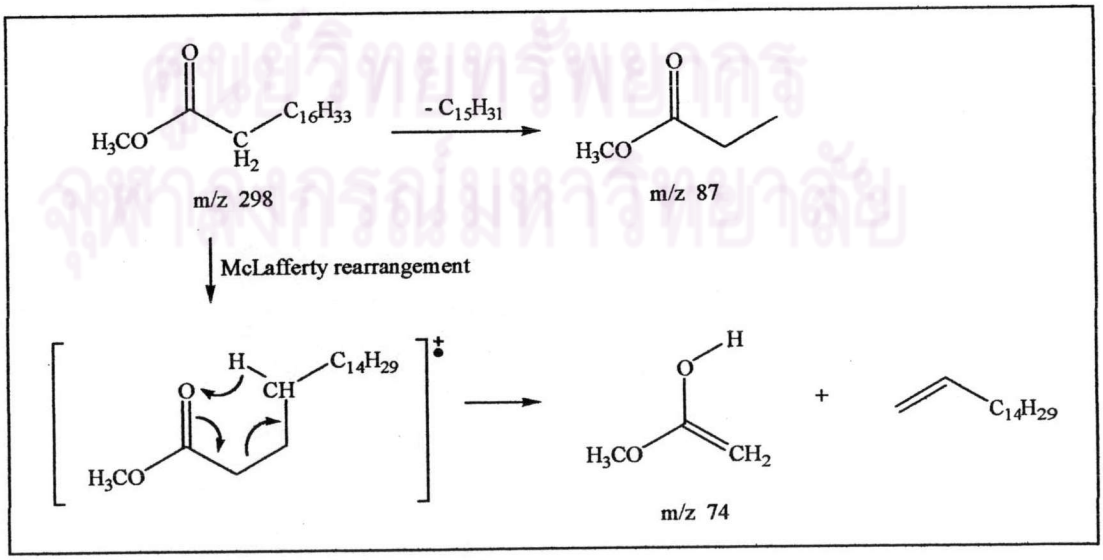

Scheme 3.3 The mass fragmentation pattern of octadecanoic acid, methyl ester

3.4.2 Structural Elucidation of Mixture 2

Colorless needle (127 mg) of mixture 2 with m.p. 126-129 °C and R_f = 0.60 (10% MeOH/CH_2Cl_2) was obtained by a treatment of subfraction E of dichloromethane crude extract using 1:3 EtOAc/CH_2Cl_2 as an eluting solvent. This substance cannot be detected on TLC under UV light, but detecting with 10% H_2SO_4 in ethanol showed pink spot. It gave a deep green color with Liebermann-Burchard's reagent suggesting the presence of steroid skeleton.

From above data , it could be suggested that the colorless needle may be β-sitosterol, stigmasterol or a mixture of steroids, the common steroid that found in plants. Due to the same R_f of two steroids on TLC, then comparison with authentic steroid on TLC could not give useful information. GC technique was then used to confirm.

The GC chromatogram(Figure 3.13, SE-30 column (2 m × 3.3 mm i.d., 5% film thickness), injection temperature 290 °C, column temperature 260 °C, carrier gas N_2, FID detector temperature 290 °C) displayed two peaks with retention time of 24.59 and 28.20 minutes which corresponded to those of an authentic stigmasterol and β-sitosterol, respectively.

The EI mass spectrum (Figure 3.14) showed molecular ion peaks, M^+, of the mixture at m/z 412 and 414 agreeable with stigmasterol and β-sitosterol.

Then it could be determined that Mixture 2 consisted of stigmasterol and β-sitosterol.

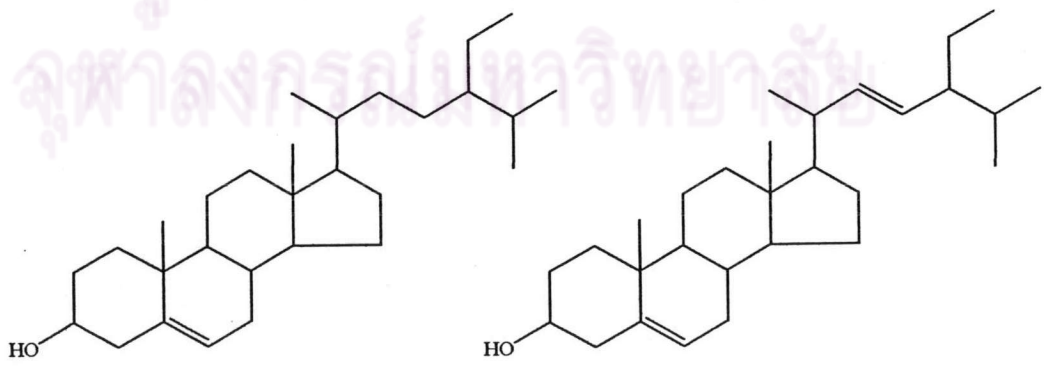

β-sitosterol stigmasterol

Mixture 2

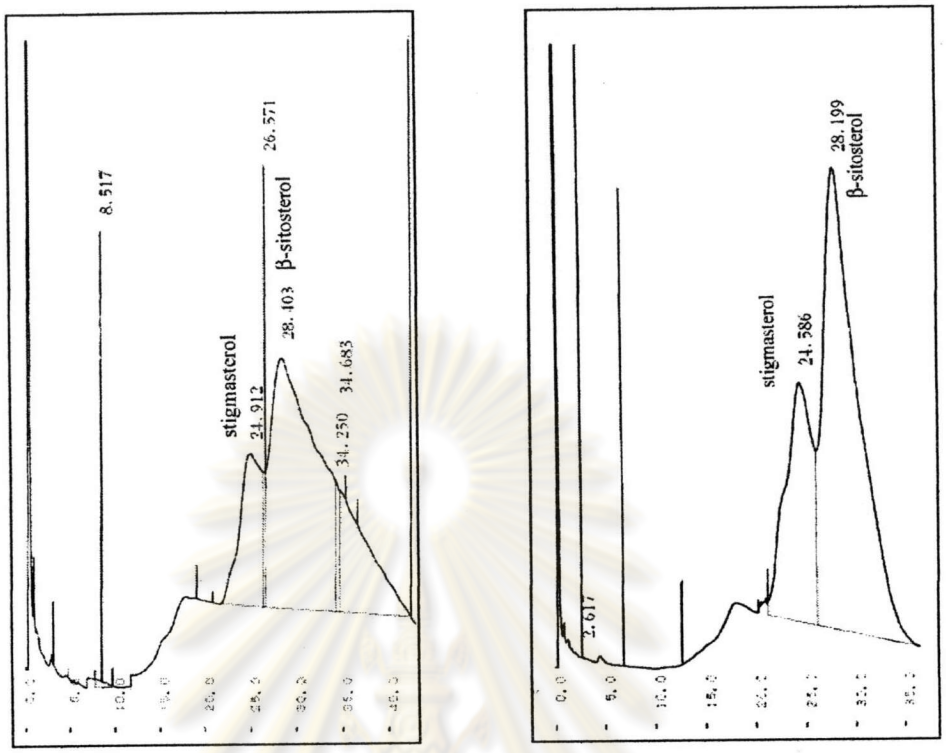

(a) **(b)**

Figure 3.13 Chromatogram of (a) standard steroids and (b) mixture 2

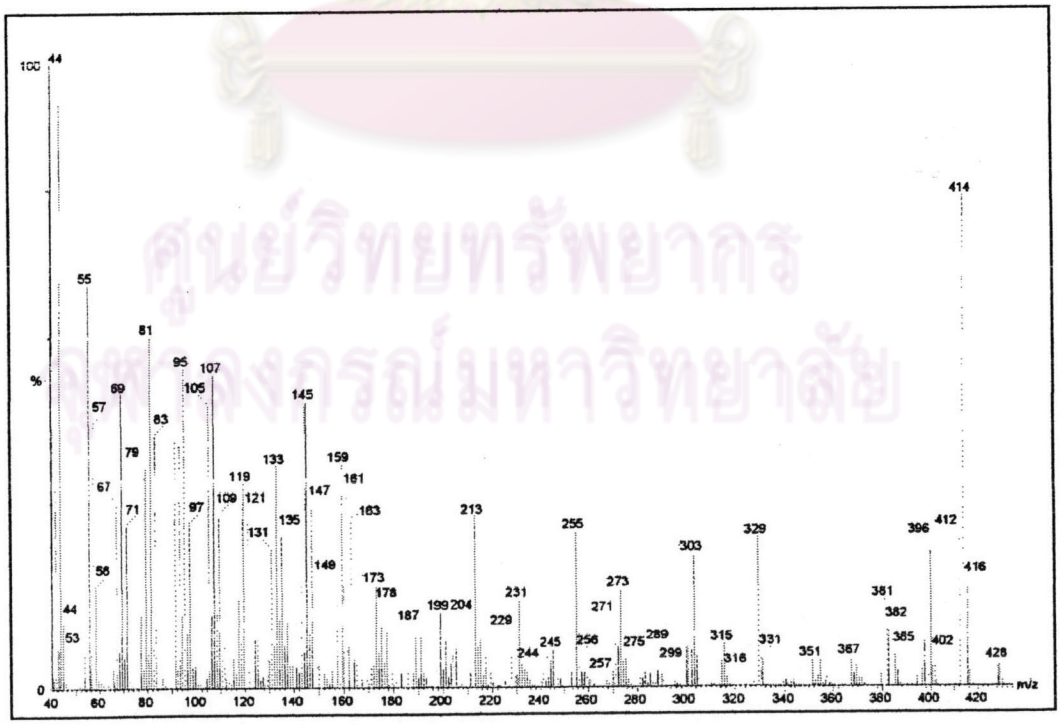

Figure 3.14 The EI mass spectrum of mixture 2

3.4.3 Structural Elucidation of Compound 1

White powder (273 mg) of compound 1 was procured from subfraction F of dichloromethane crude extract. After several recrystallization in hot 1:1 MeOH/CH_2Cl_2, a white powder which m.p. 264-267 °C (dec.) and R_f 0.46 (SiO_2 1:4 MeOH/CH_2Cl_2), was formed. From two properties of this compound, soluble in hot methanol and UV-inactive character, implied that it seemed to be a steroid or a triterpenoid glycoside. Therefore, it gave positive results (deep green color) with Liebermann-Burchard's reagent which indicated that it was composed of steroidal skeleton.

The IR spectrum of compound 1 (Figure 3.15) showed important absorption bands at V_{max} 3436 cm^{-1}(O-H stretching due to hydroxy group of sugar), 1636 cm^{-1}(C=C stretching vibration of olefin), 1078 cm^{-1}(C-O stretching vibration of glycoside linkage) and 897 cm^{-1}(C-H bending vibration of anomeric axial proton of β-sugar).

The mass spectrum (Figure 3.16) did not show the molecular peak of this compound because the sugar was lost. The peak at m/z 412 indicated (M^+) of stigmasterol moiety. Other fragments at m/z 396, 255, 213 were similar to the fragmentation pattern of stigmasterol.

The ^{1}H-NMR spectrum (Figure 3.17) showed signals at 0.65-2.0 ppm which were the signal of methyl (-CH_3), methylene (-CH_2) and methine (-CH) groups of steroids. The group of multiplet signal between 2.90-3.67 ppm was the signals of sugar moiety while an anomeric proton at 4.23 ppm(1H, d, J = 8.2 Hz) could allude to the β–anomer of sugar. The last signal at 5.33 ppm was the signal of olefinic proton (-CH=C).

The ^{13}C-NMR of compound 1 (Figure 3.18) comparison with the ^{13}C-NMR spectrum of stigmasterol (Table 3.8) was corresponded to stigmasterol. In addition a group of six carbon signals resonated at δ 100.9, 77.0, 76.8, 73.5, 70.3 and 61.3 ppm exactly resembled to a distinctive manner of D-glucose.

According to the above results and comparison with literature data indicated that compound 1 was stigmasteryl-3-O-β-D-glucopyranoside.

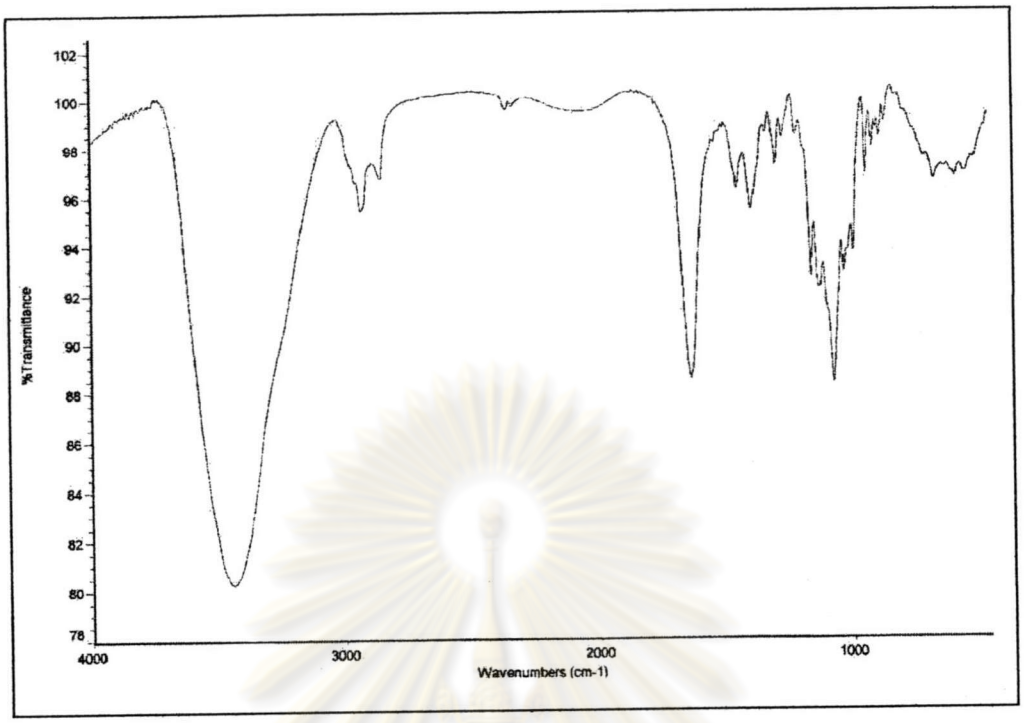

Figure 3.15 The IR spectrum of compound 1

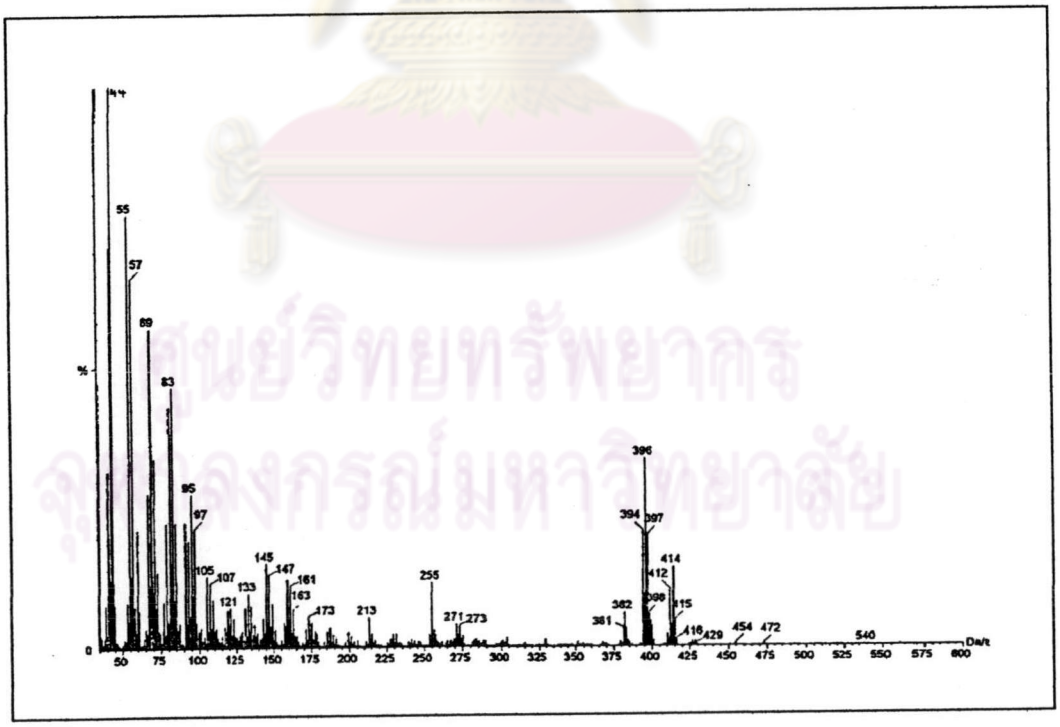

Figure 3.16 The EI mass spectrum of compound 1

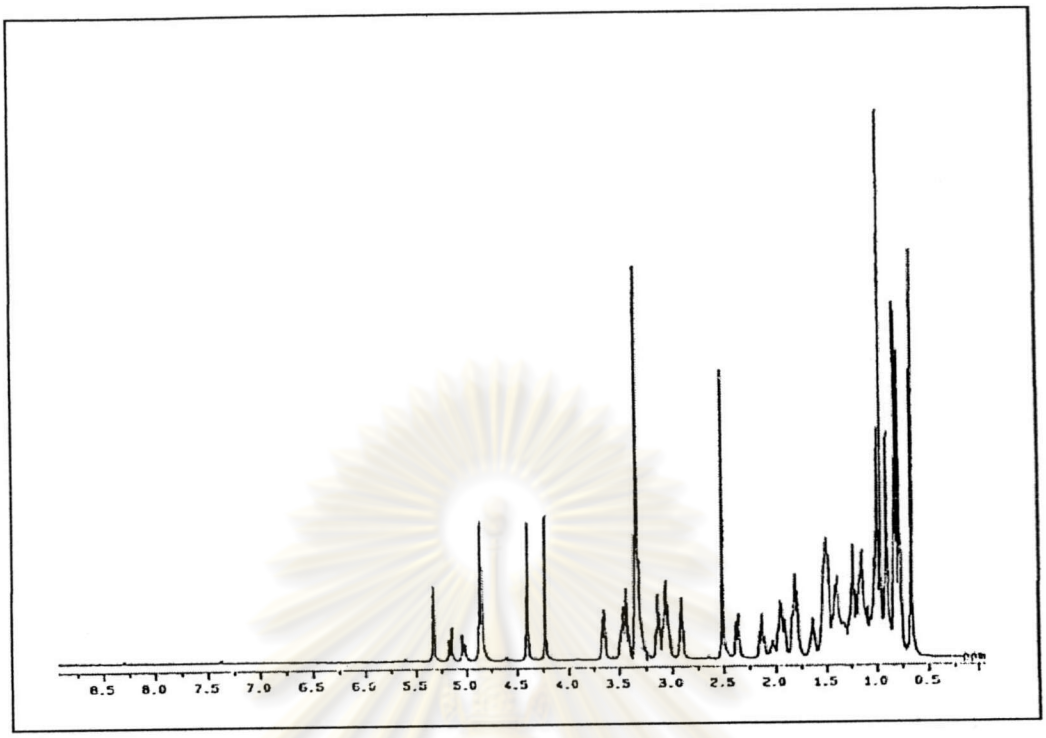

Figure 3.17 The ^{1}H-NMR spectrum (DMSO-d_6) of compound 1

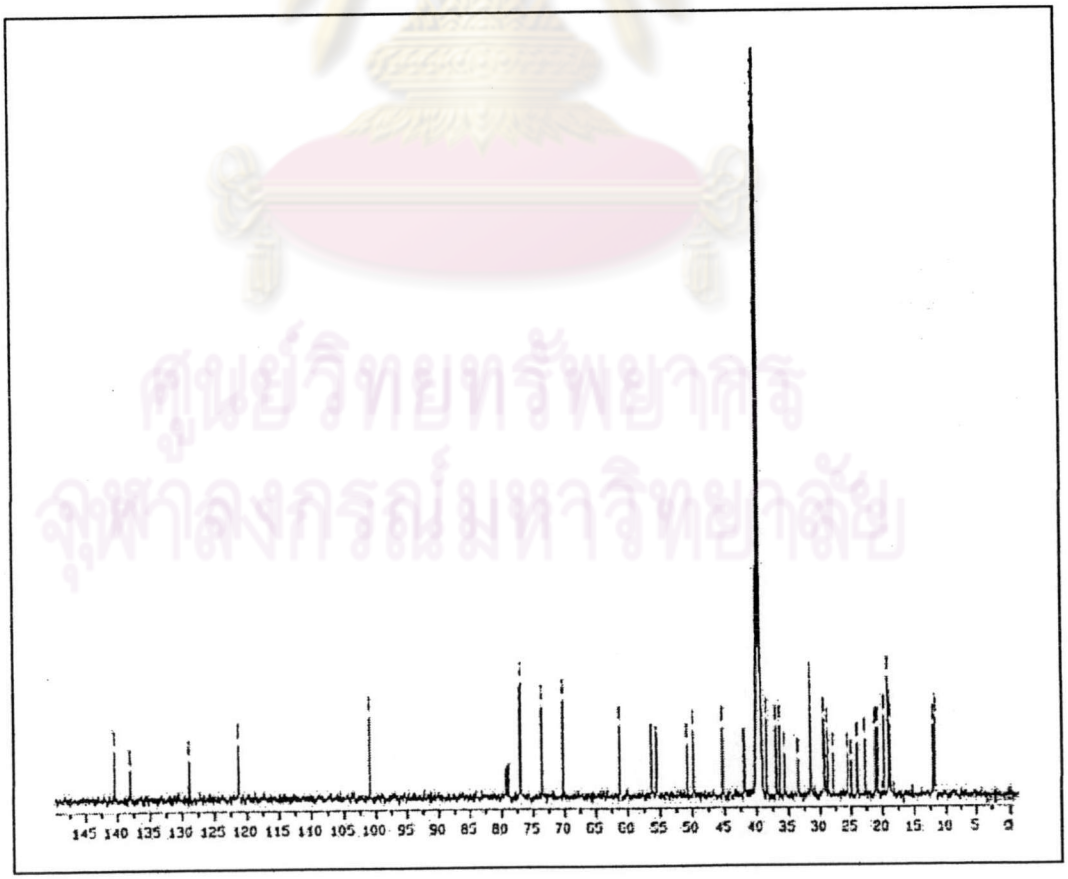

Figure 3.18 The ^{13}C-NMR spectrum (DMSO-d_6) of compound 1

Table 3.8 ^{13}C-NMR assignment of compound 1 and stigmasteryl-3-O–β–D-glucopyranoside[30]

Carbon	Chemical shift (ppm)	
	Compound 1	stigmasteryl-3-O–β–D-glucopyranoside
1	36.9	37.4
2	29.7	31.7
3	70.2	71.8
4	41.4	42.4
5	140.5	140.0
6	121.3	121.7
7	31.5	31.9
8	31.5	31.9
9	50.7	50.3
10	36.1	36.6
11	21.0	21.1
12	38.7	39.8
13	41.9	42.4
14	56.5	57.0
15	24.7	24.4
16	28.8	28.9
17	56.3	56.0
18	12.2	12.2
19	19.8	19.4
20	41.5	40.5
21	20.8	21.1
22	138.1	138.4
23	129.8	129.4

Table 3.8 (cont.) ^{13}C-NMR assignment of compound 1 and stigmasteryl-3-O–β–D-glucopyranoside

Carbon	Chemical shift (ppm)	
	Compound 1	stigmasteryl-3-O–β–D-glucopyranoside
24	51.6	51.3
25	31.5	31.9
26	19.3	19.0
27	20.7	21.1
28	25.6	25.4
29	11.6	12.0

Table 3.9 ^{13}C-NMR assignment of sugar moiety of compound 1 and glucose

Carbon	Chemical shift (ppm)	
	Compound 1	Glucose
1	100.9	100.7
2	73.5	73.4
3	77.0	77.0
4	70.3	70.1
5	76.8	76.7
6	61.3	61.1

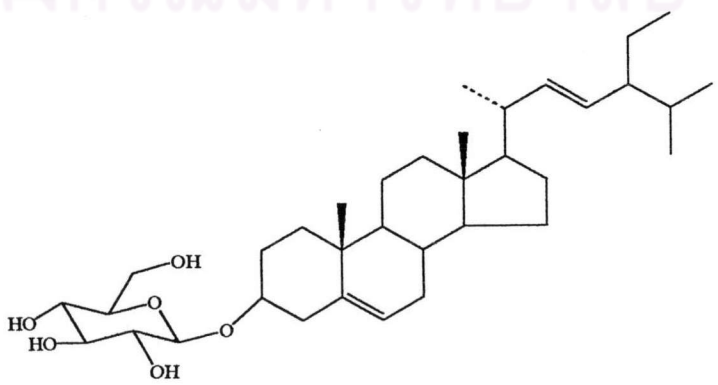

Compound 1 : Stigmasteryl-3-O-β-D-glucopyranoside

3.4.4 Structural Elucidation of Compound 2

Compound 2 (9 mg) was obtained as white amorphous solid, m.p. 292-295 °C (lit. >300 °C)[31] from subfraction E and F of dichloromethane crude extract. It was separated by column chromatography (silica gel, 80% EtOAc-CH_2Cl_2) and then repurified by HPLC (C_{18} reversed- phase, 20% H_2O-MeOH). It gave positive test, violet color, with Libermann-Burchard reagent, indicative of a triterpenoidal skeleton in this compound.

The IR spectrum (Figure 3.19) exhibited significant absorption bands at V_{max} 3439 cm^{-1} (O-H stretching), 2945 and 2847 cm^{-1} (C-H stretching), 1682 cm^{-1} (C=O stretching), 1621 cm^{-1} (C=C stretching), 1469, 1373 cm^{-1} (CH_2, CH_3 bending) and 1239 cm^{-1} (C-O stretching).

The EI mass spectrum of compound 2 (Figure 3.20) revealed a molecular ion at m/z 456, which corresponds to the molecular formula $C_{30}H_{48}O_3$ (Calcd. for $C_{30}H_{48}O_3$: MW 456.70). A base peak at m/z 248 is typical for α- or β-type triterpenes. The fundamental difference between the two triterpenes is at C-29 and C-30 of the ring E. In the α type triterpene, both methyl groups at ring E connected to C-19 and C-20 whereas in the β type the two methyl groups attached to C-20. The mass fragmentation pattern of compound 2 is shown in Scheme 3.4.

The ^{1}H-NMR spectrum (Figure 3.21) displayed methyl signal at δ 0.73-1.12 ppm. A multiplet at 5.27 ppm was assigned to the olefinic proton of C-12. A doublet of doublet signal at 2.84 ppm which a *J* value of 13.7 and 3.5 Hz indicated that this compound was of the β-type triterpene because two protons were attached to C-19. On the other hand, if this compound was of the α-type triterpene (whereby hydrogen and methyl group are attached to C-19) the coupling between proton at C-18 and C-19 would be a doublet.

The ^{13}C-NMR spectrum (Figure 3.22) showed the presence of 30 carbon signals. The signal at δ 180.1 indicated that compound 2 has carboxylic acid unit in the molecule. Furthermore, signal at δ 143.6 and 123.4 implied methine carbons.

From literature surveys, α-amyrin and β-amyrin have been isolated from this plant. By comparing the ^{1}H and ^{13}C-NMR spectra of compound 2 with, β-amyrin and its derivatives, compound 2 was identified as oleanolic acid [(3β)-3-

hydroxyolean-12-en-28-oic acid]. The carbon assignment of compound 2 and oleanolic acid are presented in Table 3.10.

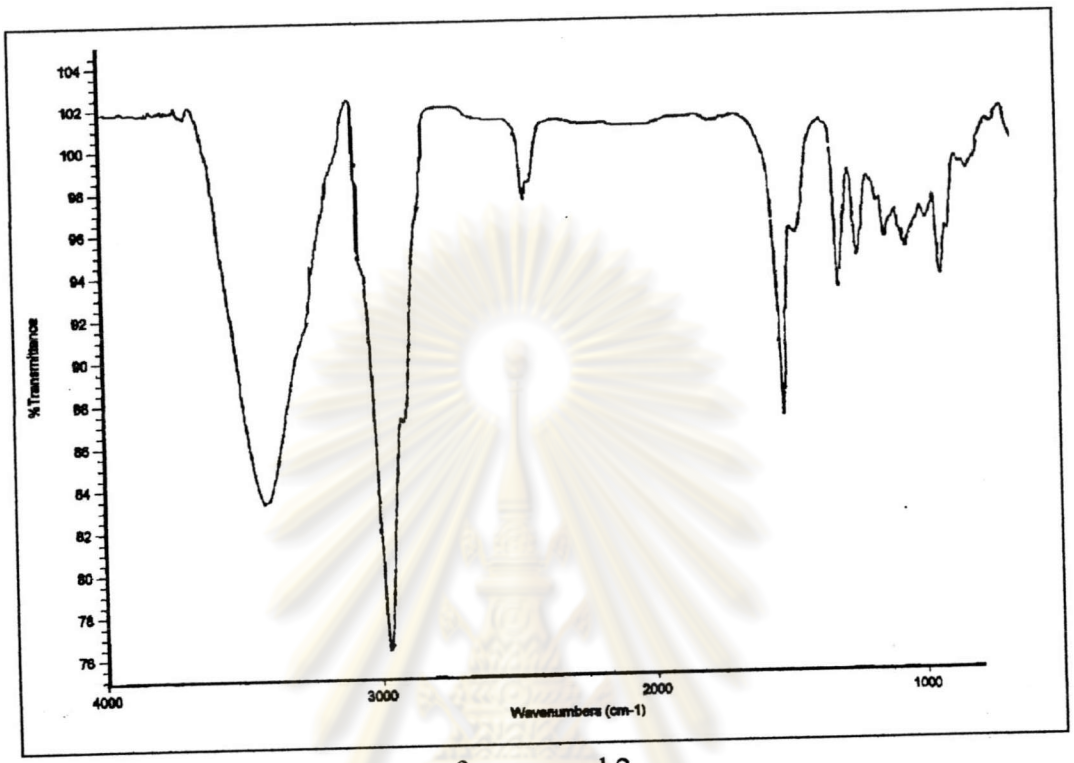

Figure 3.19 The IR spectrum of compound 2

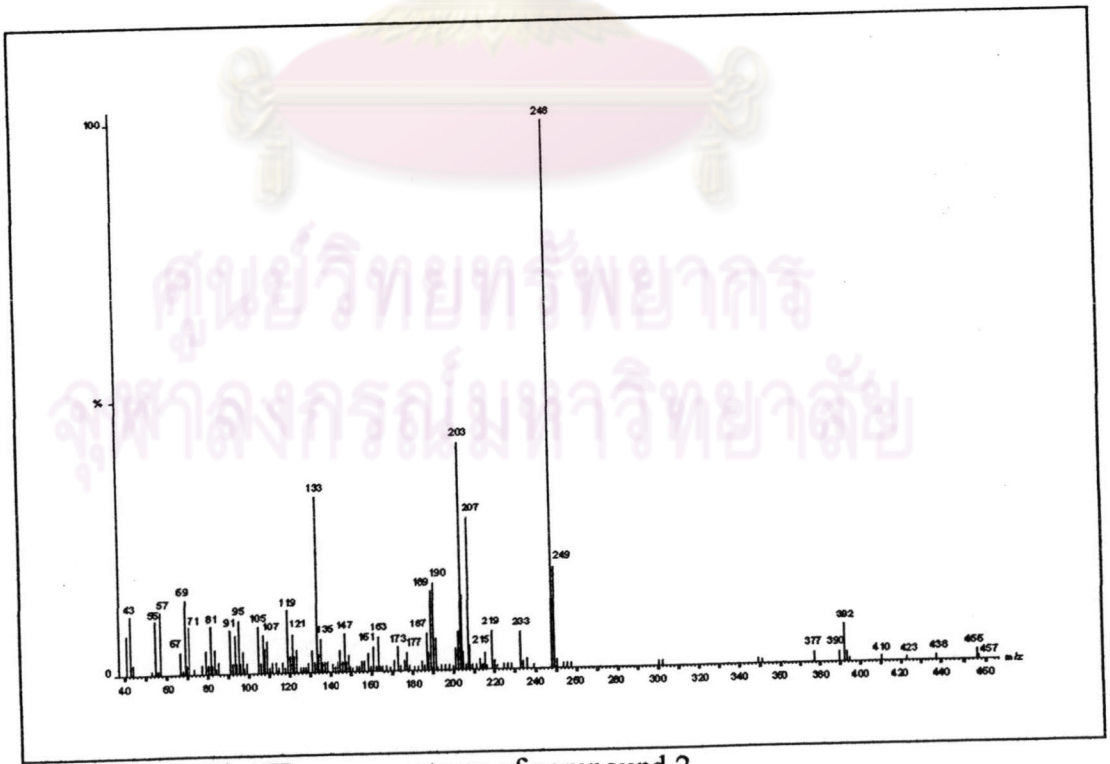

Figure 3.20 The EI mass spectrum of compound 2

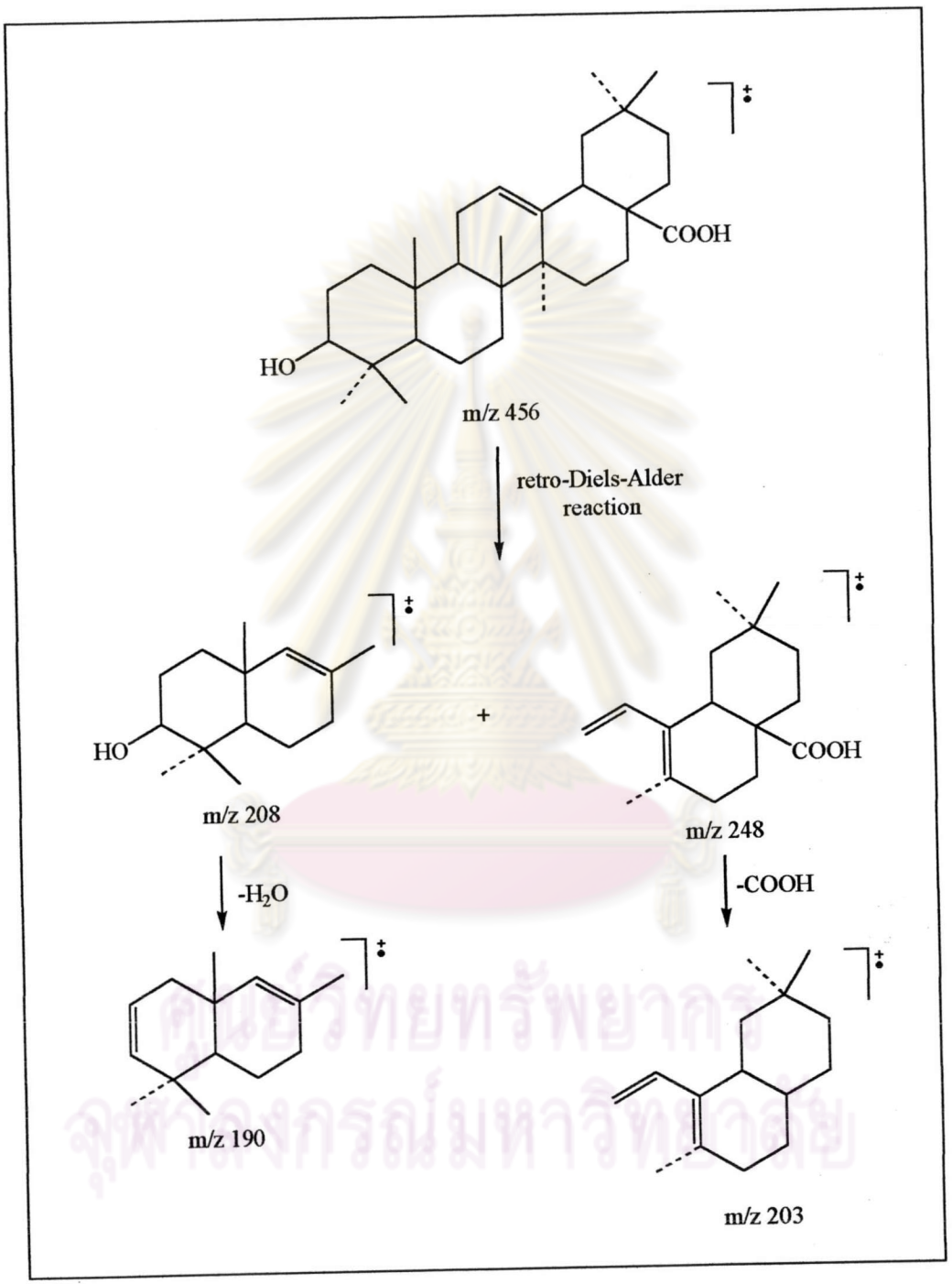

Scheme 3.4 The mass fragmentation pattern of compound 2

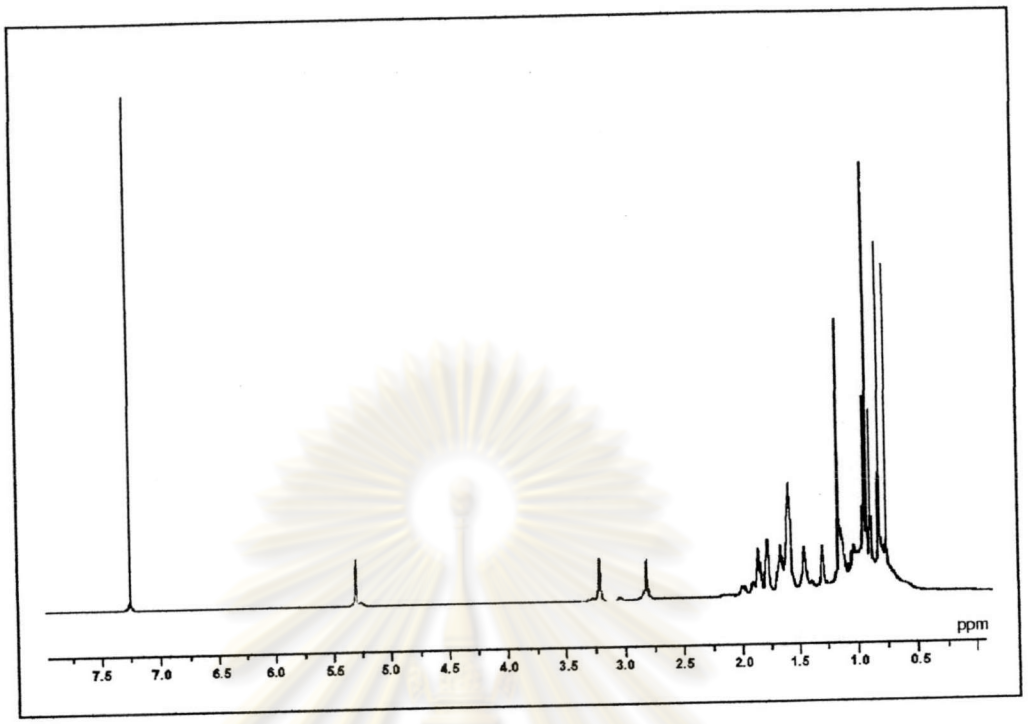

Figure 3.21 The ^{1}H-NMR spectrum ($CDCl_3$) of compound 2

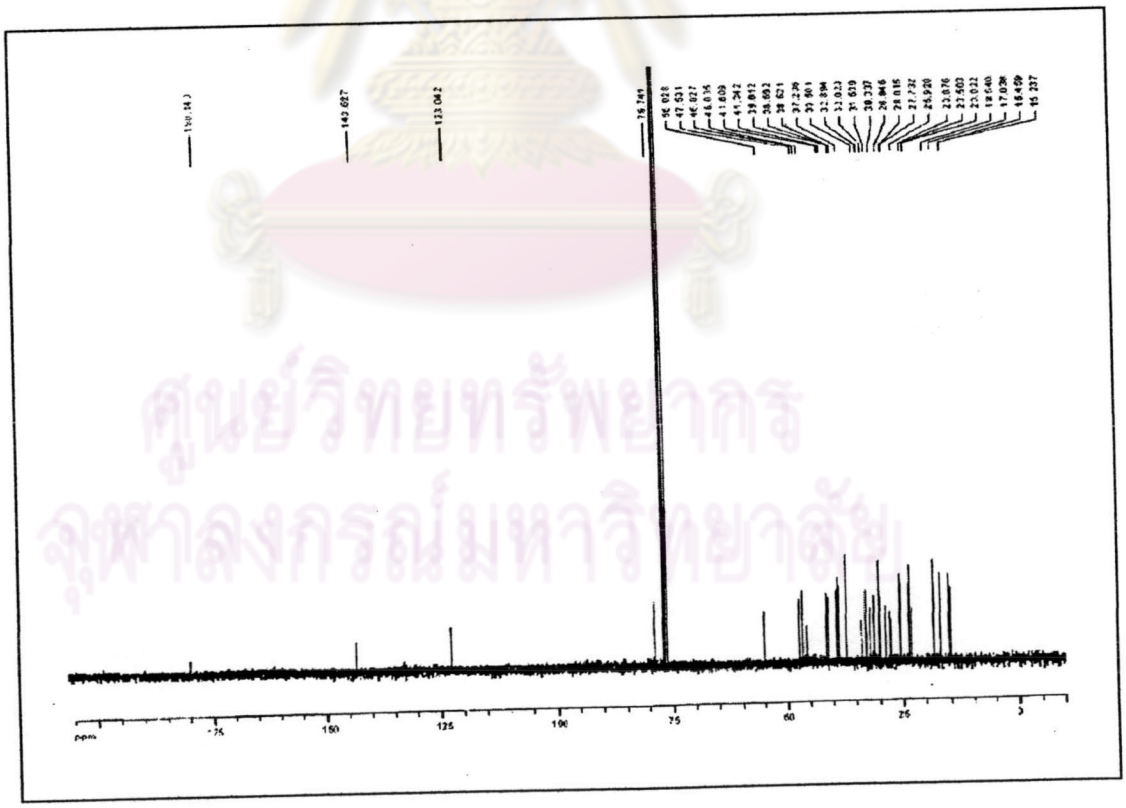

Figure 3.22 The ^{13}C-NMR spectrum (CDCl3) of compound 2

Table 3.10 The ^{13}C-NMR chemical shift of compound 2 and oleanolic acid[31] (in $CDCl_3$)

Carbon	Chemical shift (ppm)		Carbon	Chemical shift (ppm)	
	Compound 2	Oleanolic acid		Compound 2	Oleanolic acid
1	37.89	38.62	16	23.73	23.50
2	26.12	25.93	17	46.68	46.83
3	79.08	78.74	18	39.46	41.34
4	39.2	38.69	19	45.05	46.04
5	55.39	55.03	20	32.48	31.54
6	18.44	18.54	21	33.28	33.50
7	32.99	32.02	22	28.23	28.45
8	39.42	39.02	23	30.84	30.34
9	46.73	47.53	24	15.50	15.24
10	34.17	37.24	25	15.63	15.42
11	23.09	23.02	26	17.16	17.04
12	122.80	123.04	27	26.99	27.73
13	143.20	143.63	28	182.23	180.14
14	41.08	41.61	29	33.05	32.89
15	28.12	28.02	30	23.87	23.88

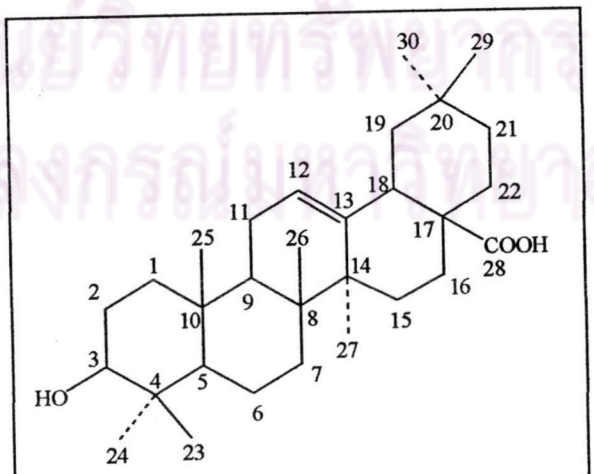

Compound 2 : Oleanolic acid

3.4.5 Structural Elucidation of Compound 3

Compound 3 (13 mg) was obtained from the same fraction with compound 2 as white amorphous solid, m.p 270-272 °C (lit. 266-267°C)[32]. It was eluted after compound 2 by HPLC (C_{18} reversed-phase, 20% H_2O-MeOH). It gave positive results (violet color) with Libermann-Burchard reagent which indicated that it was composed of triterpenoidal skeleton.

The IR spectrum (Figure 3.23) showed significant absorption bands similar to compound 2, V_{max} 3441 cm^{-1}3439 (O-H stretching), 2949 cm^{-1} (sp^3 C-H stretching), 1697 cm^{-1} (C=O stretching), 1615 cm^{-1} (C=C stretching), 1469, 1373 cm^{-1} (CH_2, CH_3 bending) and 1239 cm^{-1} (C-O stretching).

The EI mass spectrum of compound 2 (Figure 3.24) exhibited a molecular ion at m/z 456 and the other important peak as same as compound 2, then compound 3 should be α- or β- triterpene derivatives. The mass fragmentation pattern of compound 3 is presented in Scheme 3.5.

The ^{1}H-NMR spectrum (Figure 3.25) of this compound showed a doublet signal at δ 2.21 (J = 11.3 Hz). It suggested that compound 2 was of the α-orientated triterpene.

The ^{13}C-NMR spectrum (Figure 3.26) showed the presence of 30 carbon signals. The signal at δ 139.0 and 126.3 implied methine carbon. Furthermore, the signal at δ 179.9 indicated that compound 3 had carboxylic acid unit in the molecule.

From above data, the compound 3 was close to that of compound 2. Expect for the splitting pattern of proton at C-19 (δ 2.21, 1H, d, J = 11.3 Hz), ^{13}C-NMR signals represented triterpenoid skeleton. It was suggested that compound 3 might be ursolic acid because the oleanolic acid rarely occurred without its isomer, ursolic acid. By comparison the ^{1}H and ^{13}C-NMR spectra of compound 3 with ursolic acid, compound 3 was determined as ursolic acid [(3β)-3-hydroxyurs-12-en-28-oic acid]. The carbon assignment of compound 3 and ursolic acid are shown in Table 3.11.

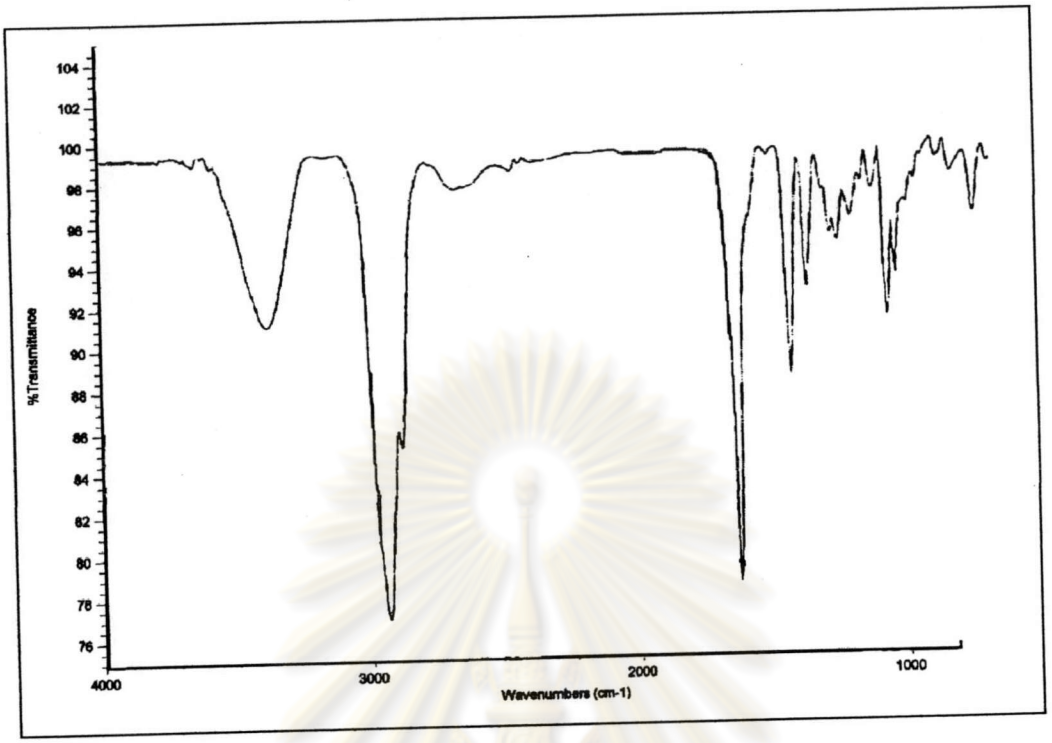

Figure 3.23 The IR spectrum of compound 3

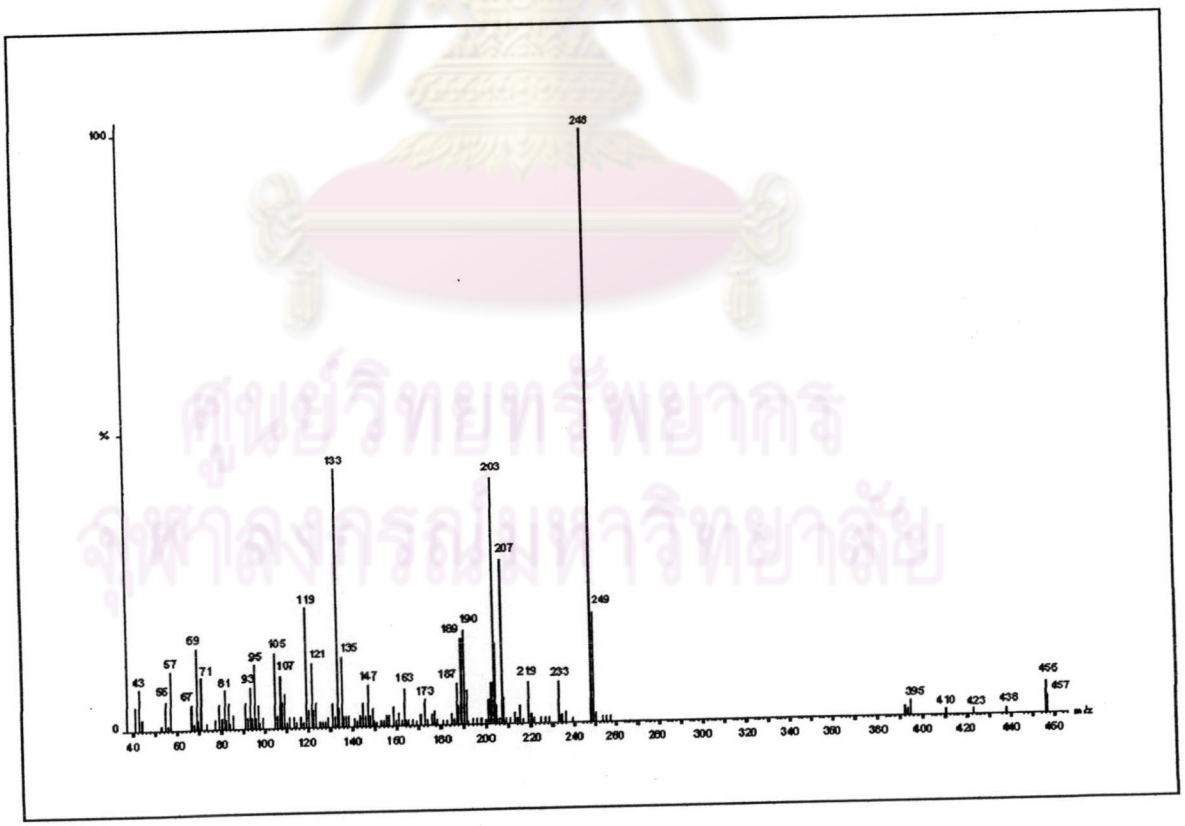

Figure 3.24 The EI mass spectrum of compound 3

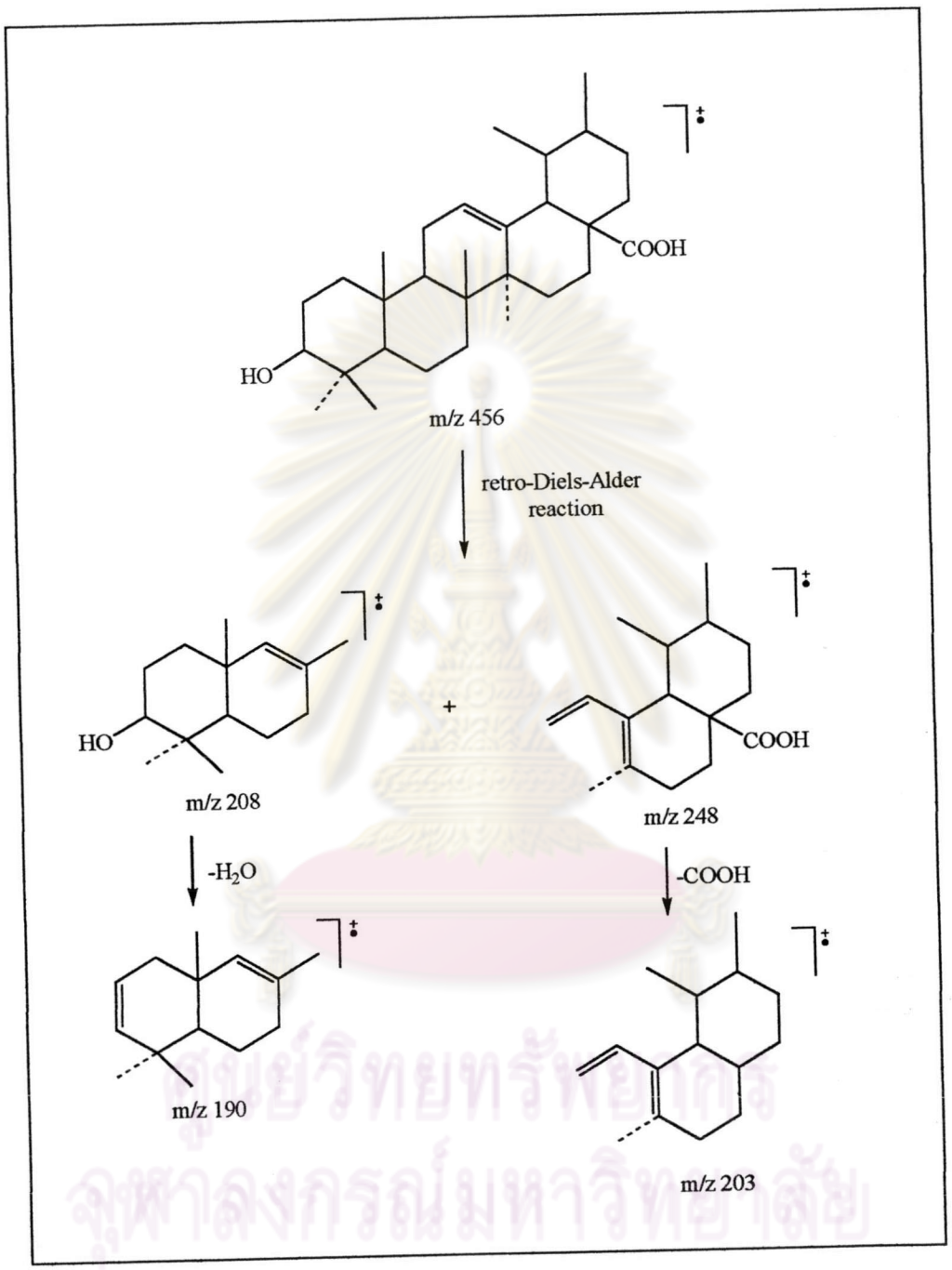

Scheme 3.5 The mass fragmentation pattern of compound 3

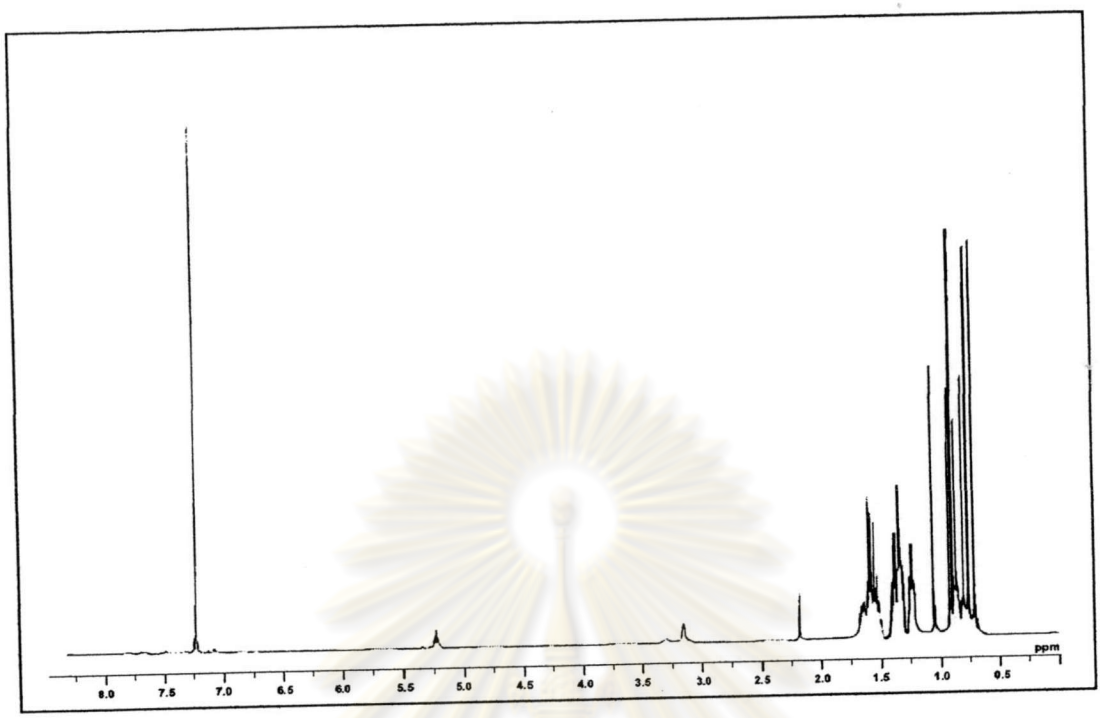

Figure 3.25 The ^{1}H-NMR spectrum ($CDCl_3$) of compound 3

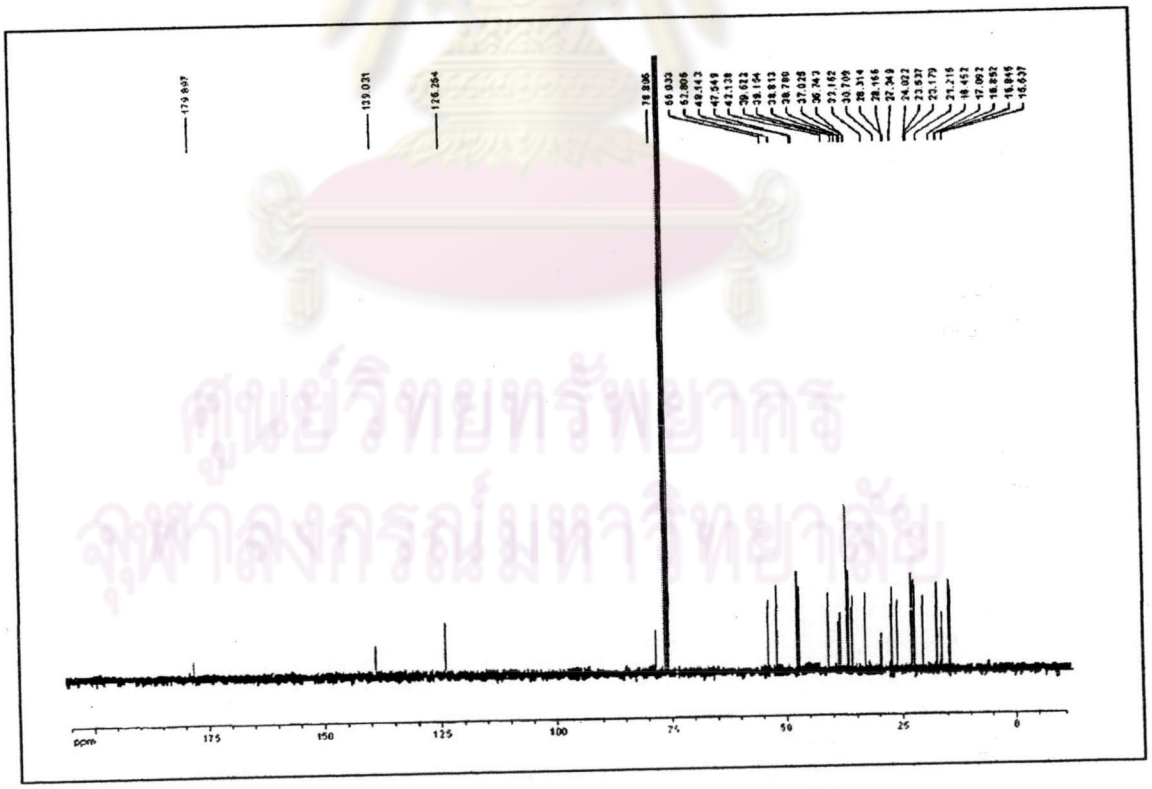

Figure 3.26 The ^{13}C-NMR spectrum ($CDCl_3$) of compound 3

Table 3.11 The ^{13}C-NMR chemical shift of compound 3 and ursolic acid[33] (in $CDCl_3$)

Carbon	Chemical shift (ppm)		Carbon	Chemical shift (ppm)	
	Compound 3	Ursolic acid		Compound 3	Ursolic acid
1	39.8	38.8	16	25.3	24
2	27.8	27.3	17	47.6	48.1
3	79.6	78.8	18	54.3	52.8
4	39.9	38.8	19	40.4	38.8
5	56.7	56	20	40.4	39.1
6	19.4	18.5	21	31.7	30.7
7	34.3	33.1	22	38.1	37
8	40.7	39.6	23	28.7	28.2
9	47.6	47.5	24	16	15.6
10	38.1	36.7	25	16.3	15.8
11	24.3	23.5	26	17.6	16.9
12	126.8	126.3	27	24	23.1
13	139.6	139	28	181.6	179.9
14	42.8	42.1	29	17.8	17.1
15	29.2	28.3	30	21.5	21.2

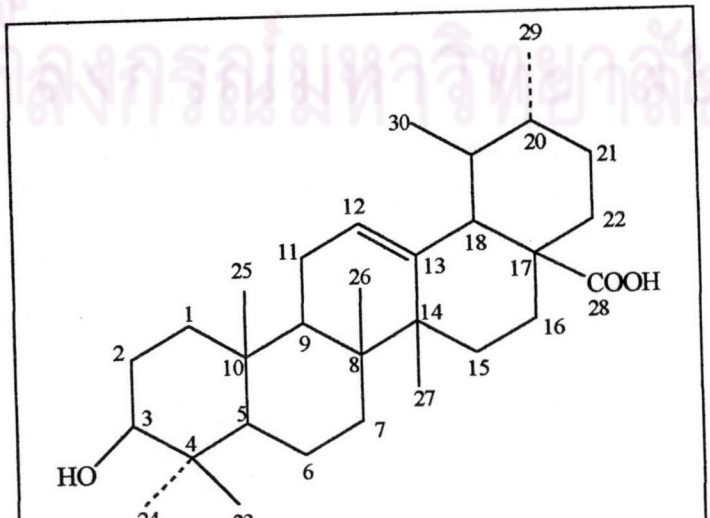

Compound 3: ursolic acid

3.4.6 Structural Elucidation of Compound 4

Compound 4 (475 mg), white needle, melting point 79-80 °C, was obtained from subfraction 3 of ethyl acetate crude extract. It was eluted with 3:7 EtOAc/CH_2Cl_2 on silica gel column chromatography and was recrystallized from 1:1 acetone/hexane.

The IR spectrum (Figure 3.27) showed distinguish absorption peak at V_{max} 3467 cm^{-1}(O-H stretching), 2929 and 2844 cm^{-1} (sp^3 C-H stretching), 1694 cm^{-1} (C=O stretching), 1467 cm^{-1} (CH_2 bending) and 1247 cm^{-1} (C-O stretching). From the IR spectrum, it was concluded that compound 4 should be a long chain carboxylic acid.

The EI mass spectrum (Figure 3.28) and collation with library data revealed that compound 4 was nonanedioic acid. It did not showed the molecular ion peak but afforded a $[M - 2H_2O]^+$ at m/z 152.

After methylation of this compound with trimethylsilyl diazomethane led to compound 4A, it was inspected by GC-MS analysis for determine the mixture component. The chromatogram of this derivative showed 1 component as in Figure 3.29.

The compound 4A had retention time at 6.78 min. Mass spectrum of this compound gave $[M+H]^+$ at m/z 217. From comparison with in library data, it was found to be a nonanedioic acid, dimethyl ester (Calcd. For $C_{11}H_{20}O_4$: MW 216.28) The mass spectrum of this compound and library data of nonanedioic acid, dimethyl ester are shown in Figure 3.30. The mass fragmentation pattern of nonananedioic acid, dimethyl ester is presented in Scheme 3.6.

Additional information was obtained from ^{1}H-NMR spectrum (Figure 3.31). It revealed the signals at δ1.35 (*m*, 6H, H-4, H-5, H-6), δ1.58 (*m*, 4H, H-3, H-7) and δ2.27 (*t*, *J* = 7 Hz, 4H, H-2, H-8).

Therefore, it was clear to conclude that compound 4 was nonanedioic acid or azelaic acid.

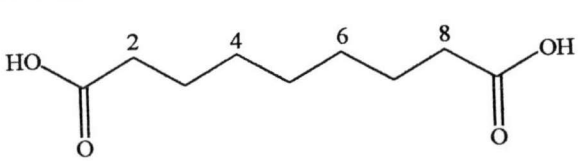

Compound 4 : Nonanedioic acid or Azelaic acid

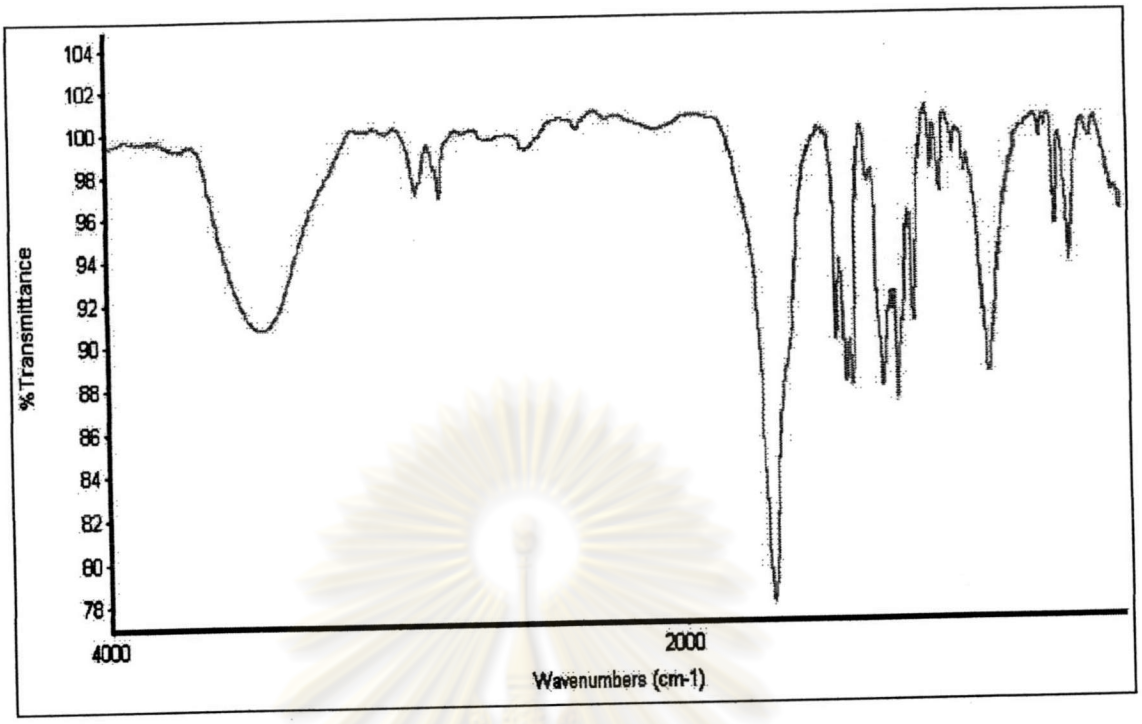

Figure 3.27 The IR spectrum of compound 4

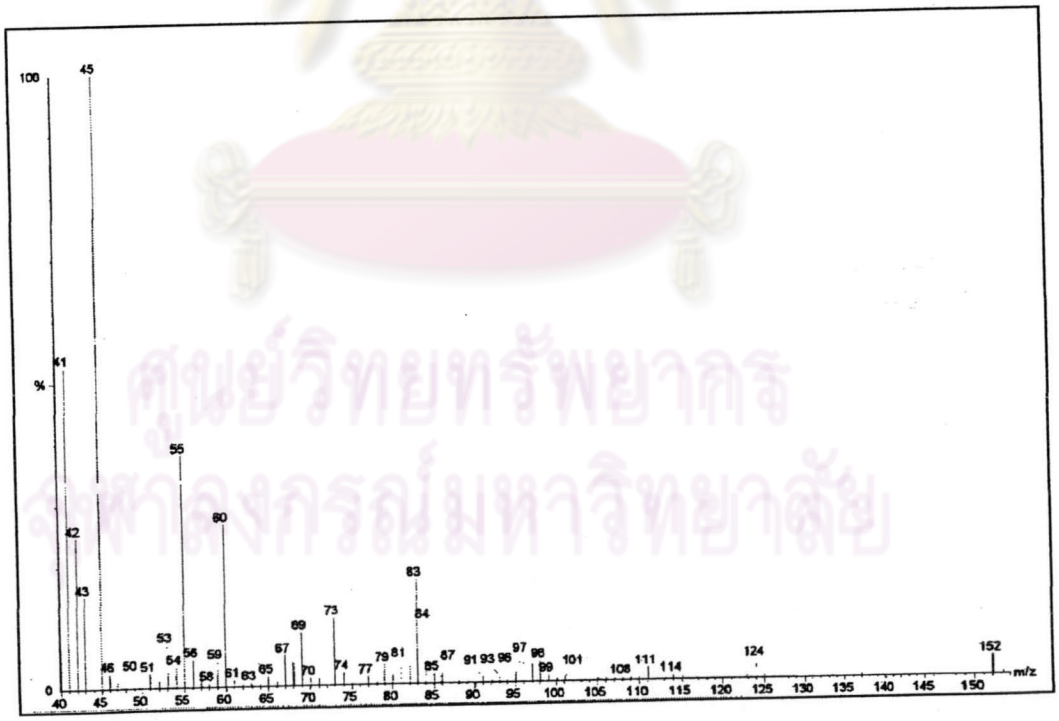

Figure 3.28 The EI mass spectrum of compound 4

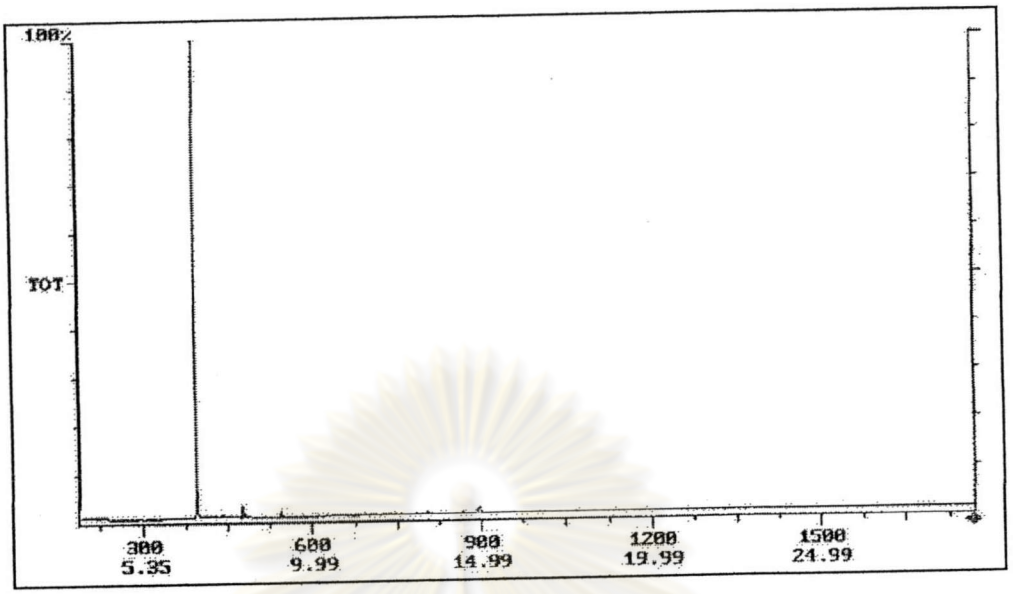

Figure 3.29 The GC chromatogram of compound 4A

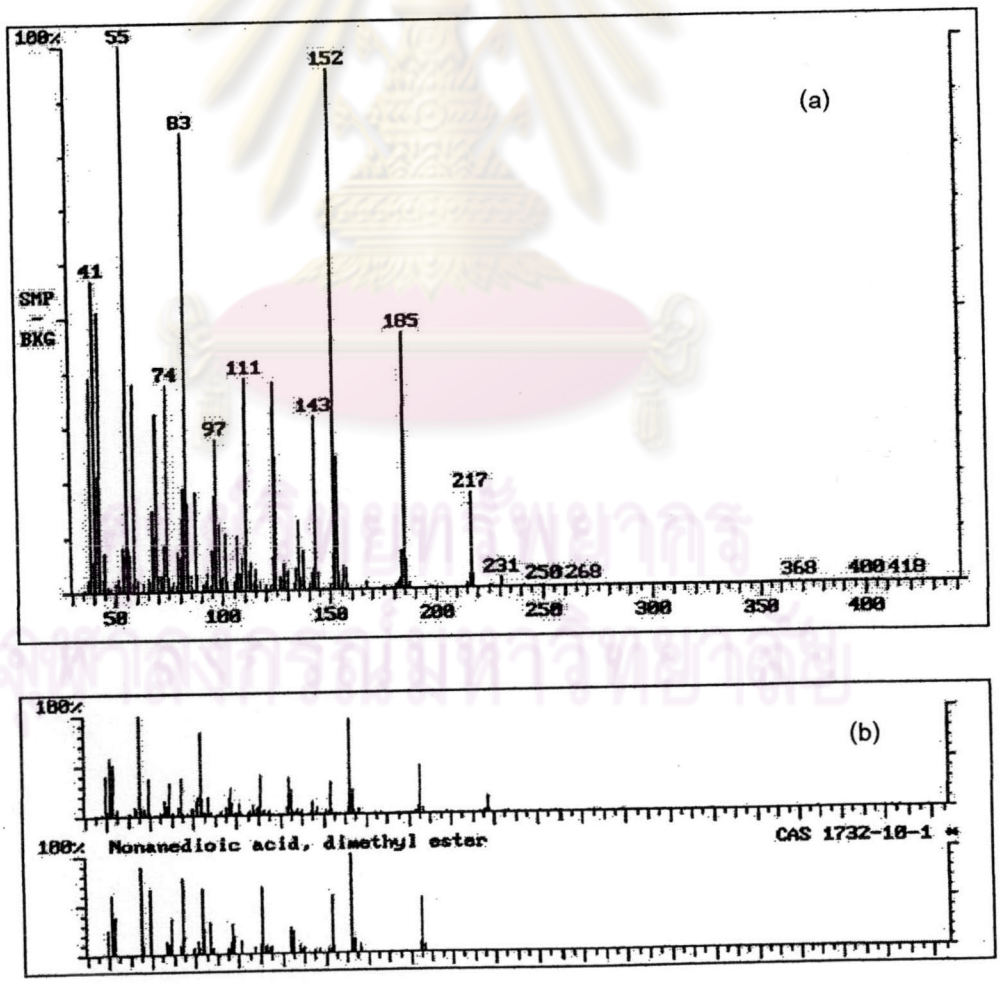

Figure 3.30 The mass spectrum of compound 4A (a) and the library data of nonanedioic acid (b)

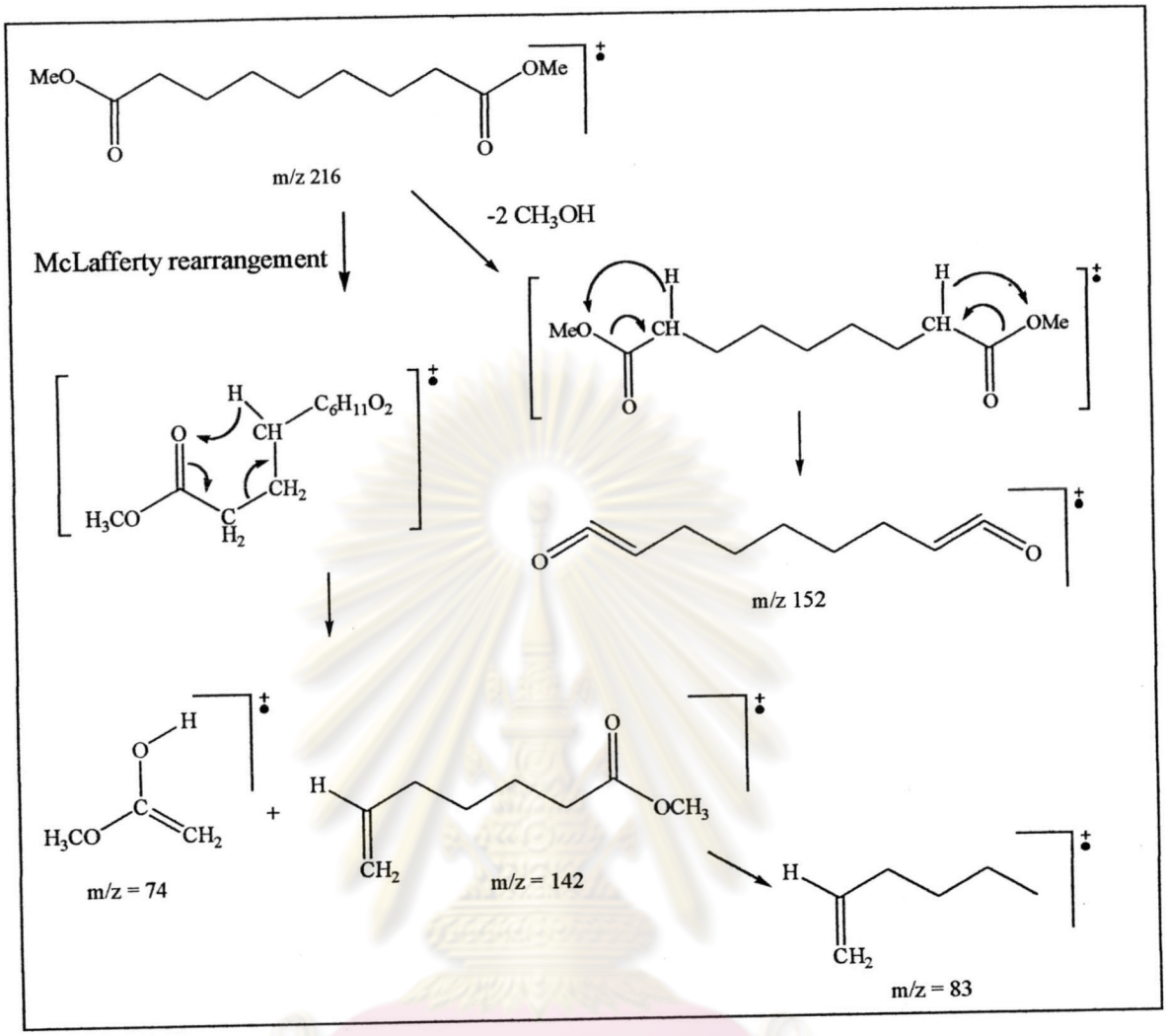

Scheme 3.6 The mass fragmentation pattern of nonanedioic acid dimethyl ester

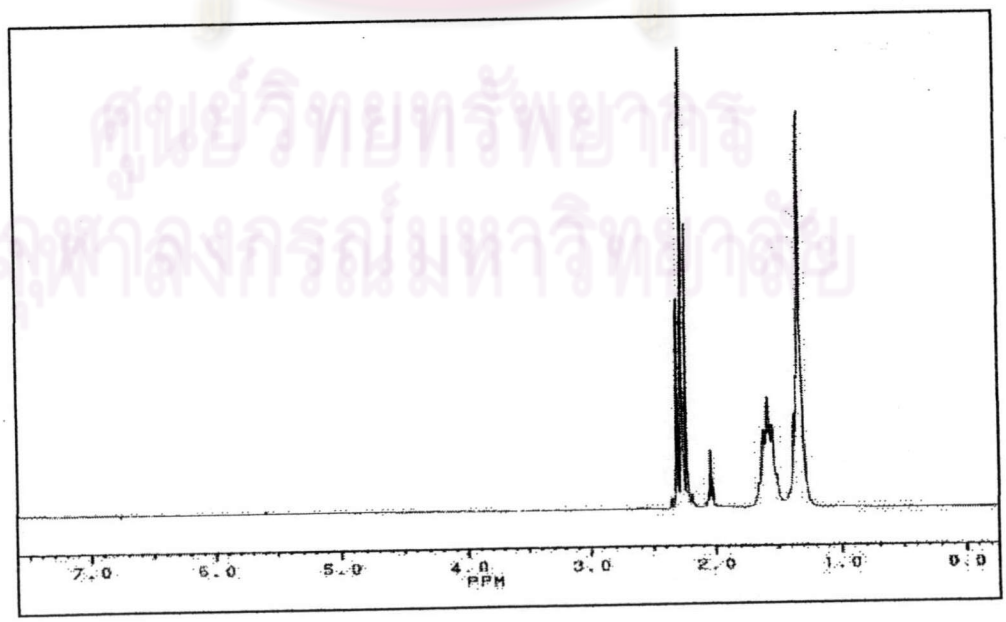

Figure 3.31 The ^{1}H-NMR spectrum (acetone-d_6) of compound 4

3.4.7 Structural Elucidation of Compound 5

Compound 5 was achieved from the same fraction with compound 4 (subfraction 3 of ethyl acetate crude extract) and was eluted by 7:13 $EtOAc/CH_2Cl_2$ on column chromatography. The appearance of compound 5 is similar to compound 4 as white needle, the melting point of compound 5 was 96-99 °C.

The IR spectrum of compound 5 (Figure 3.32) was similar to those IR spectrum of compound 4, V_{max} 3444 cm^{-1}(O-H stretching), 2925 and 2845 cm^{-1} (sp^3 C-H stretching), 1697 cm^{-1} (C=O stretching), 1463 cm^{-1} (CH^2 bending) and 1243 cm^{-1} (C-O stretching). Then, compound 5 should be a long chain carboxylic acid.

The comparison with library data of EI mass spectrum of this compound found that compound 5 was decanedioic acid. It showed the mass fragment ion $[M-2H_2O]^+$ at m/z 166. The EI mass spectrum of compound 5 and the library data of decanedioic acid are displayed in Figure 3.33.

Methylation of compound 5 was resembled with compound 4 and determined by GC-MS analysis. The chromatogram of this derivative showed 1 component as in Figure 3.34.

The methyl ester of this compound (5A) had retention time at 6.87 min. Mass spectrum of this compound gave $[M+H]^+$ at m/z 231. It was decanedioic acid, dimethyl ester (Calcd. for $C_{12}H_{22}O_4$: MW 230.30) from the basis of library data, the mass spectrum of this compound and in library data of decanedioic acid, dimethyl ester are shown in Figure 3.35. The mass fragmentation pattern of decananedioic acid, dimethyl ester was also presented in Scheme 3.7.

In addition, another information was fulfilled from ^{1}H-NMR spectrum (Figure 3.36). It exposed the signals at δ1.31 (*m*, 8H, H-4, H-5, H-6, H-7), δ1.62 (*m*, 4H, H-3, H-8) and δ2.33 (*t*, *J* = 7.3 Hz, 4H, H-2, H-9).

From all above evidences, compound 5 was deduced as decanedioic acid or sebacic acid.

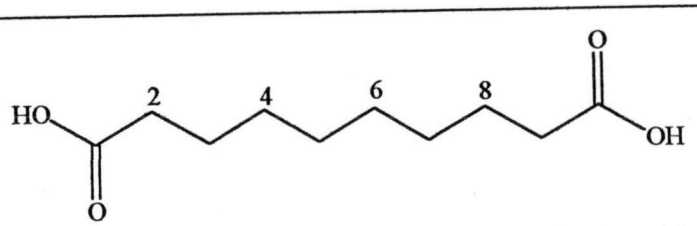

Compound 5 : Decanedioic acid or Sebacic acid

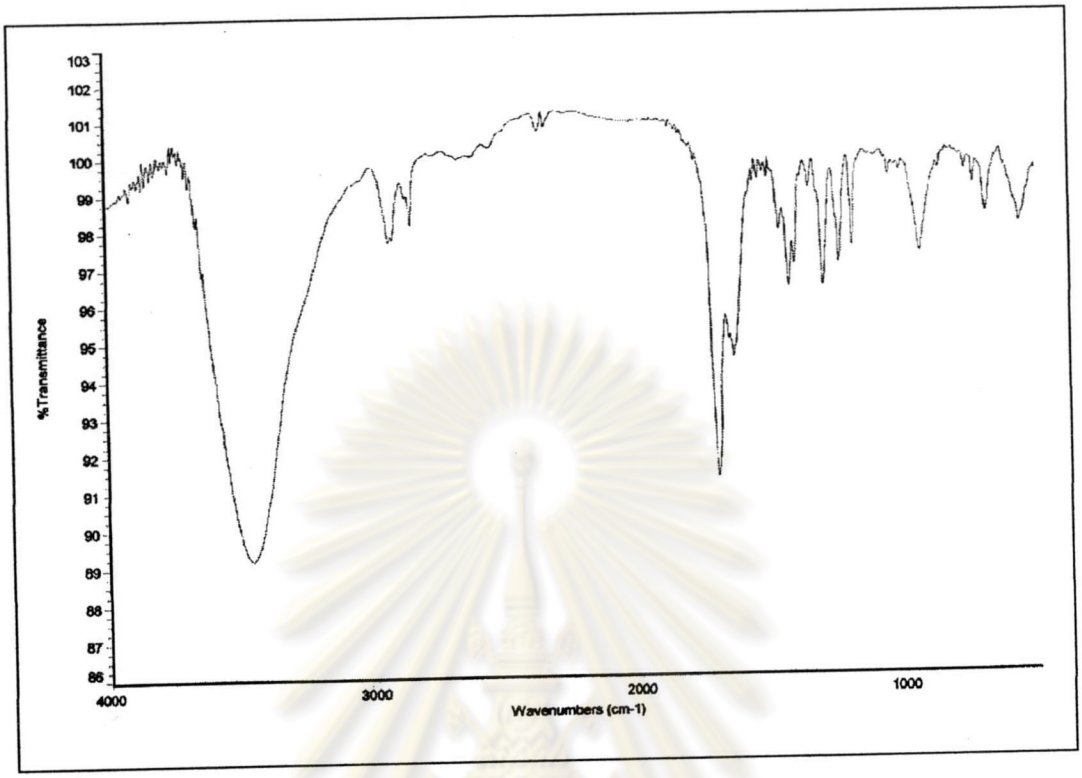

Figure 3.32 The IR spectrum of compound 5

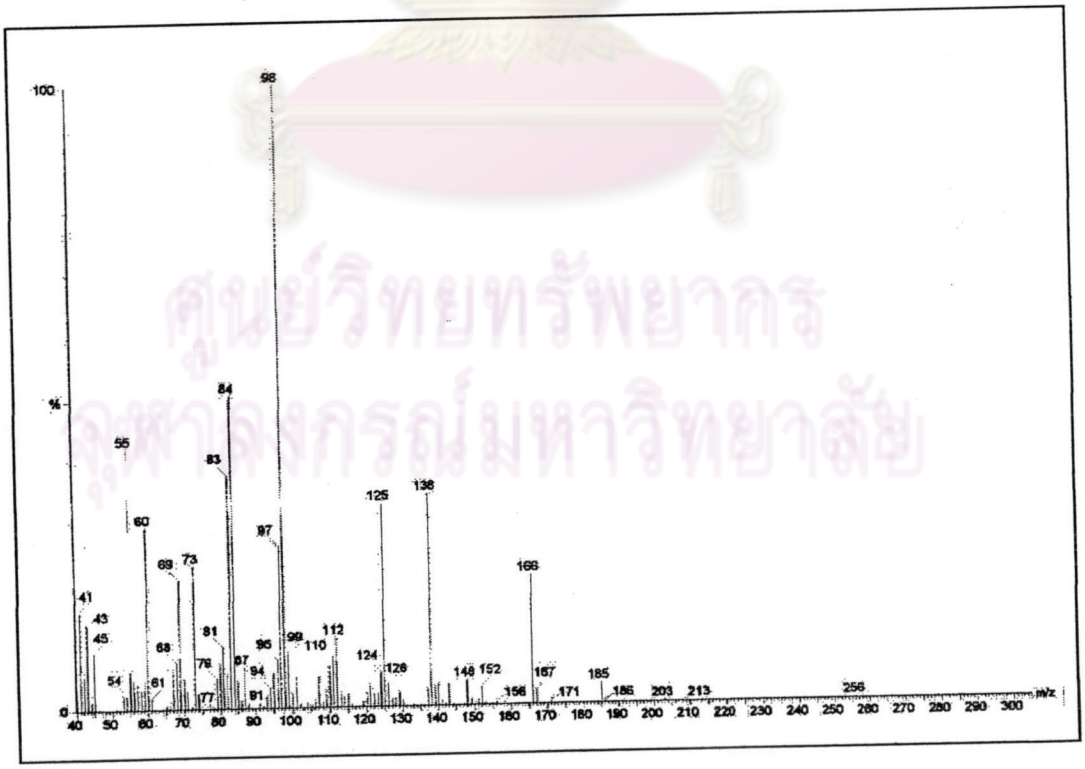

Figure 3.33 The EI mass spectrum of compound 5

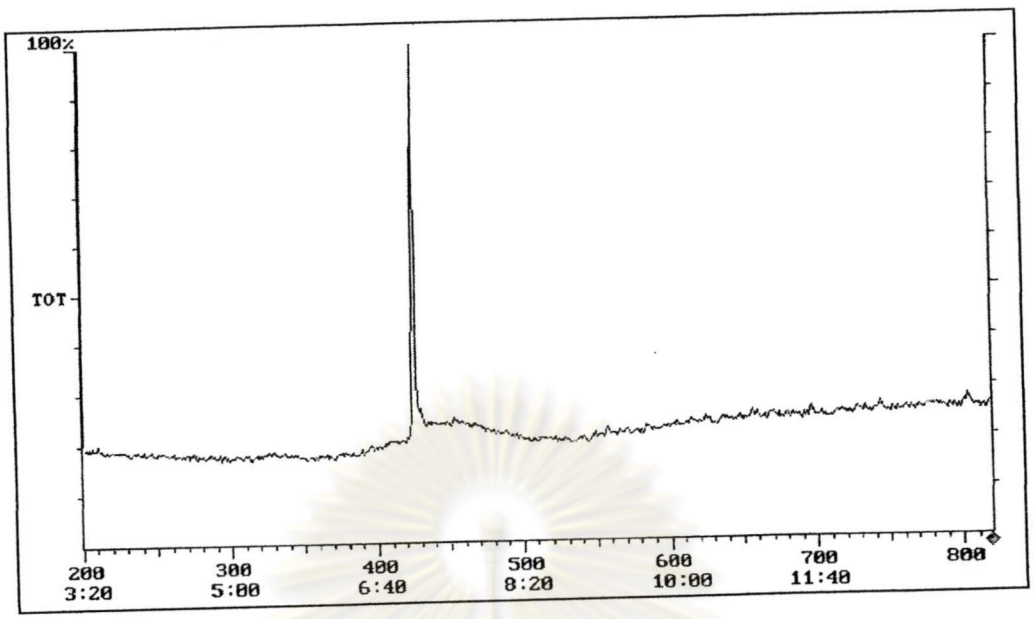

Figure 3.34 The GC chromatogram of compound 5A

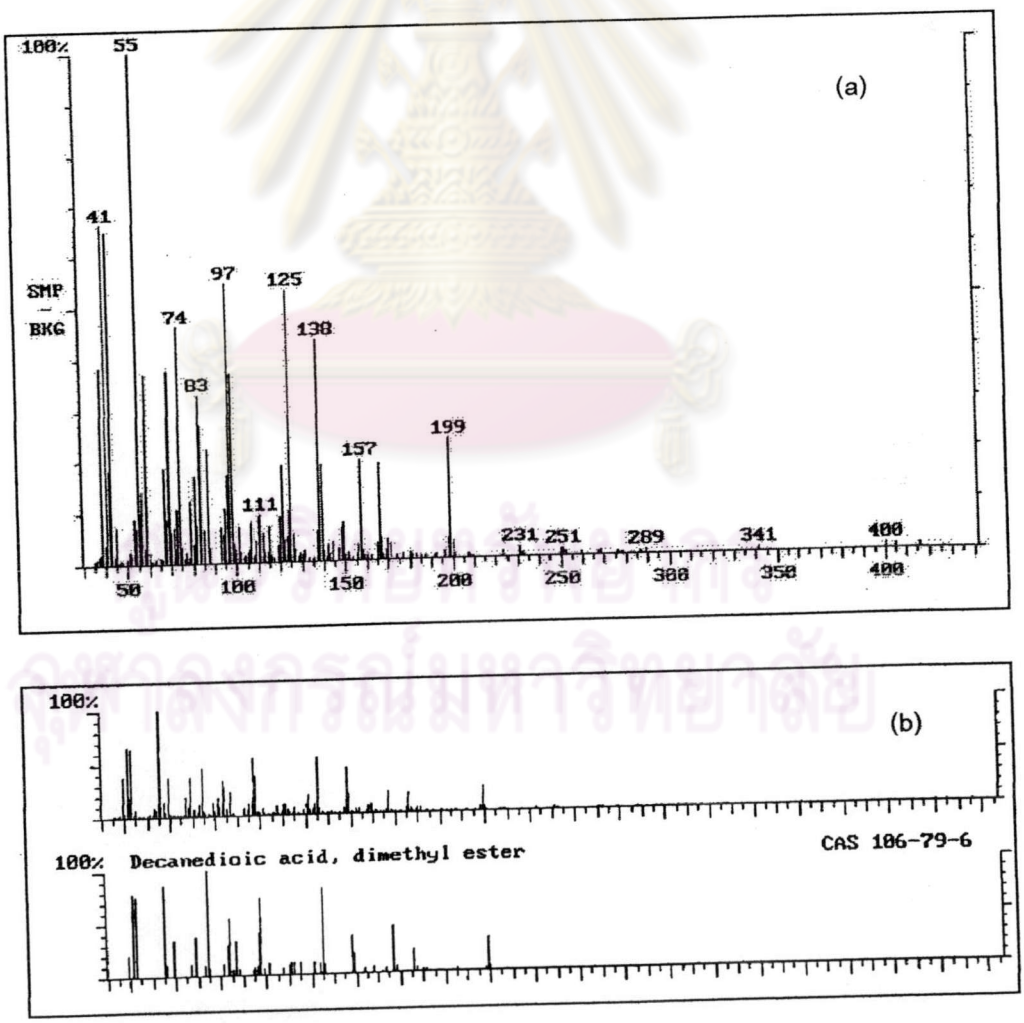

Figure 3.35 The mass spectrum of compound 5A (a) and the library data of dacanedioic acid, dimethyl ester (b)

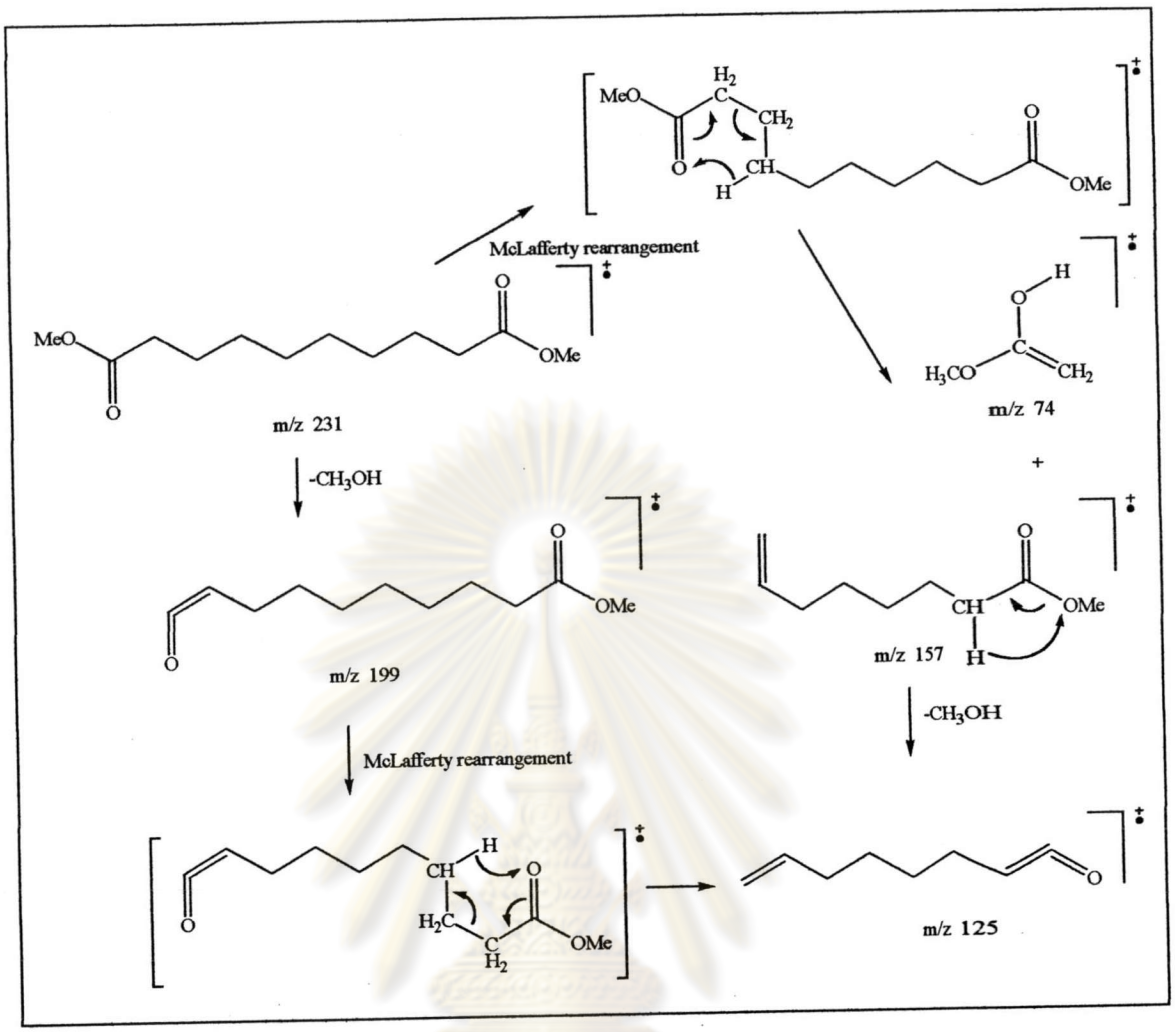

Scheme 3.7 The mass fragmentation pattern of decanedioic acid dimethyl ester (5A)

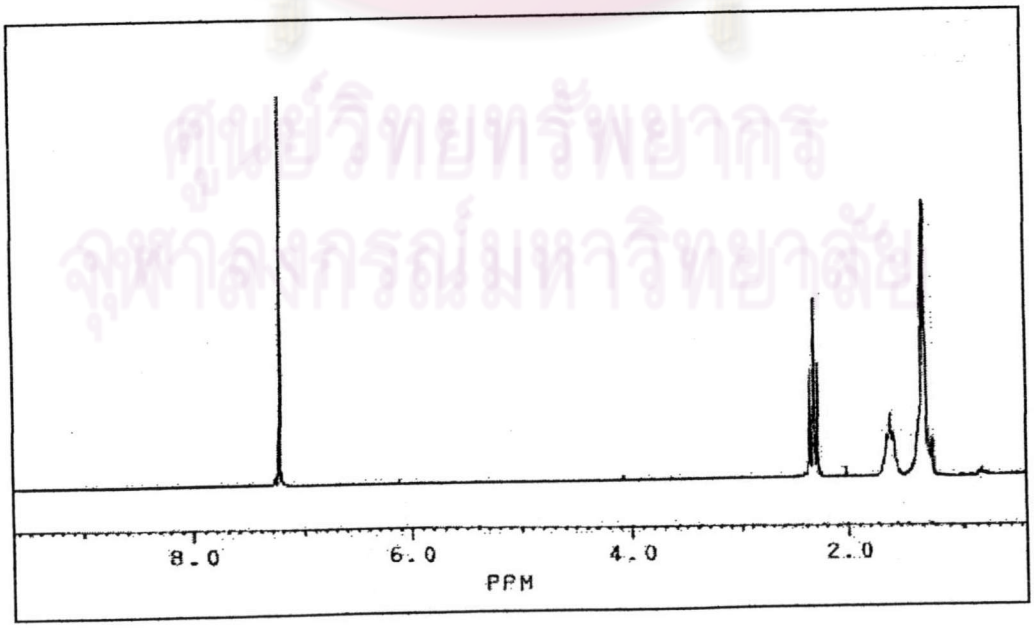

Figure 3.36 The ^{1}H-NMR spectrum (acetone-d_6) of compound 5

3.4.8 Structural Elucidation of Compound 6

Compound 6 was separated from subfraction 4 of ethyl acetate crude extract. It was subjected to chromatotron. Elution was performed with 4:1 EtOAc/hexane. Eight milligrams of this compound was obtained as a yellow powder and R_f 0.18 (SiO_2, 1:1 EtOAc/CH_2Cl_2). It exhibited bright blue fluorescence under long wavelength UV lamp (365 nm) which indicated that it might be a coumarin because the most obvious physical property of most natural coumarin is the fluorescence under the UV light[34].

The IR spectrum (Figure 3.37) presented the characteristic absorption band of unsaturated lactone of coumarin at V_{max} 1706 cm^{-1} (C=O stretching) and 1293 cm^{-1} (C-O stretching) . Otherwise, the absorption band at 1697 cm^{-1} (C=O stretching), 3461 cm^{-1} (O-H stretching) and 1245 cm^{-1} (C-O stretching) were distinguishing of carboxylic acid.

From the ^1H and ^{13}C-NMR spectrum (Figures 3.38 and 3.39, respectively) of this compound, chemical shifts of proton at δ 3.93 (*s*, 3H) and carbon at δ 56.4 were unequivocally demonstrated the presence of one methoxy group. Furthermore, signals of proton at δ 2.4 (*t*), 1.6 (*m*) and 1.3 (*m*) and carbon at δ 178.1 were indicated that $-(CH_2)_n$-COOH was another substituted group of this compound.

Two doublet peaks of aromatic proton at δ 6.23 (1H, J = 9.4 Hz) and 7.58 (1H, J = 9.4 Hz) were assigned at H-3 and H-4 in the lactone ring of coumarin. Then the substituent groups were located at an aromatic ring instead of an unsaturated lactone ring.

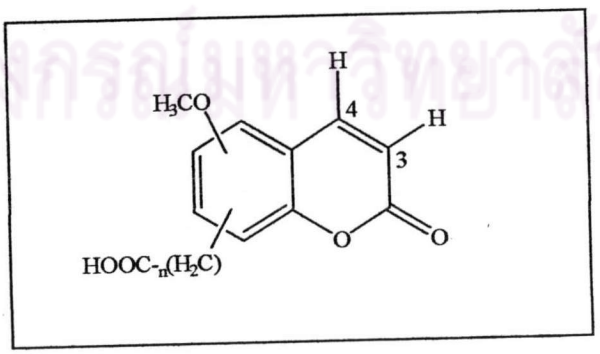

Two singlet peaks at 6.82 (1H) and 6.90(1H) on aromatic ring directed that they were not adjacent to each other. Six possible structures of compound 6 could be proposed as follow.

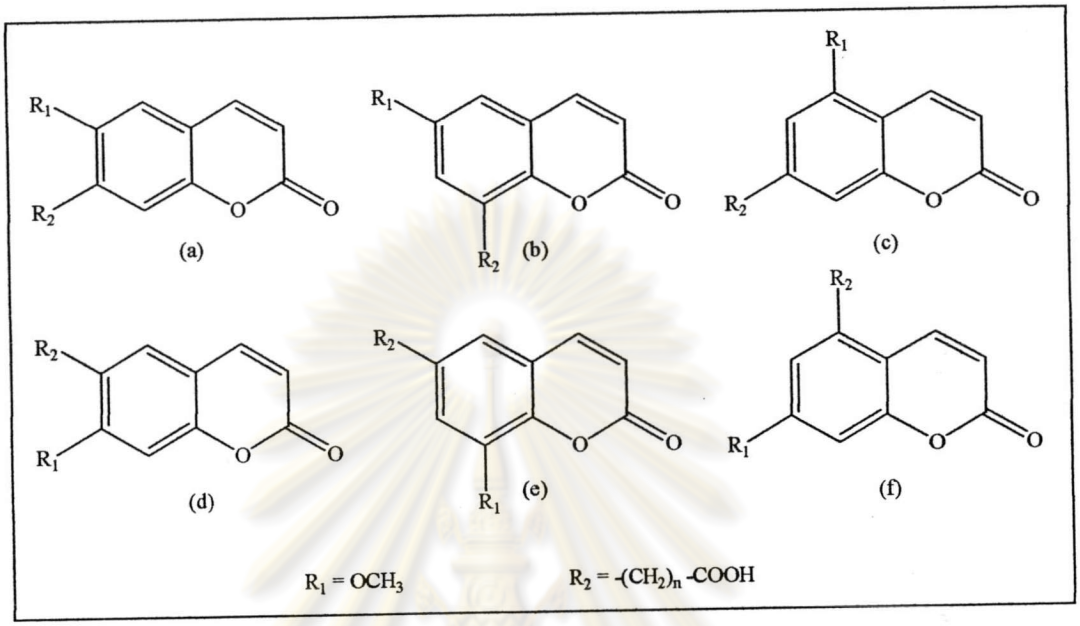

On the basis of several literature data[35-37], the R_1 and R_2 were *meta*-disubstituted in aromatic ring of coumarin, signal of two protons showed a doublet ($J \sim 2$ Hz). Therefore, structure (b), (c), (e) and (f) were eliminated.

The molecular formula $C_{22}H_{30}O_5$ was deduced from EIMS. The EI mass spectrum (Figure 3.40) showed the molecular peak, M^+, at m/z 374, then R_2 was $-(CH_2)_{11}$-COOH. The mass ion peak at m/z 329 corresponded to the loss of $COOH^+$ from the molecular ion, and also the mass ion peak at m/z 298 [329 - OCH_3].

In 6,7-disubstituted coumarins, H-5 and H-8 appeared as singlet with H-5 downfield than H-8. The methoxy group should be attached to C-6 because an oxygen substituted characteristically shifts the resonance of adjacent proton upfield by ~ 0.5 ppm but alkyl substituted should be shift the resonance to upfield by ~0.2 ppm. On the other hand, the methoxy group attached to C-7, thereby causing the resonance of H-8 to move much more the upfield than C-5 but proton signals of H-5 and H-8 were vicinity.

Thus, the structure of compound 6 could be established as 12-(6′-methoxy-2′-chromenone-7′-yl) dodecanoic acid (a). From our knowledge, this is a new compound. The assignments of ^{1}H- and ^{13}C-NMR chemical shifts are shown in Table 3.12.

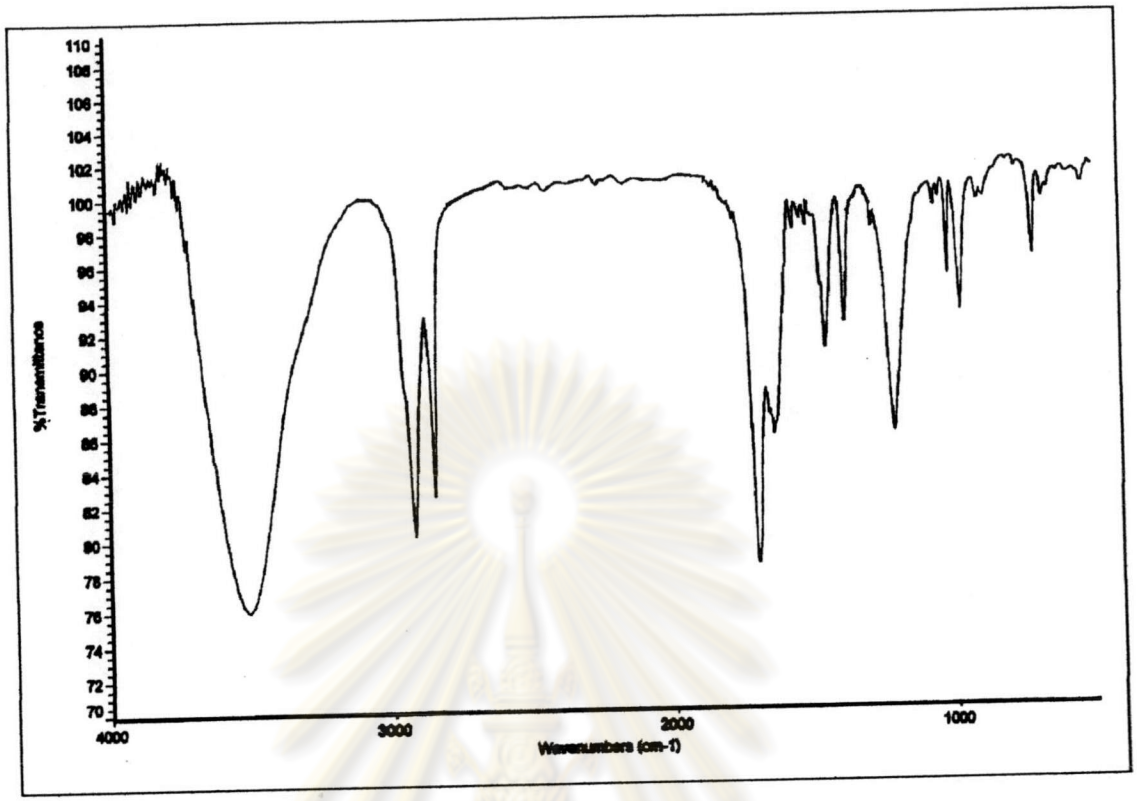

Figure 3.37 The IR spectrum of compound 6

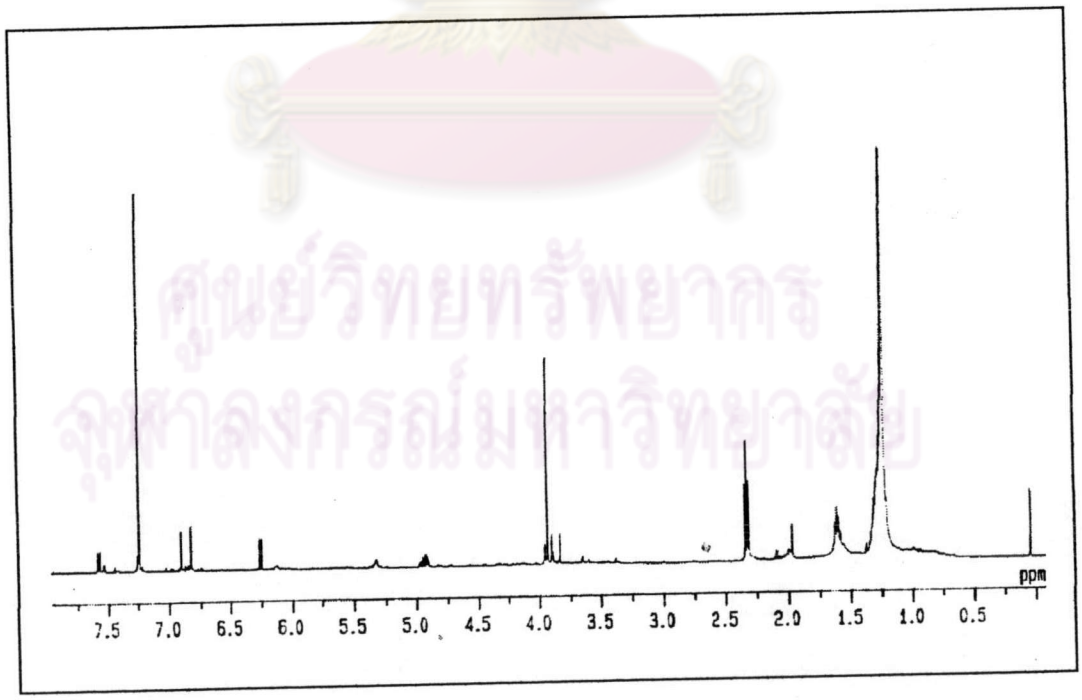

Figure 3.38 The ^{1}H-NMR spectrum ($CDCl_3$) of compound 6

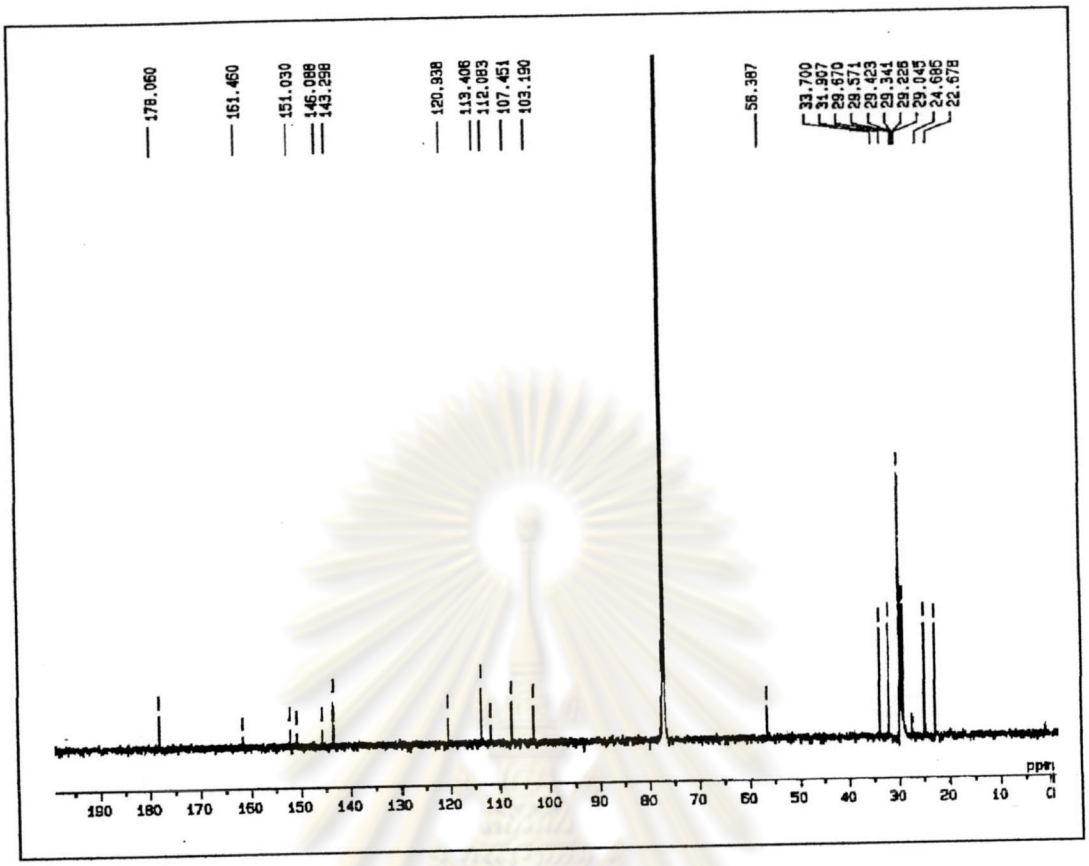

Figure 3.39 The ^{13}C-NMR spectrum ($CDCl_3$) of compound 6

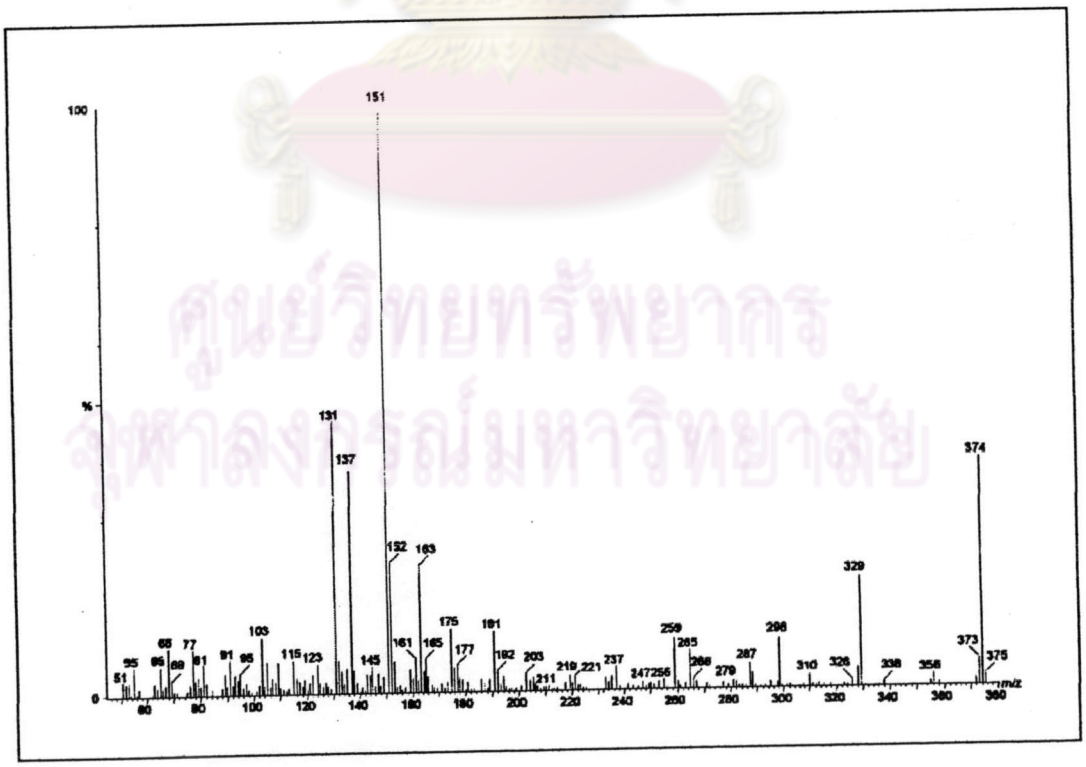

Figure 3.40 The EI mass spectrum of compound 6

Table 3.12 The assignment of ^{1}H- and ^{13}C-NMR chemical shifts of compound 6

Position	Chemical shift (ppm)	
	δ_H	δ_C
2'	-	161.5
3'	6.23 (d, 9.4)	113.4
4'	7.58 (d, 9.4)	143.3
4a	-	112.1
5'	6.82 (s)	107.1
6'	-	146.1
7'	-	120.9
8'	6.90 (s)	103.2
8a	-	151.0
2	2.4 (t)	33.7
3	1.6 (m)	22.7
4-10	1.3 (m)	29.0-29.7
11	1.6 (m)	31.9
12	2.4 (t)	24.7
-OMe	3.93 (s)	56.4
-COOH	-	178.1

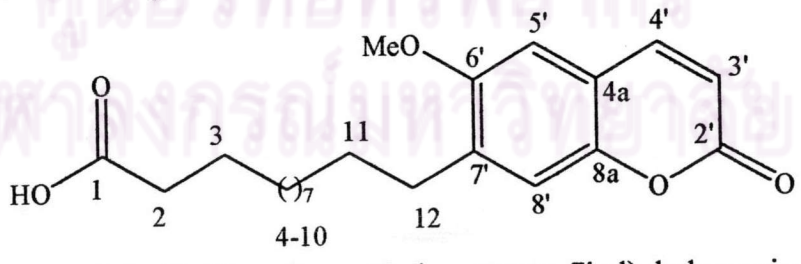

Compound 6 : 12-(6′-methoxy-2′-chromenone-7′-yl) dodecanoic acid

(new compound)

3.4.10 Structural Elucidation of Compound 7

Compound 7 was separated from alkaloid crude extract of the mixture of subfraction 5 and 6 of ethyl acetate crude extract. It was subjected to chromatotron. Elution was performed with EtOAc-MeOH (19:1 to 4:1). Seven milligrams of this compound was obtained as a yellow amorphous solid of melting point 217-220 °C (dec.) (lit. 210-213 °C (dec.))[38] and R_f 0.22 (SiO_2, 1:4 MeOH/CH_2Cl_2). It gave positive test with Dragendorff' s reagent.

The IR spectrum (Figure 3.41) presented the characteristic absorption band of at V_{max} 3400 cm^{-1} (O-H stretching), 2916 and 2848 cm^{-1} (C-H stretching), 1605, 1470 cm^{-1} (C=C stretching), 1373 cm^{-1} (N-H stretching) and 1185 cm^{-1} (C-O stretching).

The mass spectrum of compound 7 (Figure 3.42) showed a weak molecular ion peak (M^+) at m/z 395, revealed that the molecular formula of compound 7 was $C_{23}H_{25}NO_5$ (Calcd. For $C_{23}H_{25}NO_5$: MW 395.45). A peak at m/z 325 arose due to cleavage of the pyrrolidine ring by a retro-Diels-Alder reaction. It was a characteristic of phenanthroindolizidine alkaloids. The base peak at m/z 296, which resulted from expulsion of CHO from m/z 325, indicated the hydroxy function to be on C-14.

The ^{1}H-NMR ($CDCl_3$) spectrum of compound 7 (Figure 3.43) showed the presence of three methoxy groups at δ 3.87 (3H, s), 3.98 (3H, s) and 4.02 (3H, s) and four aromatic proton at δ 8.99 (1H, s), 8.17 (1H, d, J = 9), 7.35 (1H, d, J = 9) and 7.08 (1H, s). The ^{1}H-NMR values of the aromatic proton were in agreement with corresponding values of tetraoxygenated phenanthroindolizidine alkaloids. From comparison with substitution pattern of four oxygenated groups from that observed in tylophorine[39] and isotylocrebrine[40] containing the same number of oxygenated, compound 7 was suitable for isotylocrebrine type substituents.

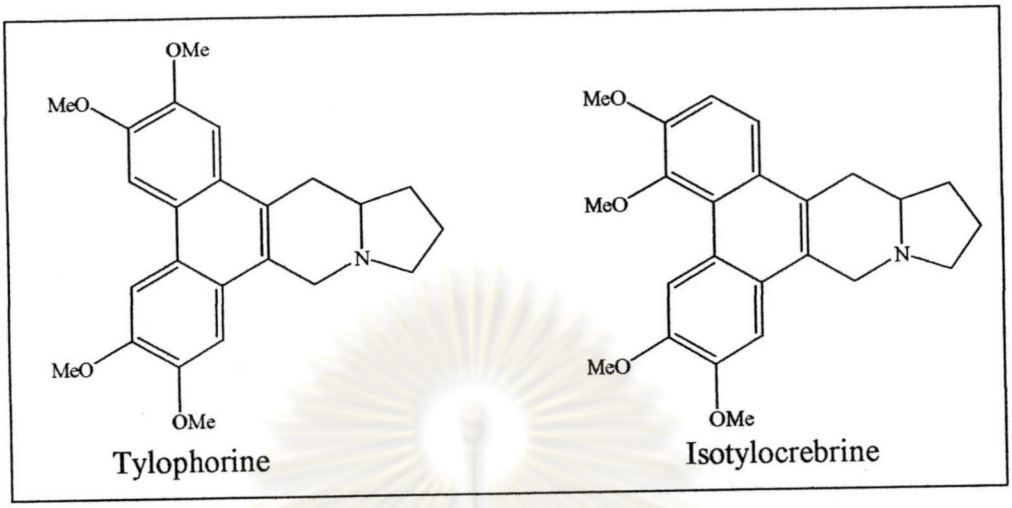

In the ^{13}C-NMR spectrum (Figure 3.44), 23 signals for carbon were observed and 14 signals (δ 102.9 –148.7 ppm) were assigned to be aromatic carbon.

By comparing the ^{1}H and ^{13}C-NMR spectra of compound 7 with isotylocrebrine phenanthroindolizidine alkaloids in plants belonging to tylophora genus, compound 7 was identified as 3-demethyl-14α-hydroxyisotylocrebrine, which have been isolated from *Tylophora tanakae* Maxim. The carbon assignment of compound 7 and 3-demethyl-14α-hydroxyisotylocrebrine are presented in Table 3.13.

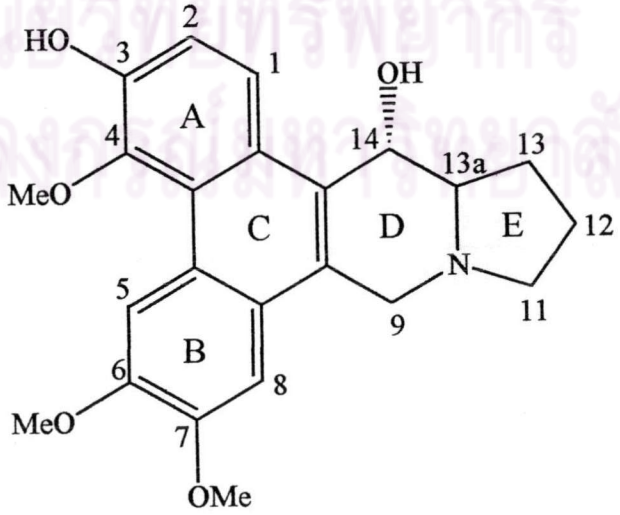

Compound 7 :3-demethyl-14α-hydroxyisotylocrebrine

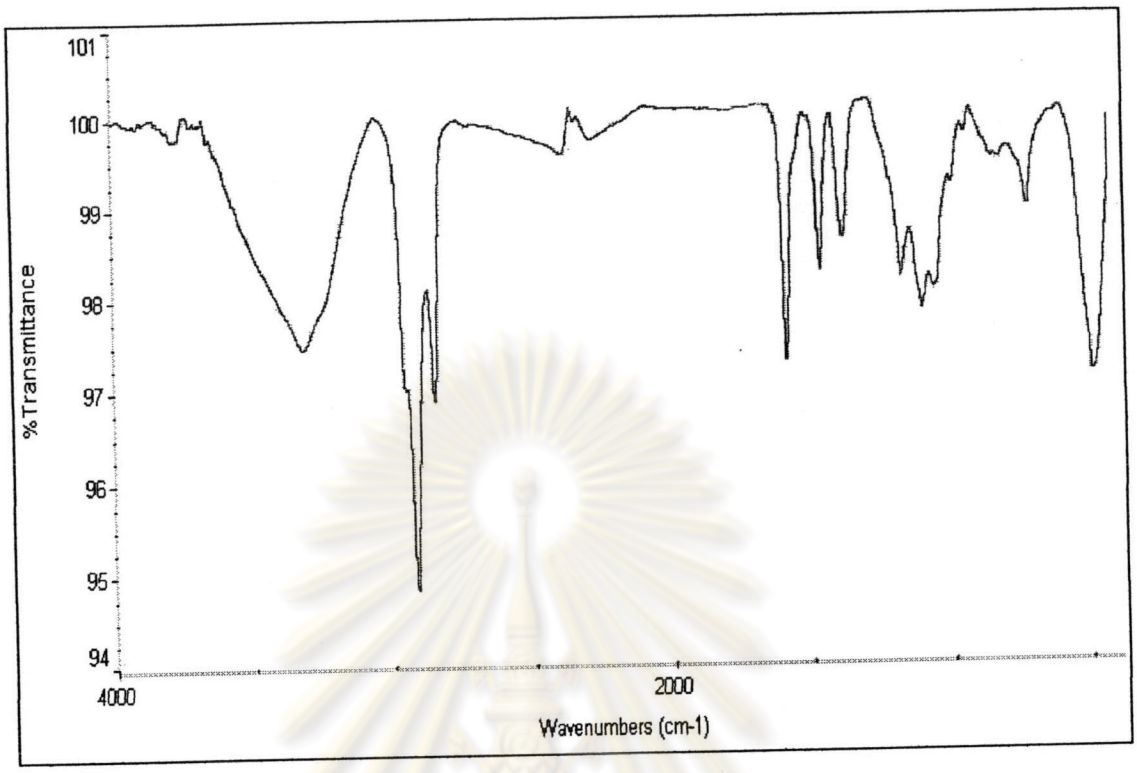

Figure 3.41 The IR spectrum of compound 7

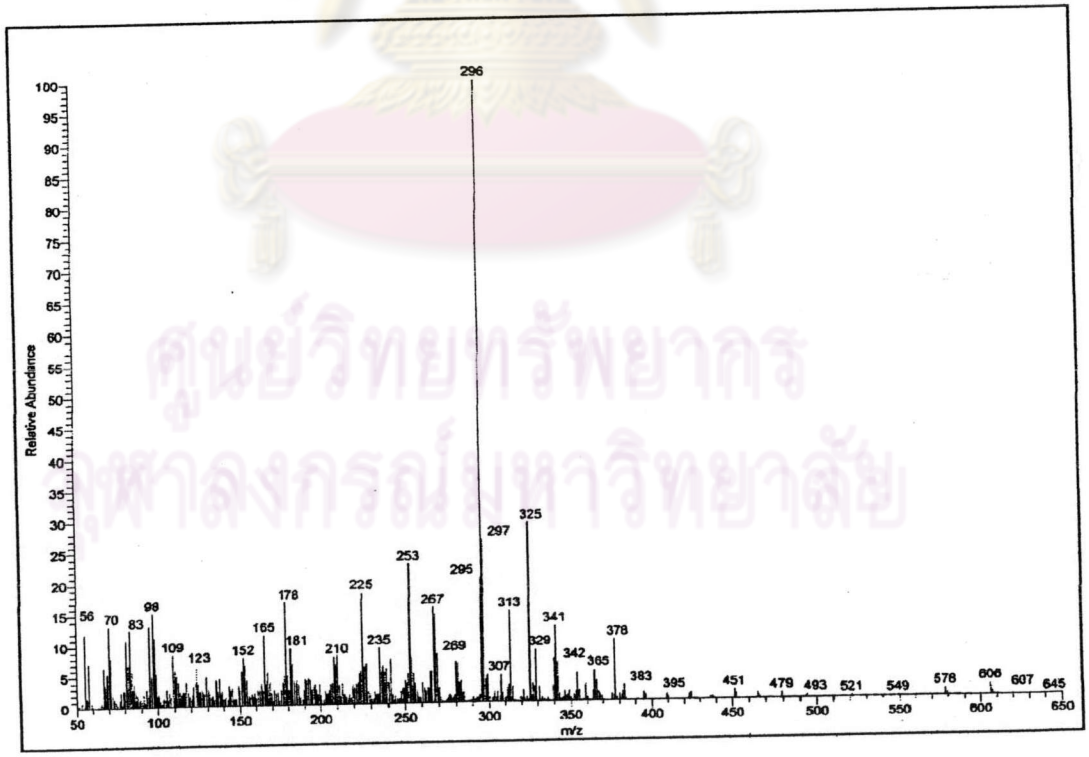

Figure 3.42 The EI mass spectrum of compound 7

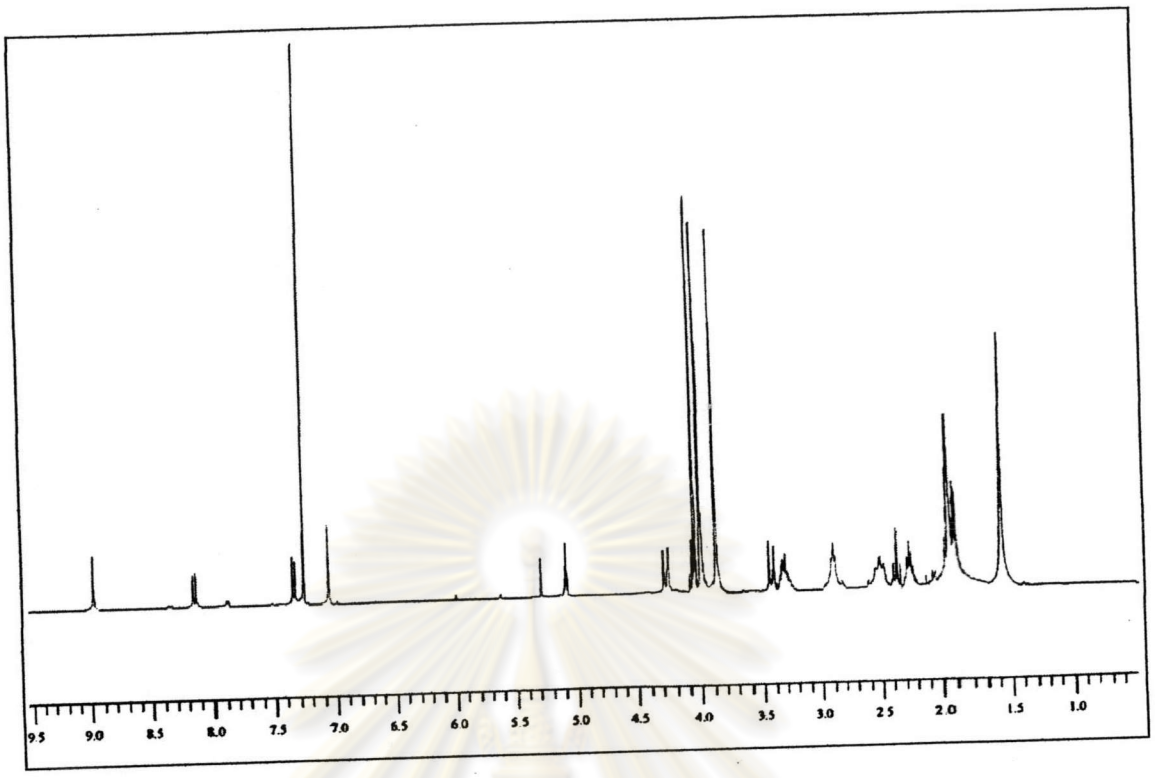

Figure 3.43 The ^{1}H-NMR spectrum ($CDCl_3$) of compound 7

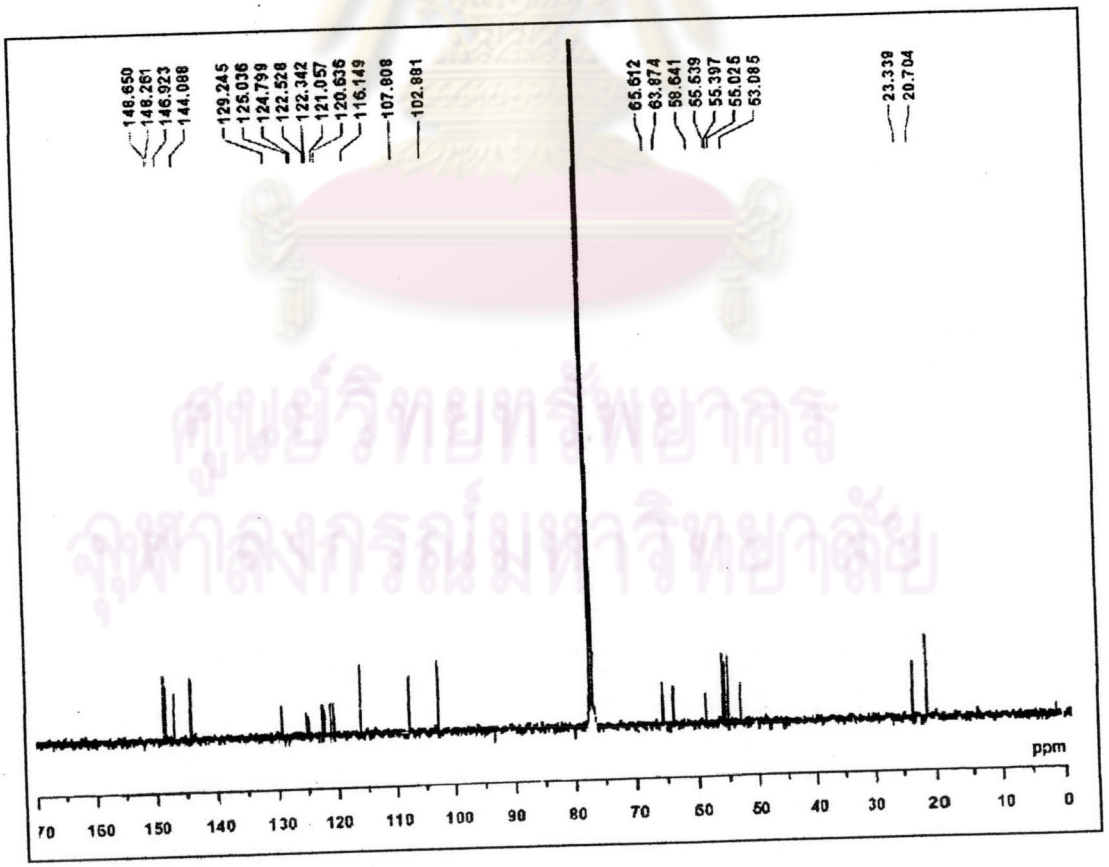

Figure 3.44 The ^{13}C-NMR spectrum ($CDCl_3$) of compound 7

Table 3.13 The ^{1}H- and ^{13}C-NMR chemical shift of compound 7 and 3-demethyl 14α-hydroxyisotylocrebrine[38]

Position	Compound 7 ($CDCl_3$)		3-demethyl-14α-hydroxyisotylocrebrine	
	^{1}H	^{13}C	^{1}H	^{13}C
1	8.17 (d, *J*=9 Hz)	120.6	8.09 (d, *J*=9 Hz)	121.0
2	7.35 (d, *J*=9 Hz)	116.1	7.29 (d, *J*=9 Hz)	116.2
3		148.3		148.1
4		144.1		143.9
5	8.99 (s)	107.8	9.19 (s)	108.3
6		146.9		147.3
7		148.7		148.1
8	7.08 (s)	102.8	6.87 (s)	102.6
9	4.24 (d, *J*=15 Hz) 3.40 (d, *J*=15 Hz)	53.1	4.17 (d, *J*=15 Hz) 3.41 (d, *J*=15 Hz)	53.5
11	3.29 (m) 2.34 (m)	55	3.34 (m) 2.41 (m)	54.9
12	1.84-1.95	20.4	1.92-2.02	21.3
13	2.48 (m) 2.21 (m)	23.3	2.32 (m) 1.99 (m)	23.6
13a	2.85 (m)	65.6	2.52 (m)	65.0
14β	5.06 (m)	63.9	5.05 (m)	64.3
ring C		129.2		128.8
		125.0		125.6
		124.8		125.5
		122.5		123.5
		122.3		123.4
		121.1		121.0
4-OMe	3.87	58.6	3.89	59.2
6-OMe	4.02	55.4	4.08	55.1
7-OMe	3.98	55.5	3.97	55.1

3.4.11 Structural Elucidation of Compound 8

Compound 8 (7 mg) was achieved from the same fraction with compound 7 as yellow amorphous solid, m.p. 220-222 °C (dec.) (lit. 215-217 °C (dec.))[10]. It was eluted after compound 7 by chromatotron. It gave a positive test with Dragendorff's reagent, which indicated the alkaloid.

The IR spectrum (Figure 3.45) presented the absorption band of at V_{max} 3394 cm^{-1} (O-H stretching), 2917 and 2850 cm^{-1} (C-H stretching), 1612, 1473 cm^{-1} (C=C stretching), 1376 cm^{-1} (N-H stretching) and 1189 cm^{-1} (C-O stretching).

The mass spectrum of compound 8 (Figure 3.46) showed a molecular ion peak (M^+) at m/z 365, suggesting a molecular formula, $C_{22}H_{23}NO_4$ (Calcd. For $C_{22}H_{23}NO_4$: MW 365.42). The base peak at m/z 296 arose due to cleavage of the pyrrolidine ring at m/z 70 from M^+ by a retro-Diels-Alder reaction. A strong peak at m/z 268 arising from 296 by loss of CO was indicative of the presence of an OH at C-14

The ^{1}H-NMR ($CDCl_3$) spectrum of compound 8 (Figure 3.47) showed the presence of five aromatic proton at δ 8.01 (1H, d, J= 9 Hz), 7.90 (1H, s), 7.75 (1H, d, J = 2 Hz), 7.10 (1H, dd, J= 10, 2 Hz) and 6.55 (1H, s) and two methoxy groups at δ 3.85 (3H, s) and 3.95 (3H, s). The ^{1}H-NMR values of the aromatic proton were in agreement with corresponding values of trioxygenated phenanthroindolizidine alkaloids.

In the ^{13}C-NMR spectrum (Figure 3.48), 22 signals for carbon were observed and 14 signals (δ 104.1 –157.5 ppm) were assigned to be aromatic carbon. The spectral data of compound 8 was in part similar to that of compound 7.

By comparison of the mass fragmentation pattern, ^{1}H- and ^{13}C-NMR spectra of compound 8 with trioxygenated phenanthroindolizidine alkaloids that had been found in *Tylophora* species. On the basis of spectral evidences of compound 8 was fully consistent with the structure of tylopholinidine, which was compared with data of tylopholinidine in the previously reported[10, 12, 40].

The mass fragmentation pattern, ^{1}H- and ^{13}C-NMR assignments are presented in Scheme 3.8, Figures 3.49 and 3.50, respectively.

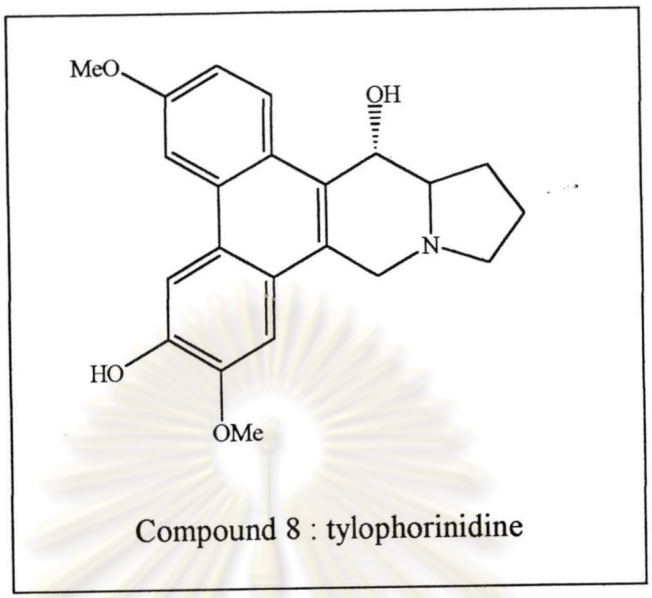

Compound 8 : tylophorinidine

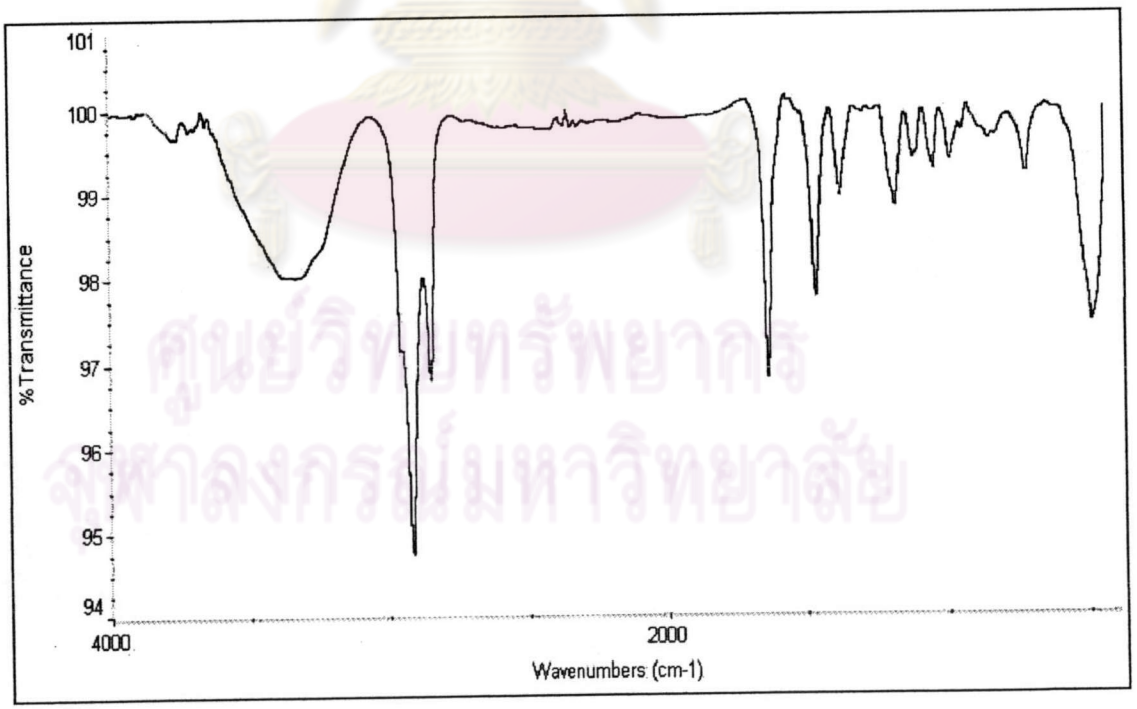

Figure 3.45 The IR spectrum of compound 8

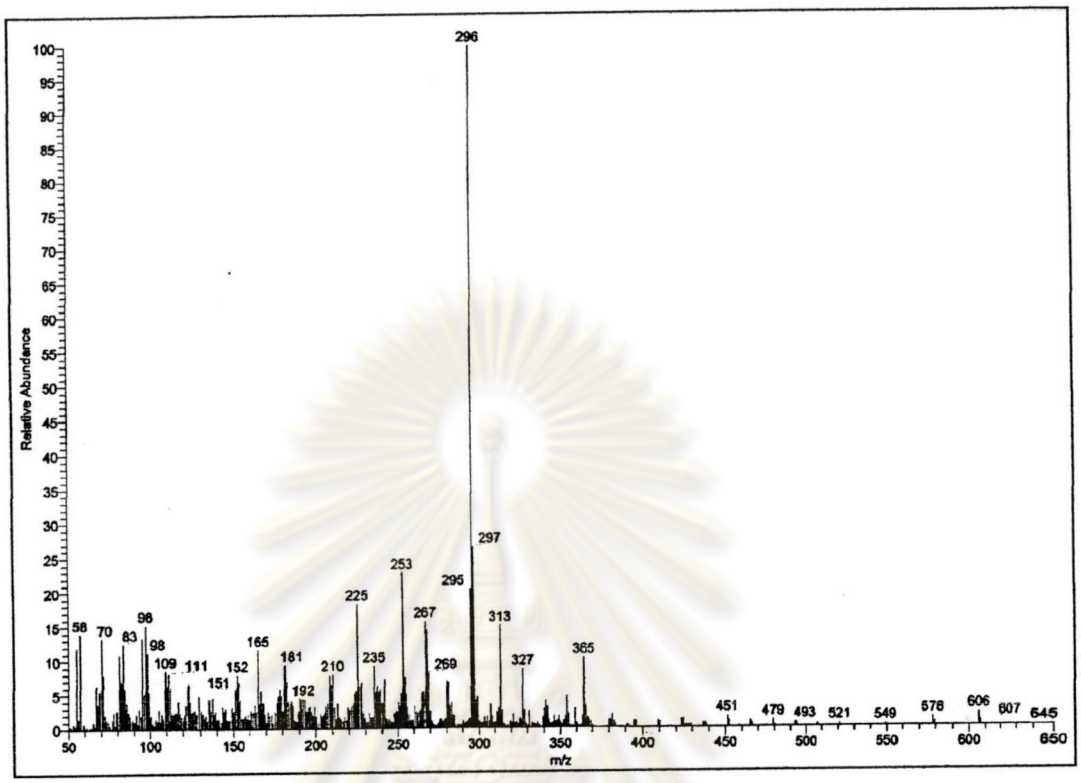

Figure 3.46 The EI mass spectrum of compound 8

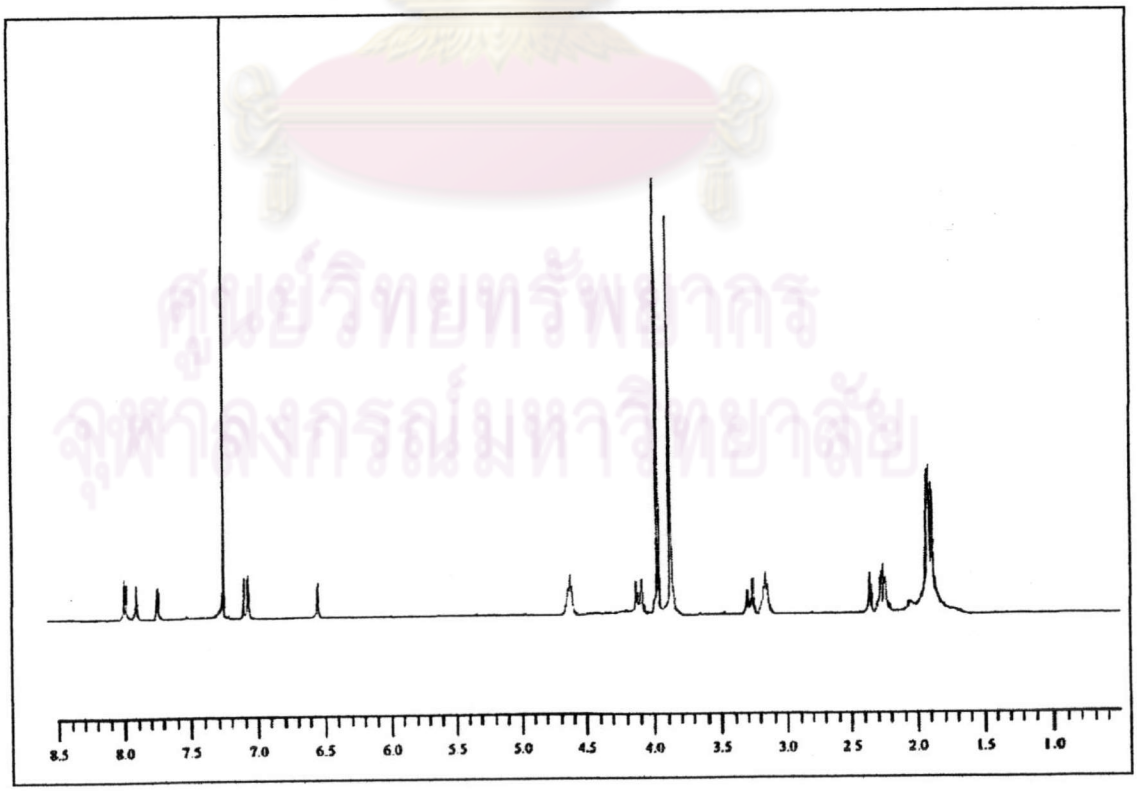

Figure 3.47 The ^{1}H-NMR spectrum ($CDCl_3$) of compound 8

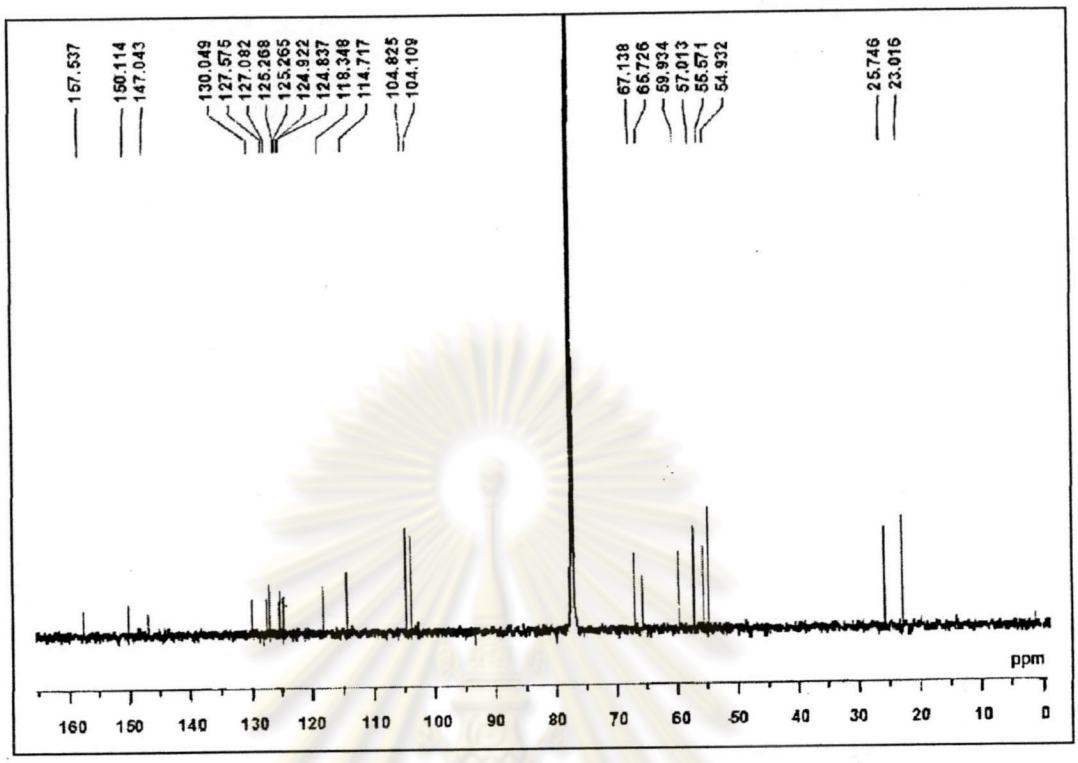

Figure3.48 The ^{13}C-NMR spectrum ($CDCl_3$) of compound 8

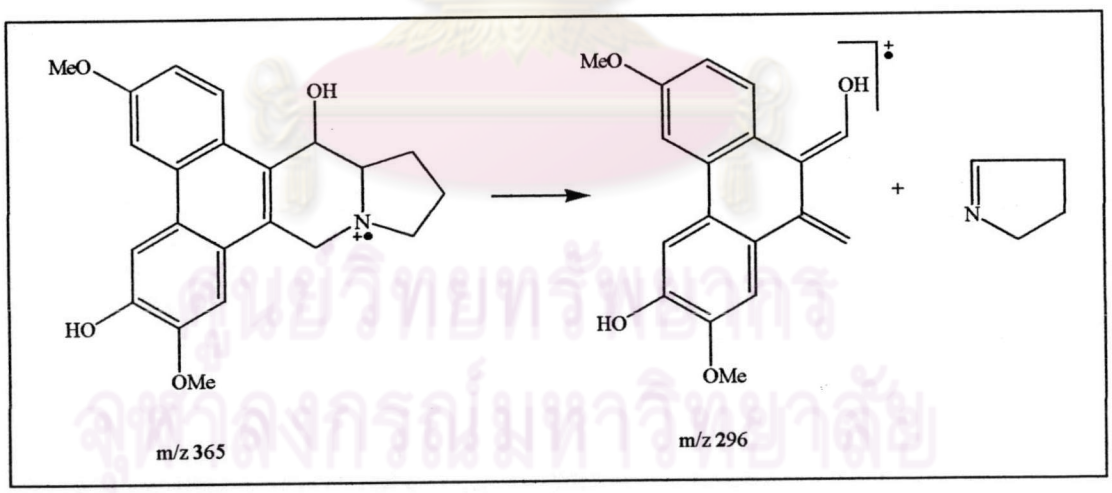

Scheme 3.8 The mass fragmentation pattern of compound 8

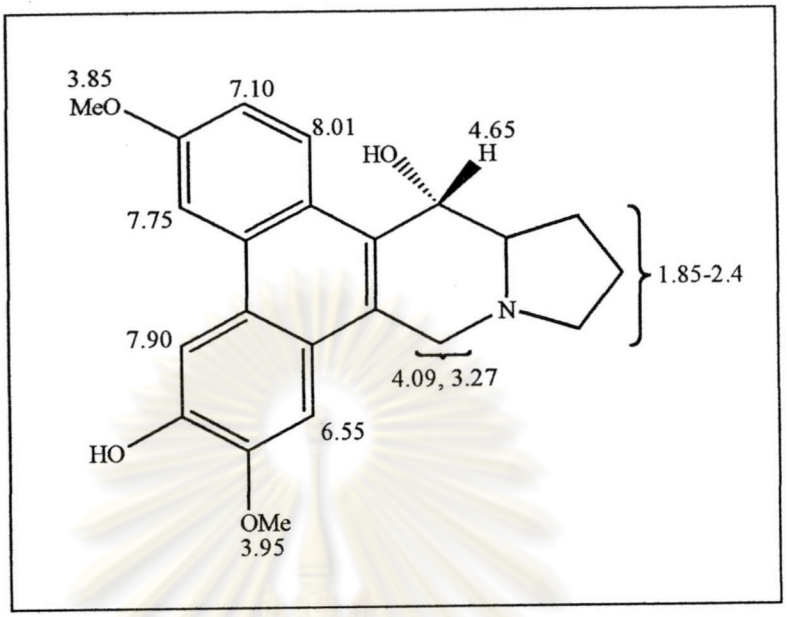

Figure 3.49 The ^{1}H-NMR assignment of compound 8

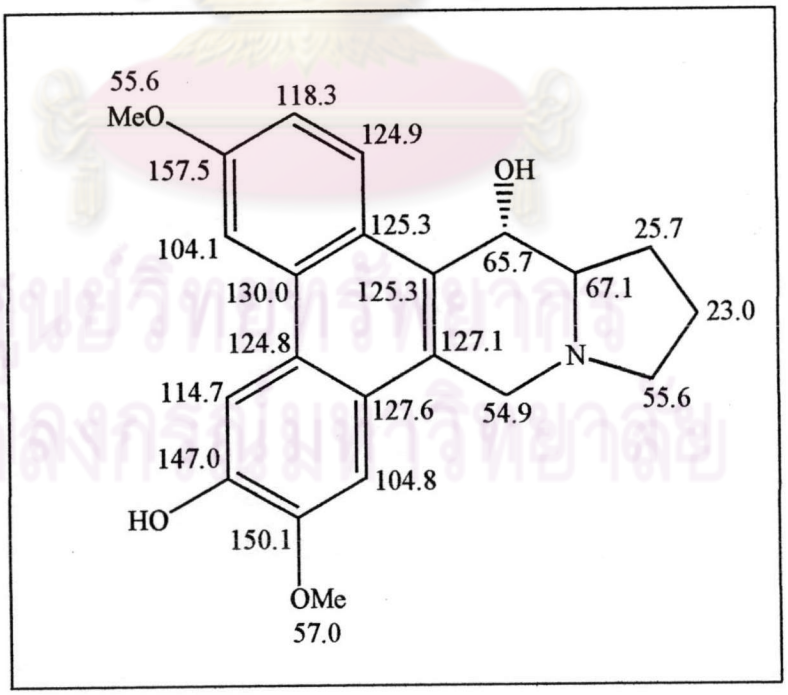

Figure3.50 The ^{13}C-NMR assignment of compound 8

3.5 Plant Growth Regulator Activity of Isolated Substances.

In order to reach the goal of this research, ten substances were isolated from the fractionation and purification from the roots of *T. indica* Merr. crude extracts which showed significant activity result in plant growth inhibition against *B. pekinensis* Rupr. Five substances, including a mixture of three fatty acid (Mixture 1), a mixture of two steroids (Mixture 2), stigmasteryl-3-O-β-D-glucopyranoside (compound 1), oleanolic acid (compound 2), and ursolic acid (compound 3) were isolated from dichloromethane crude extract. Not only that, nonanedioic acid (compound 4), dodecanedioic acid (compound 5), 6-methoxy-7-dodecanoic coumarin (compound 6), 3-demethyl-14α-hydroxyisotylocrebrine (compound 7) and tylophorinidine (compound 8) were isolated from ethyl acetate crude extract. All isolated substances and derivative of mixture 1, compound 4 and compound 5 as mixture of hexadecanoic acid, methyl ester; cis-9-octadecanoic acid, methyl ester; octadecanoic acid, methyl ester (1A); nonanedioic acid, methyl ester (4A); and decanedioic acid, methyl ester (5A) were subjected to plant growth regulator test. The results of this activity against *B. pekinensis* Rupr. are presented in Table 3.14 and Figures 3.51 and 3.52 .

Table 3.14 Inhibitory effect of isolated substances from the roots of *T. indica* Merr. on the growth of *B. pekinensis* Rupr.

Substances	Part of *B. pekinensis*	% Inhibition at various concentration		
		10 ppm	100 ppm	1000 ppm
Mixture 1	Root	-2.2	1.5	21.8
	Shoot	-4.9	0.8	-15.6
Mixture 1A	Root	-5.2	2.3	17.7
	Shoot	-1.5	3.9	7.4
Mixture 2	Root	-3.9	-1.9	-23.2
	Shoot	0.9	0.8	17.3
Compound 1	Root	6.0	9.1	24.2
	Shoot	-17.8	9.1	5.9
Compound 2	Root	-28.2	15.7	60.9
	Shoot	12.3	41.9	65.3

Table 3.14 (cont.) Inhibitory effect of isolated substances from the roots of *T. indica* Merr. on the growth of *B. pekinensis* Rupr.

Substances	Part of *B. pekinensis*	% Inhibition at various concentration		
		10 ppm	100 ppm	1000 ppm
Compound 3	Root	-20.8	18.6	63.9
	Shoot	8.4	33.4	69.1
Compound 4	Root	-27.7	0.6	100
	Shoot	3.8	13.2	34.5
Compound 4A	Root	-4.1	2.8	9.3
	Shoot	-3.7	0.8	7.3
Compound 5	Root	-22.0	11.8	90.3
	Shoot	-2.7	8.6	29.9
Compound 5A	Root	0.4	-1.3	4.3
	Shoot	-7.6	0.7	6.2
Compound 6	Root	-1.6	-4.2	30.8
	Shoot	-1.9	11.0	26.4
Compound 7	Root	-21.4	14.5	86.3
	Shoot	0.9	-24.6	-8.8
Compound 8	Root	-29.2	10.3	70.4
	Shoot	4.9	-25.2	-6.2

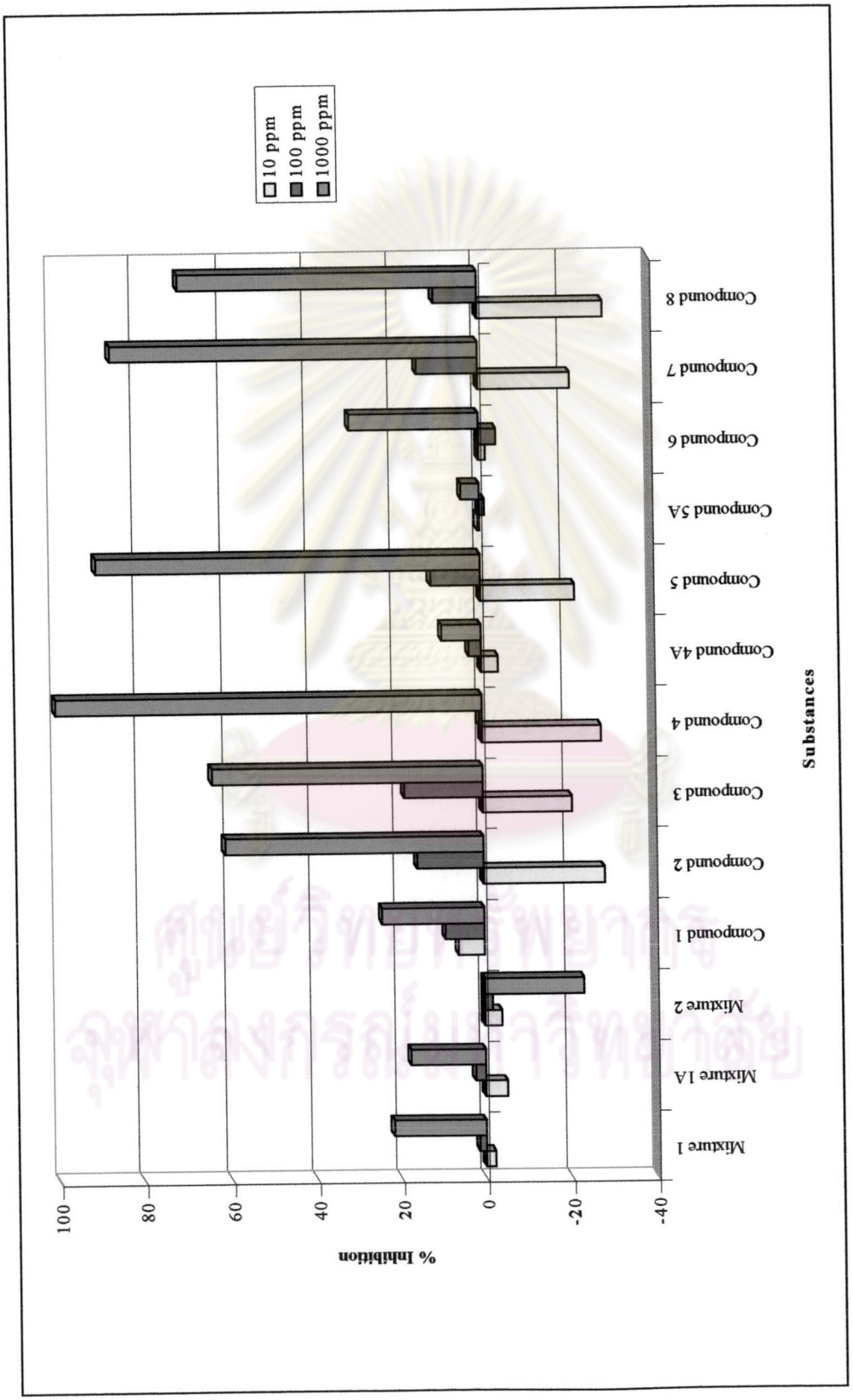

Figure 3.51 Inhibitory effect of isolated substances from the roots of *T. indica* Merr. on the root length of *B. pekinensis* Rupr.

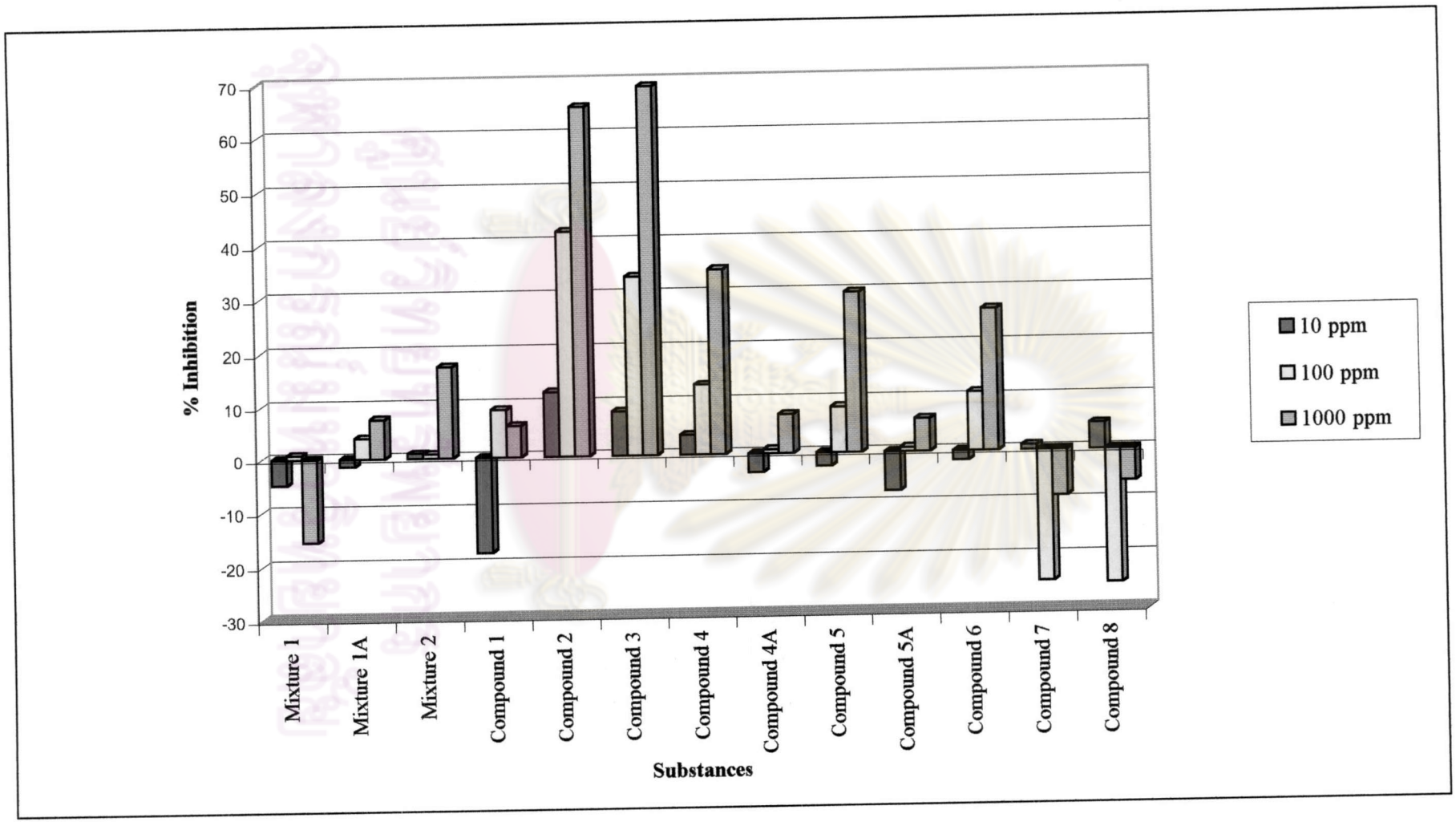

Figure 3.52 Inhibitory effect of isolated substances from the roots of *T. indica* Merr. on the shoot length of *B. pekinensis* Rupr.

The isolated substances from the roots of *T. indica* Merr. and some derivatives could be divided into 5 groups as follow: fatty acid (mixture 1, compound 4 and 5) and their derivatives (mixture 1A, compound 4A and 5A), steroid (mixture 2, compound 1), triterpenoid (compound 2 and 3), alkaloid (compound 8 and 9) and coumarin. The result of plant growth inhibition activity against *B. pekinensis* Rupr. seedling (lettuce) suggested that fatty acid could be splited to monocarboxylic acid, dicarboxylic acid and methyl ester derivatives (mixture 1A, compound 4A and 5A). Two dicarboxylic acid, nonanedioic acid and decanedioic acid, showed the strongest root growth inhibition (100 and 90.3 %, respectively). In contrast, the methyl ester of two dicarboxylic acid did not show the effect against the growth of lettuce seedling. Monocarboxylic acid, mixture 1, and its methyl ester did not exhibited significant effect on both root and shoot elongation. From these results, the carboxylic unit could play an important role in inhibitory activity. Two triterpenoids (oleanolic acid and ursolic acid) exhibited moderate effect of root and shoot length inhibition. They inhibited root elongation of lettuce seedling with 61 and 65 % and inhibited shoot length with 65 and 69 % at a concentration of 1000 ppm, respectively. Two alkaloids (3-demethyl-14α-hydroxyisotylocrebrine and tylophorinidine) showed significant results of root growth inhibition. They inhibited root growth of lettuce seedling by 86.3 and 70.4 % at a concentration 1000 ppm, while slightly accelerated both root growth by 21.4 and 29.2 % at a concentration of 10 ppm and shoot growth by 24.6 and 25.2 % (100 ppm), respectively. However, the other substances (mixture of two steroids, steroid glycoside and coumarin) did not showed significant inhibitory activity against growth of lettuce seedling.

In addition, all substances were further bioassay for plant growth inhibition against *Echinochloa crus-galli* (L.) Beauv. seedling, as a monocotyledon, which is a common and very important weed of the most agricultural areas of the world. The results of inhibitory effect are showed in Table 3.15 and Figures 3.53 and 3.54.

Table 3.15 Inhibitory effect of isolated substances from the roots of *T. indica* Merr. on the growth of *E. crus-galli* (L.) Beauv.

Substances	Part of *B. pekinensis*	% Inhibition at various concentration		
		10 ppm	100 ppm	1000 ppm
Mixture 1	Root	28.7	25.8	41.4
	Shoot	2.4	7.1	4.8
Mixture 1A	Root	0.3	3.7	5.1
	Shoot	-1.2	1.6	4.9
Mixture 2	Root	-0.3	3.1	10.3
	Shoot	6.5	11.8	13.9
Compound 1	Root	10.5	18.2	18.9
	Shoot	-5.1	0.6	2.3
Compound 2	Root	1.3	23.5	45.6
	Shoot	-0.6	7.9	32.3
Compound 3	Root	3.4	19.6	40.1
	Shoot	-3.6	5.4	22.7
Compound 4	Root	6.2	50.3	100
	Shoot	8.9	2.9	90.5
Compound 4A	Root	0.5	2.9	10.2
	Shoot	-3.4	1.6	5.6
Compound 5	Root	1.1	51.2	100
	Shoot	6.6	17.6	100
Compound 5A	Root	-1.3	3.8	8.8
	Shoot	-5.7	1.3	6.1
Compound 6	Root	16.6	10.3	66.5
	Shoot	-1.8	-15.6	13.3
Compound 7	Root	20.9	96.1	100
	Shoot	21.1	47.4	97.4
Compound 8	Root	9.6	89.0	100
	Shoot	2.9	13.5	85.6

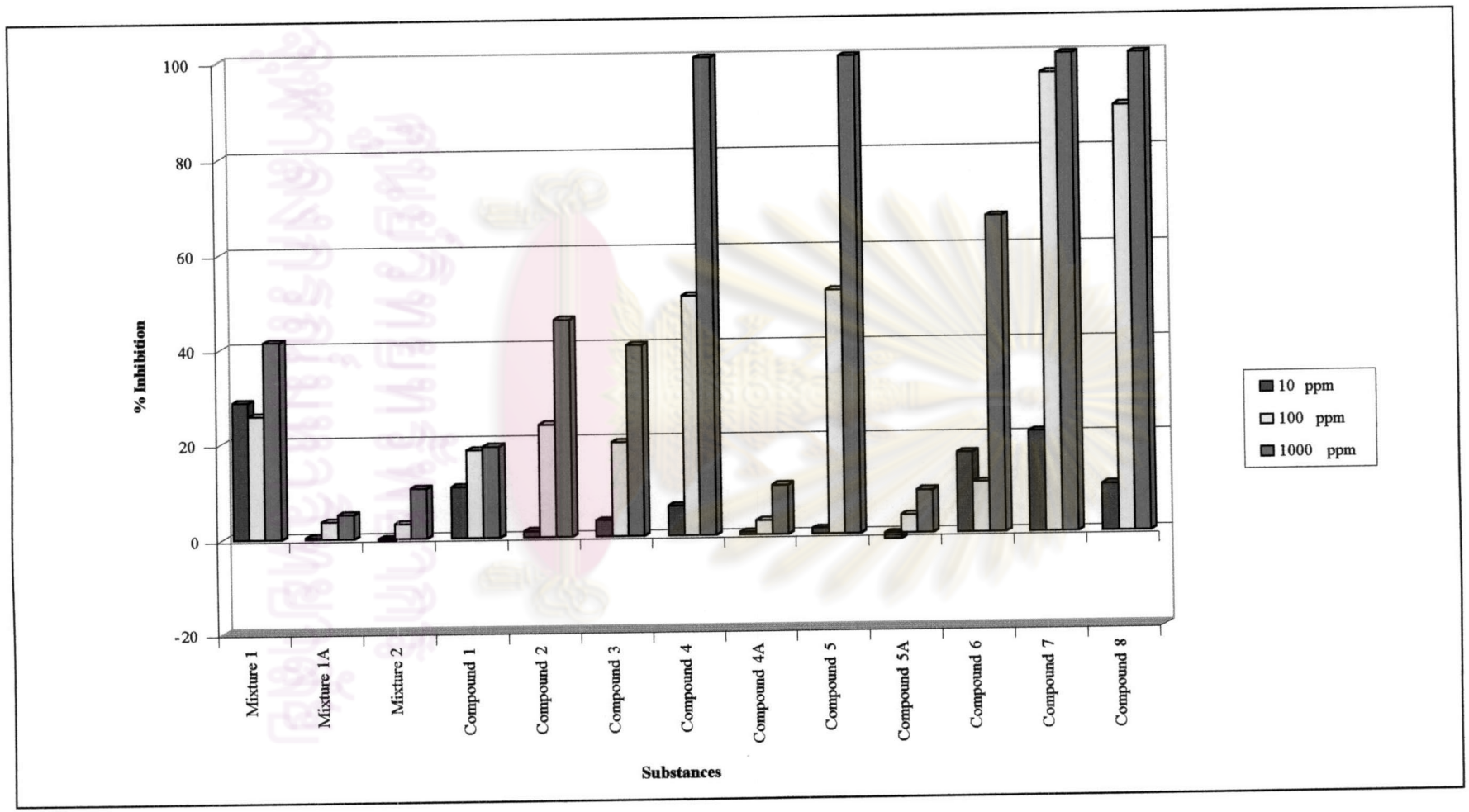

Figure 3.53 Inhibitory effect of isolated substances from the roots of *T. indica* Merr. on the root length of *E. crus-galli* (L.) Beauv.

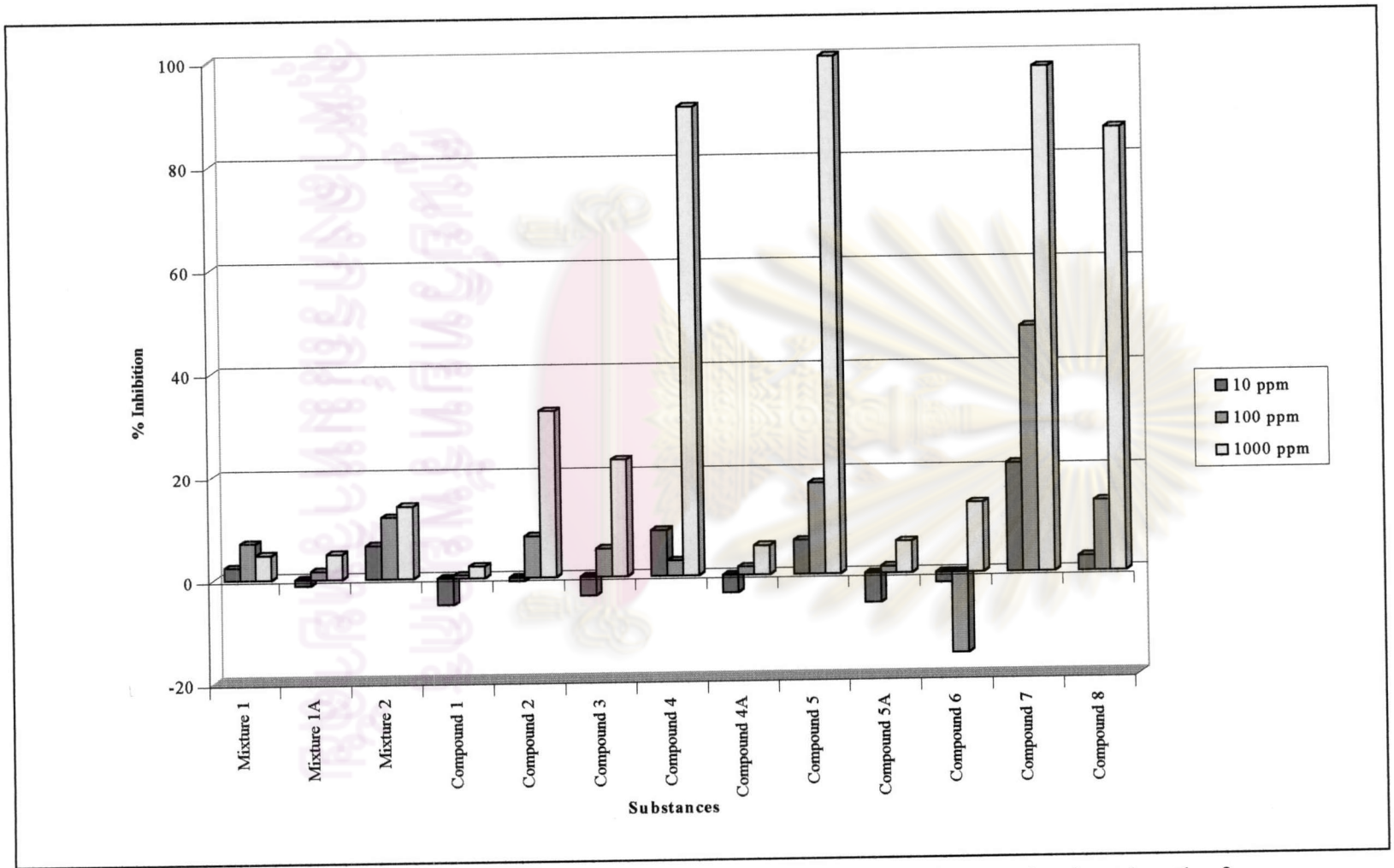

Figure 3.54 Inhibitory effect of isolated substances from the roots of *T. indica* Merr. on the shoot length of *E. crus-galli* (L.) Beauv.

From the results of inhibitory effect against the growth of *E. crus-galli* (L.) Beauv. seedling, it was revealed that two triterpenoids, oleanolic acid (compound 2) and ursolic acid (compound 3), showed moderate effect against root length inhibition. They inhibited root elongation by 45.6 and 40.1 % at concentration 1000 ppm, respectively. Dicarboxylic acid compounds, nonanedioic acid (compound 4) and decanedioic acid (compound 5), almost completely inhibited shoot and root growth at 1000 ppm and inhibited root elongation by 50.3 and 51.2 % at concentration 100 ppm, but their dimethyl ester derivatives did not affect against this activity. Coumarin derivative (compound 6) inhibited root length by 66.5 % at concentration 1000 ppm. Two alkaloids, 3-demethyl-14α-hydroxyisotylocrebrine (compound 7) and tylophorinidine (compound 8), completely inhibited root elongation at concentration 1000 ppm and still high inhibited by 96.1 and 89.0 % at concentration 100 ppm. Furthermore, they inhibited shoot length by 97.4 and 85.6 % at concentration 1000 ppm. Thus, at concentration 100 ppm, these two alkaloids were more potent inhibitory activity against this plant more than two dicarboxylic acids. The other substances did not showed any significant effect against the growth of *E. crus-galli* (L.) Beauv. seedling.

From the results of this activity against both *B. pekinensis* Rupr and *E. crus-galli* (L.) Beauv., dicarboxylic acid showed high activity against both plants. There are many literatures reported that long chain fatty acid (C_{14} – C_{22}) are allelochemicals[41-43]. This research suggested that dicarboxylic acid showed more potent inhibitory effect than C_{16} and C_{18} fatty acid.

The results of plant growth regulators of isolated substances from *Tylophora indica* Merr. against are summarized in Table 3.16.

Table 3.16 The summary of plant growth regulators of isolated substances from the roots of *T. indica* Merr. against *B. pekinensis* Rupr and *E. crus-galli* (L.) Beauv.*

Substance	*B. pekinensis* Rupr.		*E. crus-galli* (L.) Beauv.	
	Root	Shoot	Root	Shoot
mixture 1	+ (1000)		- (1000)	
mixture 1A				
mixture 2	- (1000)		- (1000)	
Compound 1	+ (1000)		+ (1000)	
Compound 2	+++ (1000) - (10)	+++ (1000) ++ (100)	++ (1000) + (100)	+ (1000)
Compound 3	+++ (1000) - (10)	+++ (1000) + (100)	+ (1000)	+ (1000)
Compound 4	++++ (1000) - (10)	+ (100)	++++ (1000) ++ (100)	++++ (1000)
compound 4A				
Compound 5	++++ (1000) - (10)	+ (100)	++++ (1000) ++ (100)	++++ (1000)
compound 5A				
Compound 6	+ (1000)	+ (1000)	+++ (1000)	
Compound 7	++++ (1000) - (10)	- (100)	++++ (1000) ++++ (100) + (10)	++++ (1000) ++ (100) + (10)
Compound 8	+++ (1000) - (10)	- (100)	++++ (1000) ++++ (100)	++++ (1000)

* The effect of isolated substances was classified as more than 80 % inhibition (++++), 60-80 % inhibition (+++), 40-60 % inhibition (++), 20-40 % inhibition (+) and 20-40 % promotion (-). The concentration of each substance is in parentheses.